Ana Cecilia Villa Parra

Admittance Control of a Robotic Knee Orthosis based on Motion Intention through sEMG of Trunk Muscles

Vitoria - Brazil

December 2017

Ana Cecilia Villa Parra

Admittance Control of a Robotic Knee Orthosis based on Motion Intention through sEMG of Trunk Muscles

Thesis submitted for the Postgraduate Program in Electrical Engineering (PPGEE), Federal University of Espirito Santo (UFES) as a preliminar requirement to obtain the PhD degree in Electrical Engineering.

Federal University of Espirito Santo - UFES

Postgraduate Program in Electrical Engineering

Supervisor: Dr. Teodiano Freire Bastos

Co-supervisor: Dr. Anselmo Frizera Neto

Vitoria - Brazil

December 2017

Ana Cecilia Villa Parra

Admittance Control of a Robotic Knee Orthosis based on

Motion Intention through sEMG of Trunk Muscles

Thesis submitted for the Postgraduate Program in Electrical Engineering (PPGEE), Federal University of Espirito Santo (UFES) as a preliminar requirement to obtain the PhD degree in Electrical Engineering.

Examined by:

_____
Prof. Dr. Teodiano Freire Bastos (PPGEE/UFES)
Supervisor
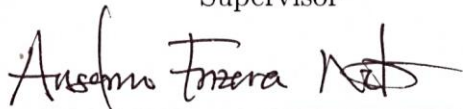
_____
Prof. Dr. Anselmo Frizera Neto (PPGEE/UFES)
Co-supervisor
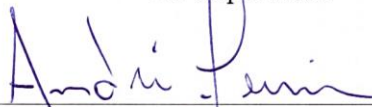
_____
Prof. Dr. Andre Ferreira (PPGEE/UFES)
Jury

_____
Prof. Dr. Eliete María de Oliveira Caldeira (PPGEE/UFES)
Jury

_____
Prof. Dr. Eduardo Rocon (CAR/CSIC-Spain)
Jury

_____
Prof. Dr. Antonio Padilha Lanari Bó (PGEA-UnB)
Jury

December 4, 2017, Vitoria - ES - Brazil

Para mi abuelito Mario, tu sonrisa permanecerá
en mi corazón por siempre.

Acknowledgements

If our work helps to improve someone's life, all efforts have been worthwhile.

Abstract

The population that requires devices for motion improvement has increased considerably, due to aging and neurological impairments. Robotic devices, such as robotic orthosis, have greatly advanced with the objective of improving both the mobility and quality of life of people. Clinical researches remark that these devices, working in constant interaction with the neuromuscular and skeletal human system, improves functional compensation and rehabilitation. Hence, the users become an active part of the training/rehabilitation, facilitating their involvement and improving their neural plasticity. For this purpose, control approaches based on motion intention have been presented as a novel control framework for robotic devices.

This work presents the development of a novel robotic knee exoskeleton controlled by motion intention based on sEMG, which uses admittance modulation to assist people with reduced mobility and improve their locomotion. For recognition of the lower-limb motion intention, sEMG signals from trunk are used, which implies a new approach to control robotic assistive devices. The control system developed here includes a stage for human-motion intention recognition (HMIR) system, which is based on techniques to classify motion classes related to knee joint. The motion classes that are taken into account are: stand-up, sit-down, knee flexion-extension, walking, rest in stand-up position and rest sit-down position. For translation of the user's intention to a desired state for the robotic knee exoskeleton, the system includes a finite state machine, in addition to admittance, velocity and trajectory controllers, which has also the function of stopping the movement according to the users intention. This work also proposes a method for on-line knee impedance modulation based on gait phases recognition using an instrumented insole. This method generates variable gains through the gait cycle for stance control during gait. The proposed HMIR system showed, in off-line analysis, an accuracy between 76% to 83% to recognize motion intention of lower-limb muscles, and 71% to 77% for trunk. Experimental on-line results of the controller with healthy and post-stroke patients showed that the admittance controller proposed here offers knee support in 50% of the gait cycle, and assists correctly the motion classes. A positive effect of the controller on post-stroke patients as users regarding safety during gait was also found, with a score of 4.64 in a scale of 5. Thus the robotic knee exoskeleton introduced here is an alternative method to empower knee movements using motion intention based on sEMG signals from lower limb and trunk muscles.

Keywords: admittance control, electromyography, robotic knee orthosis, stance control.

Glossary

2Ph Category: gait cycle divided in ST and SW phases.

4Ph Category: gait cycle divided in IC, MS, TS and SW phases.

ALLOR Advanced Lower Limb Orthosis for Rehabilitation.

AR Auto-Regressive coefficient.

BF Biceps Femoris.

C1 Classifier for sitting movements.

C2 Classifier for standing movements.

CAN Controller Area Network.

DF Drop foot.

ES Erector Spinae muscle.

F/E Knee flexion-extension.

FES Functional Electrical Stimulation.

FSM Finite State Machinne.

FSR Force sensing resistor.

G Gain.

GC Gastrocnemius.

HMIR Human motion intention recognition system.

IC Initial contact phase of the gait phase.

LDA Linear Discriminant Analysis.

LL Lower Limb.

MAV Mean absolute value.

MS Mid stance phase of the gait phase.

P1 Gain pattern based on the knee moment during gait.

P2 Gain pattern based on the knee velocity during gait.

P3 Gain pattern with a constant value equal to zero.

PCA Principal component analysis.

PI Proportional Integral.

QUEST Quebec User Evaluation of Satisfaction with Assistive Technology.

RF Rectus Femoris.

RKO Robotic knee orthosis.

RMS Root mean square.

RSD Rest sit-down.

RSU Rest stand-up.

S Subject.

SD Sit-down.

SE Semitendinosus.

sEMG Surface electromyographic.

SSC Slop sign changes.

ST Stance phase of the gait phase.

SU Stand-up.

SVM Support Vector Machine.

SVM-G Support Vector Machine with Gaussian kernel.

SVM-P Support Vector Machine with polynomial kernel.

SW Swing phase of the gait phase.

TR Trunk.

TS Terminal stance phase of the gait phase.

UW User's Weight.

VAR Variance.

VM Vastus Medialis.

W Walking.

WAMP Wilson Amplitude.

WHO World Health Organization.

WL Waveform length.

ZC Zero crossing.

List of Tables

List of Figures

Contents

Chapter 1

Introduction

1.1 Motivation

Walking is more difficult for elderly, and persons that suffer gait impairments, due to neurological disorders as stroke or spinal cord injury (SALZMAN, 2010), (JAHN; ZWERGAL; SCHNIEPP, 2010), (MAHLKNECHT et al., 2013), (BALABAN; TOK, 2014). These conditions often lead to possible traumas, injury, disability, risk of falls, loss of independence and reduction in their quality of life (WEERDESTEYN et al., 2008), (BRADLEY; HERNANDEZ, 2011), (LEWEK et al., 2014).

In order to assist these people with reduced mobility and improve their locomotion, some robotic devices that include powered exoskeletons have been proposed recently, which apply functional compensations at the lower limb during gait (COWAN et al., 2012), (CHEN et al., 2013), (DZAHIR; YAMAMOTO, 2014), (YAN et al., 2015), (CHEN et al., 2016).

Preliminary findings report promising results, as the fact of: sub-acute stroke patients experimenting added benefit from exoskeletal gait training (LOUIE; ENG, 2016); powered exoskeletons providing individuals with thoracic-level motor-complete SCI the ability to walk (LOUIE; ENG; LAM, 2015); and that the use of a exoskeleton in combination with conventional therapy may be safe and reduce the metabolic cost (VITECKOVA; KUTILEK; JIRINA, 2013).

Clinical and biomechanical researches that involve robotic platforms remark that these devices must work in constant interaction with the neuromuscular and skeletal human system, for functional compensation and rehabilitation. In fact, the users and the exoskeleton must work together in an intuitive and synergistic way to provide more natural movements to enable them to take an active part of the training/rehabilitation, facilitating their involvement in an attempt to improve their neural plasticity (TUCKER et al., 2015). In addition, for the implementation of proper gait training and rehabilitation plans, control strategies that consider both the ability and impairment of the user are required (CAO et al., 2014).

Studies have demonstrated that cells in motor cortex and various pre-motor areas discharge with execution of voluntary movements in relatively specific and reliable ways (FETZ, 2007). Then, diverse ranges of limb movements and flexibility of digital control must clearly be correlated. In this sense, the biggest challenge related to control strategies for exoskeletons is that they must be adapted to the functional capabilities of users for seamless cognitive and physical interaction (VITECKOVA; KUTILEK; JIRINA, 2013), (TUCKER et al., 2015), (HUO et al., 2016). In this context, control strategies to obtain direct volitional control through motion intention detection may provide the user with the ability to modulate the exoskeleton's behavior (TUCKER et al., 2015).

For this purpose, some control approaches based on motion intention detection have been presented as a novel control framework for exoskeletons to improve their performance. The goal is to detect the user's motion intention and follow the user when a predefined movement is imposed (RIENER; LüNENBURGER; COLOMBO, 2006), in order to execute an action that is both appropriate for the task and corresponds to the user's expectations. This information can be used to adapt the robotic assistance to the user's motor abilities allowing them to contribute as much as possible to the movement (RIENER et al., 2005). Hence, the user executes an appropriate locomotion with the generation of voluntary commands in a human-centered system to assist the movement with minimal cognitive disruption (TUCKER et al., 2015). The system must be also autonomous, easy to use, and capable of providing a high level of comfort and functionality.

In recent times, some impedance/admittance controllers have been proposed for assistive robots to regulate the interaction between the exoskeleton and the user, incorporating human motion intention (CAO et al., 2014). Impedance is intricately related to the mode and amount of muscle activation involved in the performance of as given task. Therefore, control of the mechanical impedance of the limb joints is an important feature of the neuromuscular system (MIZRAHI, 2015). Due to the fact that humans change their joint impedances during gait by regulating the postures and the muscle-contraction levels to maintain the stability, impedance controllers are of interest to develop control strategies for gait assistive devices. Theses controllers offer the possibility of regulating the mechanical impedance at joints according to the user's disability level and their voluntary participation in order to provide an effective human support through assisting their limited motor capability (CAO et al., 2014), (TSUJI; TANAKA, 2005), (HUSSAIN; XIE; JAMWAL, 2013).

Interaction forces exist between the device, the user, and the environment which can be sensed as an input to controllers based on motion intention detection. Force and surface electromyography (sEMG) signals have been used to recognize the human-motion intention (TUCKER et al., 2015). Force sensors may detect the patient's remaining muscular efforts reflected in joint moments, and sEMG signals contain enough information to allow the motion intention detection even although no movement is performed (KIGUCHI; TANAKA; FUKUDA, 2004), (FLEISCHER et al., 2006). In fact, studies show that sEMG signals can be detectable shortly before muscle producing movement, and these signals contain information able to both predict the intended motion (LEE et al., 2015b) and detect gait events, due to the natural and repeatable relationship between sEMG and events during gait.

Pattern recognition–based techniques that employ classification theory to extract the user's intent from multiple sEMG signals have the potential to more accurately detect a greater set of motion intention. As advantages of this approach, some studies report that a smaller learning effort might be expected from users using devices with control systems based on it (JIMéNEZ-FABIáN; VERLINDEN, 2012). Additionally, studies report that using sEMG the user can perform a desired movement, or try to do so, without creating an additional mental load (FLEISCHER et al., 2006).

In studies focused on lower-limb motion recognition (CHEN et al., 2013), sEMG signals from lower limb muscles are recorded as primary actor in locomotion (SAWICKI; FERRIS, 2009), (KIGUCHI; IMADA, 2009), (MENG et al., 2010), (JIMéNEZ-FABIáN; VERLINDEN, 2012), (JOSHI; LAHIRI; THAKOR, 2013), (LEE et al., 2015a), (LEE et al., 2015b). However, few works consider alternatives in cases where the user cannot generate sufficient amplitude of sEMG signals from their lower limbs due weakness or atrophy. These conditions do not allow to discern and interpret the physiological state and desires of the user (SUZUKI et al., 2007).

In this context, there are studies related to sEMG analysis during walking that report that, in addition to lower limb muscles, the *erector spinae* (ES) muscle of the trunk, on different spinal levels plays an important role in the organization of this task (LAMOTH et al., 2002), (AN-DERS et al., 2007), (SèZE; CAZALETS, 2008), (SWINNEN et al., 2012a) and also participate actively in motor tasks (CECCATO et al., 2009). On the other hand, the (ES) muscle is also involved in maintaining the trunk equilibrium during several forms of locomotion or rhythmic motor tasks in humans (SèZE et al., 2008). In (WENTINK et al., 2013), the feasibility of real-time intention detection of gait initiation based on lower limb muscles and ES muscle (lumbar region) was analyzed. The results show that the ES muscle can provide valuable information on postural changes and be used for detection of heel strike. Additionally, the muscle recruitment of trunk precedes the muscle recruitment of the lower limb, then the trunk begins to move earlier (KARTHIKBABU et al., 2012). A sEMG study also suggests that the ES muscle activity anticipates propulsive phases in walking with a repetitive pattern (CECCATO et al., 2009). Thus, this muscle can be considered to estimate gait phases.

It is important to understand how the locomotion is controlled in humans and how the user's state and intent can be sensed. In neurological cases, such as spinal cord injury and post-stroke, patients present spasticity and paralyzed muscles, but the trunk musculature may have been preserved (KARTHIKBABU et al., 2012), (ESPINOSA, 2013). Regarding post-stroke, it is reported that although the trunk muscles have a potential to deteriorate their function, the recovery after stroke is possible (KARTHIKBABU et al., 2012).

Elderly have significantly higher co-activation of lower-limb muscles than middle-aged adults at

their preferred gait speed; the trunk co-activation is significantly lower (LEE et al., 2017), but studies show that the relationship between trunk co-activation and locomotor instability can be used to develop robotic gait assistance of elderly people to prevent fall (LEE et al., 2017). However, the literature review does not report applications of sEMG of trunk muscle for motion intention recognition, gait phase identification and locomotor instability applied to the control of exoskeletons for movement assistance or rehabilitation (YAN et al., 2015), (TABORRI et al., 2016). This fact opens then the possibility of exploring the alternative of obtain motion intention of lower limb movements, but using sEMG of the trunk, and use this information to control robotic devices for gait assistance and rehabilitation. For our knowledge, the literature does not report studies that use sEMG features of trunk muscles for motion intention recognition in gait applications, even although these muscles are involved in the organization of locomotor patterns during walking and other various rhythmic motor tasks. In this context, the ES muscle is investigated in our research as an option to propose a method for motion intention recognition and gait phases for a control system. Furthermore, a strategy to assist gait using impedance controllers is also proposed. This research also allows defining specific recommendations and guidelines for electrode location of the trunk muscles to control assistive devices for gait. In addition, as pattern recognition-based control currently has limited clinical implementation, this study contributes to define optimal parameters for the control system, in order to maximize the user's performance of the motion intention detection methods based on sEMG signals. The system proposed here could be used in other applications related to gait technologies and, together with a variable impedance controller also proposed, can can be considered as promising orthotic intervention for assistive devices using residual motor skills of users. This control strategy also provides the possibility of investigating knee impedance variations during gait, which is of vital interest for researchers involved with the design and control of prosthetic and orthotic devices (TUCKER et al., 2013).

1.2   Context

Based on the report on ageing and health of the World Health Organization (WHO) (World Health Organization, 2015), ageing is emerging as a key policy issue due to elderly around the world is increasing dramatically. In fact, currently Japan exceeds 30% of the proportion of people aged 60 years or older, and by the middle of the century, countries in Europe, North America and South America will have a similar proportion.

Regarding the stroke, the WHO reports that in 2004 annually 15 million people worldwide suffered a stroke, and of these, 5 million died and another 5 million were left permanently disabled (MACKAY; MENSAH, 2004). Stroke is a leading cause of serious long-term disability in North America and is considered among the top 18 diseases contributing to years lived with disability (BENJAMIN et al., 2017). Nowadays, about 92.1 million North American adults are living with some form of cardiovascular disease or the after-effects of stroke, and with the increase in the aging population, the prevalence of stroke survivors is projected to increase, especially among elderly women (BENJAMIN et al., 2017). Stroke is a serious and disabling global health-care problem due to the number of affected continues to increase because of the ageing population and unhealthy lifestyle. Thus, due to the significant increase of population affected with gait impairment, the development of strategies to improve gait rehabilitation and assistance with robotic devices is an important goal. Among the main contributors related to movement assistant for people with disabilities are the active orthosis and exoskeletons.

Currently, the Assistive Technology Group at UFES/Brasil develops a robotic system for assistance and rehabilitation of human walking. The systems is composed of a robotic knee orthosis and a smart walker with forearm supports. The smart walker guides the users during the gait and assists them to keep a stable posture, and the orthosis provides assistance to the knee. The orthosis comes with a signal acquisition system for force, angle, electroencephalography and surface electromyography signals, which is used to develop control strategies based on user's motor intention. The control of the knee motion in different gait phases is the current goal of the mentioned research. The main goal is to implement different impedances at the knee joint during stance and swing phases, providing robustness when the motor intention detected by

brain and muscle patterns is generated by the user.

1.3 Hypothesis

The hypothesis of this research work is that a system for motion intention recognition based on sEMG from ES muscle together a admittance controller for a robotic knee orthosis may be quite robust to assist knee joint movements.

1.4 Objectives

The main objective of this research is to propose an admittance control for a robotic knee orthosis that uses human motion intention based on sEMG from ES muscle. This, in order to assist patients with difficulty in voluntarily initialize knee movement. Around this main objective, several challenges define the following partial objectives:

1. Design of a protocol to acquire sEMG signals from trunk muscles during gait over ground in both intact and neurologically impaired individuals. This objective is focused on designing a safe protocol for the individuals and defining the correct positioning of electrodes to obtain a database oriented to lower-limb motion analysis.

2. Development of a human motion intention recognition system based on sEMG from ES muscle in neurologically intact as well as neurologically impaired individuals. This represents a new approach in which the trunk muscles, specifically the ES muscle, can be used to extract information to control the assistive gait device.

3. Development and validation of a stance control strategy for a robotic knee orthosis to assist the knee movement during gait, based on the modulation of admittance parameters. The orthosis varies the knee support while performing walking, in order to allow a natural gait pattern.

1.5   Organization

This document is organized in the following chapters:

Chapter 2 presents a background related to gait, robotic knee orthosis technology, control strategies for movement assistance and recognition systems based on sEMG signals. In addition, a brief state of art of the role of trunk and lower limb muscles during gait is presented. This in order to support the hypothesis that ES muscle can be explored as a source for a gait phase recognition system. From this analysis, controller criteria and signal processing techniques are derived to guide the developments and proposals of this research. Additionally, electrode locations are derived to design the protocol to acquire sEMG signals and obtain a database.

Chapter 3 presents the materials and methods used in this research, with the description of the platform to implement the controller to assist knee movements. These include the description of the motion intention recognition system, implemented with Support Vector Machine (SVM) classifier and the protocol to acquire sEMG signals of trunk muscles. Then the description of the components of the admittance control strategy with the impedance adjustment method, the gait phase detection system composed of an instrumented insole, the robotic knee orthosis employed, the experimental protocol used to validate the controller.

Chapter 4 presents the experimental results of experimental tests with healthy and impaired subjects to evaluate the controller and the discussion.

Finally, chapter 5 presents the conclusions and future works of this research.

Chapter 2

Background

This chapter presents the background and rationale of this research. It starts by giving an overview of gait disorders and robotic knee orthosis developed for gait assistance and rehabilitation. Next, relevant aspects related to knee impedance during gait, in addition to admittance controllers as strategies that can improve the knee motor assistance during gait are addressed. Consequently, the chapter follows by explaining the approach based on sEMG to develop a system to detect the human motion intention related to knee movements. Subsequently, characteristics of sEMG activity of the trunk muscles during walking, and muscle condition in post-stroke patients are reviewed.

2.1 Gait Cycle

The gait cycle starts when one leg goes forward and the corresponding heel strikes the ground, and ends when the same foot goes forward again and touches the ground. These events define two major phases of the gait cycle, called stance phase (ST) and swing phase (SW) (AGOSTINI; BALESTRA; KNAFLITZ, 2014).

Figure 2.1(a) shows the gait phases during the gait cycle. ST designates the period during which the foot is in contact with the ground and the leg supports the body weight, representing approximately 60% of the gait cycle. On the other hand the SW applies to the period that the
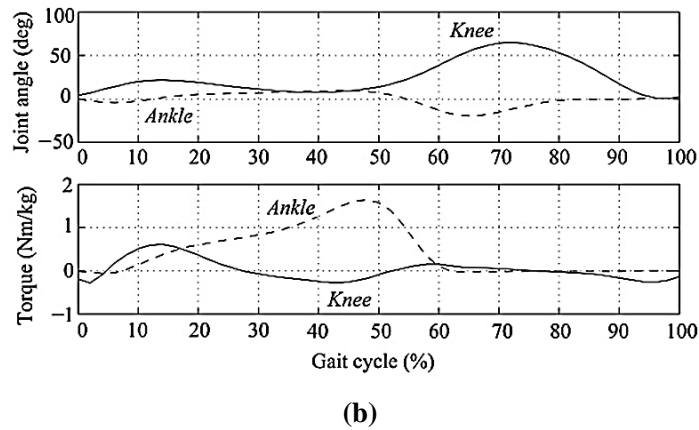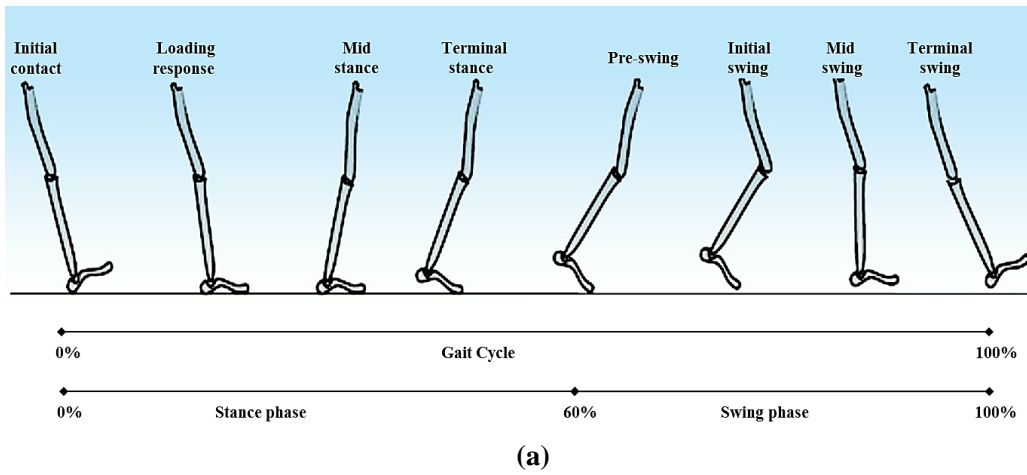
Figure 2.1: (a) Gait phases during the gait cycle. Representation of knee and ankle values during walking (PERRY, 2010); (b) joint angle and torque (PONS et al., 2007).

foot is in the air for limb advancement.

Usually, the gait cycle for stance analysis is divided in the sequence of the following sub-phases (CHEN et al., 2015): 1) Initial contact (IC), defined by the heel contact; 2) Loading response and mid-stance (MS), defined by a flat foot contact; 3) Terminal stance (TS), defined by the heel off; 4) Swing (SW), defined by the foot off.

During normal gait, hip, knee and ankle joints play important roles in all locomotion aspects, which include motion control, shock absorption in the ST, stance stability, balance, energy conservation, and propulsion (SHORTER et al., 2013), (PONS et al., 2007). Figure 2.1(b) shows the angle and moment of the knee and ankle joints, considering anthropometric characteristics of the users with average heights (from 1.5 to 1.85 m), weights (from 50 to 95 kg) and average gait speed (approx 1.4 m/s) (MCGIBBON; KREBS, 2004), (PONS, 2008), (WINTER, 2009).

Regarding normal and pathological cases, during gait, both normal and pathological subjects use different sequences of gait phases, then, they do not show the same type of GC (AGOSTINI; BALESTRA; KNAFLITZ, 2014). Thus, the next section describes gait disorders and characteristics of pathological gait.

2.2 Gait Disorders

Gait impairments are frequent injuries for elderly and post-stroke individuals, which would often lead to disability (WEERDESTEYN et al., 2008), (SALZMAN, 2010), (HENDRICKSON et al., 2014), (BALABAN; TOK, 2014).

Regarding elderly, the characteristics of gait include: reduction of velocity and stride length, an increased stance width and time spent in the double support phase (i.e., with both feet on the ground), bent posture and less vigorous force development at the moment of push off (SALZMAN, 2010). These changes may due to adaptations to alterations in their sensory or motor systems to produce a safer and more stable gait pattern (SALZMAN, 2010).

On the other hand, for post-stroke individuals, the typical characteristics are the spatial and temporal asymmetry of the hemiplegic gait, higher cadence and shorter stride length (JONSDOTTIR et al., 2009). For this individuals the impaired ability of the paretic limb to control balance contributes to gait asymmetry (HENDRICKSON et al., 2014), which may be related to their high number of falls (LEWEK et al., 2014). Gait deficits include reduced propulsion at push-off, decreased hip and knee flexion during the swing phase (SW), and reduced stability during the stance phase (ST)(WEERDESTEYN et al., 2008). Due to their balance deficits these individuals present reduced postural stability during quiet standing and delayed and less coordinated responses (WEERDESTEYN et al., 2008). The gait disorder termed drop foot (DF) also is a motor disability that affects post-stroke individuals people, which is often the result of a paralysis and/or weakness in the individuals's dorsiflexor muscles, causing an unsuccessful foot clearance during the SW (MELO et al., 2015). The subjects usually start the gait cycle (GC) with a forefoot contact instead a heel strike, causing kinematic and kinetic changes

at the lower limb joints and increasing the risk of falls. During SW, disturbances of hip, knee, and ankle motions in the hemiplegic limb are characterized by limited or reduced hip flexion, reduced knee flexion, and reduced ankle dorsiflexion or continuous plantar flexion (BALABAN; TOK, 2014). (BURPEE; LEWEK, 2015) reports that unsuccessful foot clearance events during SW are characterized by an increase in the knee extension moment during late stance and ankle plantarflexion angle at toe-off as well as a reduction in the knee flexion velocity at toe-off. In addition, elevation of the pelvis on the side of the swinging leg and lateral sway of the trunk are another compensation for achieving foot clearance (BALABAN; TOK, 2014).

For these individuals and elderly, gait assistance through robotic devices may be of great help (PONS et al., 2007). In fact, robotic gait assistive technology has greatly advanced to assist individuals with excessive knee flexion, droop foot, limb paralysis and other mobility-limiting disorders (KOZLOWSKI; BRYCE; DIJKERS, 2015), (HUO et al., 2016).

2.3   Lower-limb Robotic Orthosis

Lower-limb robotic orthoses are devices that act in parallel with the human body to assist impairment in lower limbs during the execution of hip, knee or ankle movements (HERR, 2009), (DíAZ; GIL; SáNCHEZ, 2011), (ANAM; AL-JUMAILY, 2012), (CHEN et al., 2013), (KOZLOWSKI; BRYCE; DIJKERS, 2015); which cannot be accomplished due to muscles or joints weak, ineffective or injured for a disease or a neurological condition (WALDNER; TOMELLERI; HESSE, 2009), (YAN et al., 2015), (CHEN et al., 2016). Some studies (VITECKOVA; KUTILEK; JIRINA, 2013) have also demonstrated that these robotic orthoses may reduce the metabolic cost and increase the walking speed, in addition to be used to assist gait in individuals with paraplegia, spinal cord injury and elderly (ZEILIG et al., 2012), (KOZLOWSKI; BRYCE; DIJKERS, 2015). Additionally, some studies report that the use of robotic gait assistive technology in combination with conventional therapy may be a safe and effective way towards reduction of disablement due to neurological injury (KIM et al., 2015), (STAM; FERNANDEZ, 2016). According to (KOZLOWSKI; BRYCE; DIJKERS, 2015), theses devices offer the following functions: (a) exercise modality to promote physical, mental, and social wellness; (b)

gait training modality for inpatient or outpatient rehabilitation; (c) facilitate an environment for plasticity in which neurologic repair can take place.

A special case of lower-limb robotic are robotic orthoses for knee, which are used to assist knee flexion and extension in order to supply assistive torque at the joint and alleviate the load, reducing pressure and relieving the strain and stress acting on the knee joint (IR; AZUAN, 2015). These robotic knee orthoses (RKO) typically actuate on the the sagittal plane, due to the motion range of the joint is greater in this plane than in other planes during walking (WINTER, 2009), (PERRY, 2010). Several robotic devices have been developed to provide active knee assistance, such as: the orthosis KAFO (SAWICKI; FERRIS, 2009), assitive knee brace (MA et al., 2013), CSCO (SHAMAEI; NAPOLITANO; DOLLAR, 2014), knee orthosis rotary SEA mechanism (SANTOS; SIQUEIRA, 2014), running knee (SHAMAEI et al., 2014), COWALK-M (KIM; KIM; CHOI, 2015) and the powered knee orthotic (FIGUEIREDO et al., 2017). Figure 2.2 shows some of these devices.

Assistive Knee Brace 2013	*CSCO 2014*	*Knee Orthosis Rotary SEA mechanism 2014*	*Running Knee 2014*	*COWALK-M 2015*	*Powered Knee Orthotic 2017*
2 Kg	3 Kg	2.9 Kg	2.63 Kg	4.8 Kg	2.02 Kg
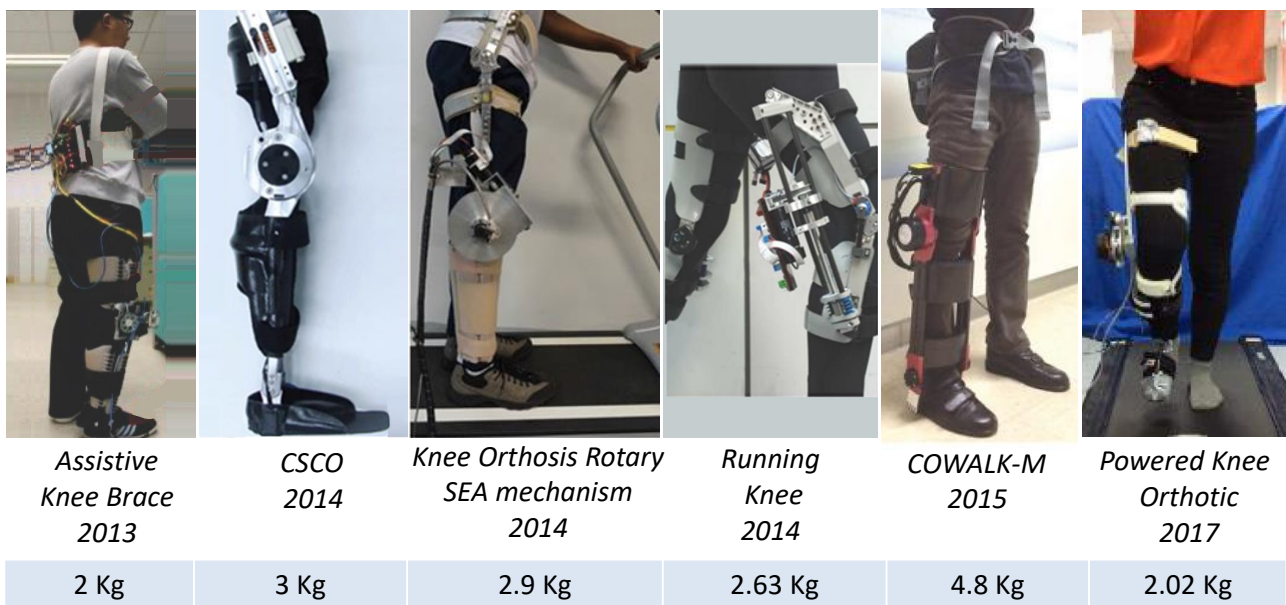
Figure 2.2: Robotic knee orthoses for gait assistance and rehabilitation.

To ensure that the orthosis moves together with the individual, a mechanical structure is normaly attached to the individual's joints, whose design is based on the mechanism and kinematics of the human body, following the basic principles of ergonomy (SHORTER et al.,

2013). Links and joints of the robotic orthoses are placed on correspondence of those of the human body, and are connected to the limbs in multiple points (DONATI et al., 2013). This mechanical structure is typically wearable, compact and light to minimize the energetic impact to the user and ensure safety (SHORTER et al., 2013), (VITECKOVA; KUTILEK; JIRINA, 2013), (HUO et al., 2016). Regarding the joint actuators, these provide the power needed to maximize the residual abilities of the user and regain functional mobility during walking (ANAM; AL-JUMAILY, 2012), (HUSSAIN; XIE; LIU, 2011), (PONS et al., 2007), which are selected in terms of their velocity and torque (ONEN et al., 2013). Table 2.1 summarizes some required for robotic knee orthoses reported in (PONS et al., 2007), (HUSSAIN; XIE; LIU, 2011), (VITECKOVA; KUTILEK; JIRINA, 2013), (ONEN et al., 2013), (SHORTER et al., 2013), (HUO et al., 2016).

Table 2.1: Design criteria for active orthoses.

Criteria	
Mechanical structure	Alignment with user's joints
	Adaptability to different users
	Light weight and hardness and firmness
	Stops to inhibit to go beyond the physiological ranges of motion
	Allow active and passive movements
	Easy to wear, safe and ergonomic
Actuator	Powerful (joint torques comparable to healthy individuals)
	Low mechanical impedance[a]
	Light weight and safe
	Highly compliant and zero backlash
	Compact design and efficient
	Accuracy and repeatability in positioning

[a]Relationship between moment applied by the robotic orthosis and the joint angle.

2.4   Control Strategies

Robotic knee orthoses require control strategies to identify, compensate and finally overcome disabilities of the users to induce an effective movement assistance (HUSSAIN; XIE; LIU, 2011), (LOW; YIN, 2007), (LOBO-PRAT et al., 2014). Feedback information to the controller are typically joint angles and interaction forces, which can be obtained through encoders, inertial

measurement units (IMUs) and force sensors.

In adition, for a precise control, the device must identify the gait phases in order to apply the assistance to achieve a correct knee angle. Different configurations of controllers are proposed in literature, such as "trajectory tracking" control, "assist-as-needed" control algorithms, and "impedance" control (AMA et al., 2012), (CAO et al., 2014), (YAN et al., 2015), (HUO et al., 2016). Some examples of robotic knee orthoses are the Vanderbilt active orthosis, which uses a Hall-effect sensors to get angle measurements in each hip and knee joint, in addition to a 3-axis accelerometer and gyroscope in each thigh segment. The control system is composed of a trajectory control, and a supervisory based on event-driven finite state machine (QUINTERO; FARRIS; GOLDFARB, 2012), (FARRIS; QUINTERO; GOLDFARB, 2011).

(BULEA et al., 2012) use an impedance control to apply a variable damping on the knee to substitute the stabilizing effect of eccentric quadriceps contractions during stance flexion in walking. Also, there is the robotic orthosis reported in (HUSSAIN; XIE; JAMWAL, 2013), which uses an adaptive impedance control to provide assistance at low compliance level for severely impaired individuals and increased compliance for individuals with less severe impairments. The CSCO robotic knee orthosis (SHAMAEI; NAPOLITANO; DOLLAR, 2014) uses a quasi-passive compliant system for stance control. Nevertheless, for the use of these robotic orthosis for gait assistance and rehabilitation, control strategies must consider both the skill and impairment of the individual (CAO et al., 2014). In this sense, an impedance controller offers the possibility of regulating the mechanical impedance at joints according to the individual impairment level and their level of skill to promote a compliant human-robot interaction (TSUJI; TANAKA, 2005), (HUSSAIN; XIE; JAMWAL, 2013). Here, the impedance actuates in function of the relation between force, position and its time-derivate, which is given by three components: stiffness, damping and inertia. Thus, a robotic-assisted system which impedance control will be able to provide interactive gait training and adjust the amount of support to be assisted in rehabilitation (CHEN et al., 2016). In fact, some reviews report that the use of an adaptive impedance controller provides a gait motion training that is comparable to the one provided by physical therapists (DZAHIR; YAMAMOTO, 2014).

On the other hand, humans change their joint impedances during gait by regulating the postures

and the muscle-contraction levels to maintain their stability, then the robotic device must also integrate methods for a suitable impedance modulation to assist the movement through the gait cycle. Impedance modulation allows promoting a compliant human-robot interaction to provide an effective human support through assisting the limited motor skill of the user (CAO et al., 2014), (TSUJI; TANAKA, 2005). Despite this, few studies have explored suitable and reliable methods to execute this modulation in gait applications, which very important in rehabilitation robots to guarantee a dynamic performance (MENG et al., 2015).

The literature does provide information about impedance modulation, such as the "assist-as-needed" control, which is based on the interaction torque and reference trajectory (CHEN et al., 2016), (CAO et al., 2014), (MENG et al., 2015), (FIGUEIREDO et al., 2017). However, in this case, a common limitation is the discontinuous model, just like to turn on or off the robotic assistance, rather than offering a seamless impedance tuning process (MENG et al., 2015). Robots that use manual impedance level adjustment to adapt the support to individual's skills or training progress have also been reported (CAO et al., 2014). Some methods try to set the impedance through the estimation of the joint stiffness using sEMG combined with kinetic and kinematic measurements to estimate the muscle force, together with models that relate muscle force to stiffness (PFEIFER et al., 2012), (SARTORI et al., 2015), which would be of great interest for control strategies. However, these methods have not yet been applied in control systems for robotic gait assistance.

On the other hand, the stance control is reported as a strategy that can be used to increase the walking speed and reduce both energy expenditure and gait asymmetry (to both affected and unaffected legs), allowing less stressed paretic musculature in patients with muscular weakness (ZISSIMOPOULOS; FATONE; GARD, 2007), (RAFIAEI et al., 2016b), (ZACHARIAS; KANNENBERG, 2012). It is an important strategy which is considered as a new generation of orthotic intervention that could potentially be significant in assisting to improve the gait kinematics (RAFIAEI et al., 2016a), and that can be aboard with impedance control. A stance control strategy consists of the following: (1) suitable free knee motion in the swing phase (SW) to allow free joint rotation in flexion and extension; (2) suitable lock of the knee joint to resist knee flexion while allowing free knee extension (YAKIMOVICH; LEMAIRE; KOFMAN, 2009),

(TO et al., 2011), (TO et al., 2012), (YAN et al., 2015).

Hence, SC provides knee stability and protects the joint from collapsing during the standing and stance phase of walking, releasing the knee to allow free motion during the swing phase (IR; AZUAN, 2015). Figure 2.3 shows the knee angle during walking tests using lower limb orthosis under stance control strategy.
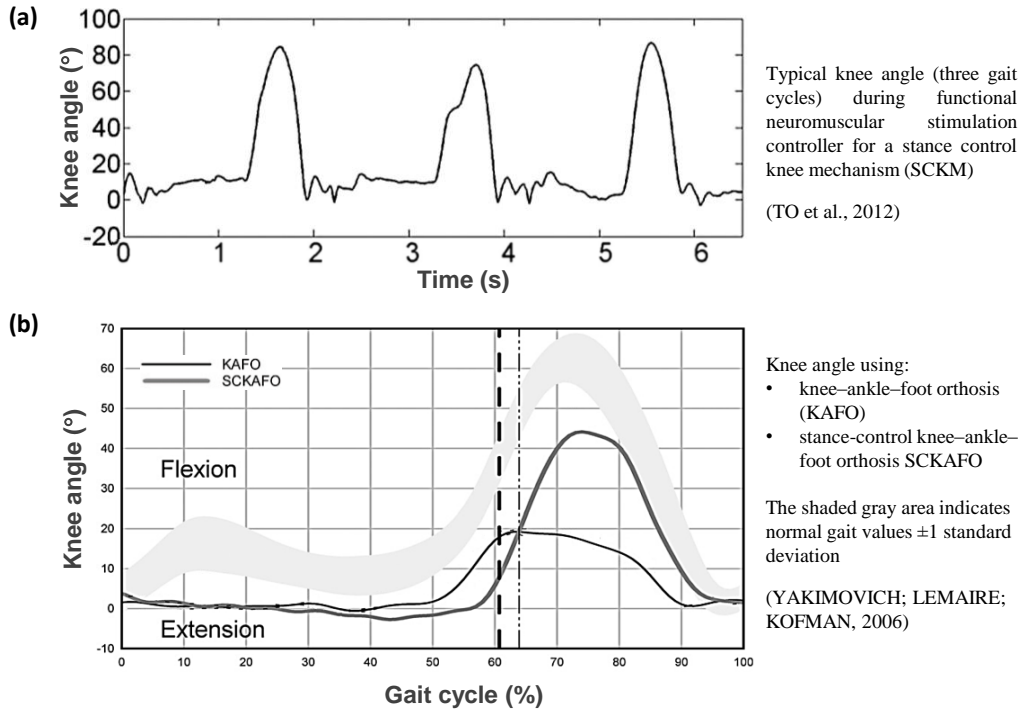
Figure 2.3: Knee angle during walking tests using lower limb orthosis under stance control strategy.

It is reported in literature that the SC improves the gait kinematics (increased knee range of motion, stride and step lengths), user satisfaction in addition to have reduced energy expenditure (ZACHARIAS; KANNENBERG, 2012), (McMillan et al., 2004), (YAKIMOVICH; LEMAIRE; KOFMAN, 2009). Also, SC allows less stressed paretic musculature in individuals with muscular weakness.

The ideal controller should have a very quick reaction time (<6 ms) when switching between stance and swing modes. Additionally, for smooth progression of the body center of mass and shock absorption, controlled knee flexion and assisted knee extension during stance phase (ST) are required (YAKIMOVICH; LEMAIRE; KOFMAN, 2009). To stabilize the knee, it is also required a gait phase recognition system to allow a smooth and quick switching between

stance and swing phase (YAKIMOVICH; LEMAIRE; KOFMAN, 2009), (TO et al., 2011), (IR; AZUAN, 2015).

SC can be implemented using an impedance control with a suitable impedance modulation that allows a smooth switching between the stance phase and swing phase, which is a remarkable challenge to guarantee a suitable response of a robotic orthosis (YAKIMOVICH; LEMAIRE; KOFMAN, 2009), (IR; AZUAN, 2015). Also, a study about the mechanics of the knee during the stance phase of the gait, reported in (SHAMAEI; DOLLAR, 2011), suggests that, ideally, the mechanism that adjust the knee impedance should be based on the gait speed and weight, in order to mimic the behavior of the human knee joint. Thus, sense, a stance control implemented with a variable impedance controller can be considered to provide adequate knee stability and allow a more normal gait.

2.5   Human Motion Intention Detection

An important aspect for robotic knee orthoses is the detection on the motion intention. Motion intentions originate with the subject, whose physiological state and desires must be discerned and interpreted. This intention to execute a movement can be estimated through the sensing of cortical and neuromuscular activity, posture, locomotive state, and physical interaction with the environment and the robotic assistive device (CHEN; ZHENG; WANG, 2014), (TUCKER et al., 2015). Robotic orthoses used the concept of "patient-cooperative" or "subject-centered" based on the motion intention and motor abilities to feed information back to the individual in order to adapt the robotic assistance (RIENER; LüNENBURGER; COLOMBO, 2006). The detection of the motion intention may be obtained through sEMG signals (KIGUCHI; TANAKA; FUKUDA, 2004), (SUZUKI et al., 2007). The richness of information is related to both the variety of discernible activities and the specificity of motion intention obtainable through a given modality. The reviews (JIMéNEZ-FABIáN; VERLINDEN, 2012) report that a smaller learning effort might be expected from users using devices with control systems based on motion detection.

There are some lower-limb robotic orthosis (also termed exoskeletons) that employ sEMG sig-

nals based-assistance: HAL (Hybrid Assistive Limb) (HAYASHI; KAWAMOTO; SANKAI, 2005), KAFO (SAWICKI; FERRIS, 2009) and NEUROExos (LENZI et al., 2012). These devices use control interfaces that detect the motion intention based on sEMG pattern recognition, which are commonly acquired during daily life tasks, both static (sitting) and dynamic (walking) ones. In the review (MENG et al., 2015) an sEMG-triggered control is used, which is a muscular activation controlled method that predicts the user's motion intention in advance, and the robot assistance is triggered when it reaches a certain threshold.

Surface electromyography (sEMG) allows to sense peripheral nerve signals and is a noninvasive technique,in which electrodes are placed on the muscle of interest. Among the advantages of using sEMG in robotic orthoses are (FLEISCHER et al., 2006): (1) If the muscles are weak the motion intention can still be detected; (2) sEMG signals are emitted unconsciously, then, if the user trying to do a desired movement no additional mental load is created; (3) the sEMG signals are emitted early, before the muscles contract, due to the signal propagation delays and the muscle fibers need some time to contract. In fact, biosignals possess enormous potential for human–machine interaction, because these signals offer for machines an alternative means to communicate with people with physical disabilities (LEE et al., 2015b). Disadvantages can include that sEMG activity is susceptible to changes in electrode-skin conductivity, motion artifacts, misalignment of the electrodes, fatigue, and cross-talk between nearby muscles (HOOVER; FULK; FITE, 2012), (TUCKER et al., 2015). sEMG is also non-stationary during a dynamic activity, needing necessitates the use of pattern recognition techniques and calibration each time the device is put on (DAWLEY; FITE; FULK, 2013), (VILLAREJO et al., 2013), (TUCKER et al., 2015). However, pattern recognition–based techniques have the potential to more accurately detect a greater set of motion intention. Under this approach, the sEMG also allows the identification of gait phases (TABORRI et al., 2016), due to the lower-limb muscle activity occurs in a repeatable way during gait cycle (HOF et al., 2002).

2.5.1   sEMG Processing Techniques

Several signal processing techniques are used to detect the motion intention through sEMG. Motion intention for standing up and knee flexion-extension can be detected through neural network as proposed in (TANG; WANG; TIAN, 2017). In (AI et al., 2017) Gaussian kernel-based linear discriminant analysis (LDA) and multi-class support vector machinne (SVM) are used to lower-limb motion recognition. In (KIGUCHI; IMADA, 2009) and (KIGUCHI; HAYASHI, 2015), a neuro-fuzzy technique for motion detection of lower-limb. (LAUER et al., 2004) use an adaptive neuro-fuzzy technique for motion intention detection with the application of functional electrical stimulation (FES) to produce leg movements.

For gait phase recognition, pattern recognition–based techniques are commonly used. They employ classification theory to extract the user's motion intention from multiple sEMG signals, and has the potential to more accurately recognize a greater set of motions. Among the works that report systems for gait phase recognition from lower-limb sEMG signals, the following may be mentioned: Meng et.al (MENG et al., 2010), which applies hidden Markov model (HMM) as a classifier to recognize gait phases. In that work, the gait is divided into five phases, including early stance, mid stance, pre-swing, swing flexion, and swing extension, according to the posture angle of the thigh, shank, and knee joint. In (LEE et al., 2015a), gait sub-phases during stairs ascending (weight acceptance, pull up, forward continuance, foot clearance) and stairs descending (weight acceptance, controlled lowering, leg pull through, foot placement) are recognized through LDA according with the knee angle.

(LEE et al., 2015b) report a method that identifies nine gait phases from sEMG and a combination generated by four force sensing resistor (FSR) installed on the toe and heel.

Independently of the processing technique used, an effective real-time operation requires a quick and accurate response to the user, regardless of the control method employed. Since raw sEMG signals are not suitable as input signals to a controller, their features must be extracted (KIGUCHI; HAYASHI, 2015). Feature selection is an essential stage in recognition due to the significance of features during classification. Table 2.2 summarizes the features of sEMG that present best results in gait analysis and motion intention detection in real-time.

Table 2.2: Features for sEMG signal processing

Feature	Description
Root mean square (RMS)	- Allows quantifying the intensity and duration of several events of sEMG signals - Reflects the level of physiological activities in the motor unit during contraction
Mean absolute value (MAV)	- Provides a maximum likelihood estimate of the amplitude when a signal is modelled as a Laplacian random process - It is used for low contractions and fatigued muscles analysis
Waveform length (WL)	- Provide information on the waveform complexity in each segment - Contains the fluctuation frequency information of the signal
Zero crossing (ZC)	- A simple frequency measure can be obtained by counting the number of times the waveform crosses zero - Provides an estimation of frequency domain properties
Slop sign changes (SSC)	- Frequency measured by counting the number of times the slope of the waveform changes sign - Represent the frequency information of sEMG signals
Variance (VAR)	- Uses the power of sEMG signals as a feature
Wilson Amplitude (WAMP)	- It is related to the firing of motor unit action potentials and muscle contraction level - Used to reduce noise effects
Auto-Regressive coefficients (AR)	- Describes each sample of sEMG signal as a linear combination of previous samples plus a white noise error term

Table 2.2 is according with different studies and reviews (ZECCA et al., 2002), (OSKOEI; HU, 2007),(PHINYOMARK; LIMSAKUL; PHUKPATTARANONT, 2009), (MENG et al., 2010), (FUKUDA et al., 2010), (NAJI; FIROOZABADI; KAHRIZI, 2012), (JOSHI; LAHIRI; THAKOR, 2013), (VILLAREJO et al., 2013), (LEE et al., 2015a), (LEE et al., 2015b), (AI et al., 2017). The mathematical representation of these features are presented in Appendix A.

Results of researches have shown that sEMG features, such as zero crossings, mean power frequency, median power frequency and second order cumulants of extensor muscles are most sensitive to flexion angle variation (NAJI; FIROOZABADI; KAHRIZI, 2012).

The window length parameter is representative for the accuracy of the pattern recognition classification and for the controller delay experienced by the user (SMITH et al., 2011). Specifically, for lower limb active orthoses, the window length that enables the best performance is between 50 to 250 ms (JOSHI; LAHIRI; THAKOR, 2013).

Regarding to feature projection, principal component analysis (PCA) and LDA are the two main linear mapping functions used in different researches (OSKOEI; HU, 2007). PCA is superior to other methods of features dimension reduction, it avoids overloading the classifiers. LDA maximizes the ratio between-class variance to the within-class variance in any particular data set, thereby achieving maximal separability (OSKOEI; HU, 2008). An advantage of this algorithm is that it does not require iterative training, avoiding problems with over-training, such as occurs in artificial neural networks.

On the other hand, as classifiers, methods based on machine learning are the more common for pattern recognition for upper and lower limb (OSKOEI; HU, 2008), (VILLAREJO et al., 2013) and (LEE et al., 2015a). SVM is a classifier that considers the input data as an n-dimensional feature space, then an $(n-1)$ dimensional hyperplane separates the space into two parts. The high generalization and classification linearly-inseparable of patterns with small computational complexity are characteristics of the SVM, which can be useful to classify sEMG signal patterns whose features tend to change with time and can allow a real-time motion classification (OSKOEI; HU, 2008). For SVM, three different kernels can be considered: linear, Gaussian (also known as RBF) and polynomial (VILLAREJO et al., 2013).

Joshi et al. (JOSHI; LAHIRI; THAKOR, 2013) proposed a control system for a foot-knee exoskeleton based on the processing of eight sEMG outputs, four for each leg. Four time domain features were computed and the application of a combination of Bayesian information criteria (BIC) and LDA allowed identifying eight gait phases. The results obtained an accuracy around 80%.

Regarding the classification theory applied to trunk muscles only (as these muscles also are activated after motion intention), Naji et al. (NAJI; FIROOZABADI; KAHRIZI, 2012) evaluated a wide range of sEMG features in these muscles to find the best feature spaces that discriminate among postural task involving different trunk flexion angles, using features evaluation index as Davies-Bouldin (DB) and Calinski-Harabasz (CH).

2.6 Lower Limb and Trunk Muscles for Motion Intention Detection

In different researchs sEMG signals from lower limb are measured as primary actor of locomotion (SAWICKI; FERRIS, 2009), (KIGUCHI; IMADA, 2009), (MENG et al., 2010), (JIMéNEZ-FABIáN; VERLINDEN, 2012), (JOSHI; LAHIRI; THAKOR, 2013), (LEE et al., 2015a), (LEE et al., 2015b). The more common muscles used for motion intention detection based on sEMG from lower limb are *gluteus maximus, rectus femoris, vastus lateralis, biceps femoris* and *semitendinosus* (MENG et al., 2010), (JOSHI; LAHIRI; THAKOR, 2013), (LEE et al., 2015a), (LEE et al., 2015b). *Rectus femoris* appears to be the muscle that guarantees the best performance in terms of accuracy and time delay. However, the muscular condition in post-stroke individuals do not allow, in all the cases, the use of sEMG signal from lower limb (SUZUKI et al., 2007), as the characteristics of sEMG patterns during gait of hemiplegic individuals include a reduction in the magnitude of the sEMG signals obtained from the muscles in the paretic limb, premature onset and peaks of activity that differ from normal patterns (BALABAN; TOK, 2014). In addition, prolonged muscle activation of the hamstrings and quadriceps during (ST) occurs in the non-paretic limb and, at slow speeds, the stability of stance requires

increased muscle activity (JONSDOTTIR et al., 2009).

Profiles of the sEMG signals strongly depend on walking speed and, in pathological gait, post stroke individuals do not usually walk at normal speeds (HOF et al., 2002).

Researches conducted about the trunk muscles activity of hemiparetic and control subjects during therapeutic exercises, which includes trunk rotation, leg and arms elevation, reveal that the *erector spinae* (ES) muscle does not present inter-group difference (PEREIRA et al., 2011). The primary contribution of trunk muscles is to allow the body to remain upright, adjust weight shifts, and provide an appropriate equilibrium between flexibility and stiffness during walking, which has an impact on balance and functional ability of subjects (KARTHIKBABU et al., 2012), (SWINNEN et al., 2012b). Among the functions of the trunk segment during gait, it can be mentioned: (1) transfer and absorb the forces generated by the lower limbs to limit excessive vertical and lateral displacement of the head; (2) control movements against constant pull of gravity, which is considered central key point of the body; (3) maintain equilibrium and balance within the base of support; (4) contribute to the initiation and control of gait speed (WINTER, 2009), (KARTHIKBABU et al., 2012).

Trunk muscles are involved in the organization of locomotor patterns during walking and other various rhythmic motor tasks (LAMOTH et al., 2002), (ANDERS et al., 2007), (SèZE et al., 2008), (CECCATO et al., 2009), (SWINNEN et al., 2012b).

From literature, it is know that the muscle recruitment of trunk precedes the muscle recruitment of the lower limb, then the trunk begins to move earlier (KARTHIKBABU et al., 2012). In studies for sEMG analysis of the trunk muscles during walking, the back and abdominal muscles have been considered with low back muscles, showing activity of about 12% maximal voluntary contractions while walking (SWINNEN et al., 2012b), (WATANABE et al., 2006). It was revealed that ES muscle, on different spinal levels, demonstrates an important role in the organization of this task (LAMOTH et al., 2002), (ANDERS et al., 2007), (SèZE; CAZALETS, 2008), as it EMG activity decreases significantly with increasing walking velocity (LAMOTH et al., 2004).

The ES muscle is the most superficial muscle that is covered by the cervical and thoracolumbar

fascia, separating them from the intermediate and superficial planes of the back muscles (SèZE; CAZALETS, 2008). Also called *ES group*, it is the extensor muscle of the spinal column, composed of long columns of these muscles on either side of the vertebral column, which extends the back and helps to return the trunk to an upright position, termed as *iliocostalis*, *longissimus* and *spinalis*. Figure 2.4(a) presents an overview of the entire group, which has a common origin. Figure 2.4(b) shows the anatomical location of the ES muscle, which has been that have been considered for electrode placement during walking analysis (SèZE; CAZALETS, 2008).
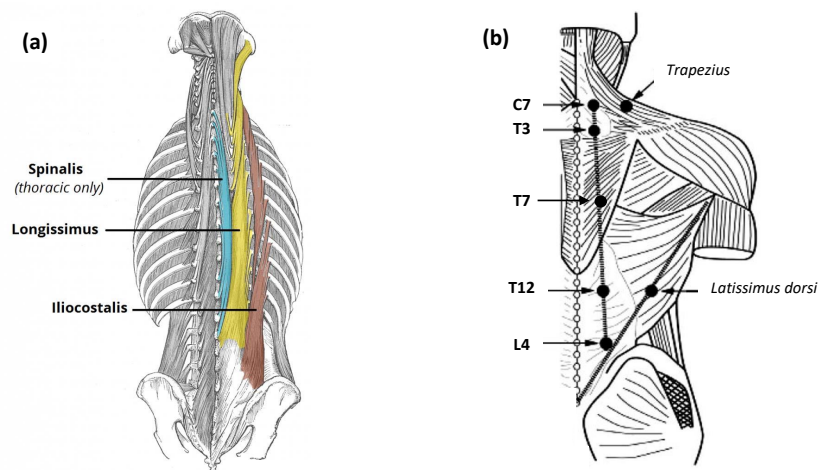
Figure 2.4: (a) Erector spinae group (SERIES, 2017); (b) Anatomic location of electrodes over ES muscle levels. (SèZE; CAZALETS, 2008)

(BENEDETTI; AGOSTINI; BONATO, 2012) evaluated muscle activation patterns during common activities of daily life, such as walking, using sEMG signals acquired from the trunk and lower limb muscles. In all subjects, the ipsilateral ES muscle was activated around the initial contact and between terminal stance and pre-swing during gait. Ceccato et al. (CECCATO et al., 2009) investigated the trunk movement during gait initiation and walking from ES muscle records, monitored bilaterally at various spine levels. They concluded that the trunk movement during gait initiation and walking shares similarities at the metachronal activation of the ES muscle and that this muscle activity occurs just before the double support phase during walking. (WENTINK et al., 2013) studied the feasibility of real-time motion intention detection of gait initiation based on lower limb muscles and ES muscle (lumbar region). The results show that toe-off and heel-strike of the leading limb can be detected using sEMG and kinematic data. The study also reports that the ES muscle may give valuable information on postural

changes and may be used for detection of heel strike. The levels of the ES muscle that have been reported in studies for walking analysis are C7, T1, T3, T7, T9, T12, L1, L2, L3, L4, L5 and L6. In (WHITE; MCNAIR, 2002) the analysis of patterns of muscle activation during gait in lumbar muscles using cluster analysis was developed. Here, in the ES muscle (L4 and L5 levels) peaks of activity were observed close to foot-strike, and thereafter the sEMG activity decreased considerably. Authors considered that this activity is related to weight transference between the limbs (WHITE; MCNAIR, 2002).

Figure 2.5 shows the typical ES muscle activity during a classical gait cycle reported by the following studies: (LAMOTH et al., 2004), (BENEDETTI; AGOSTINI; BONATO, 2012), (ANDERS et al., 2007).
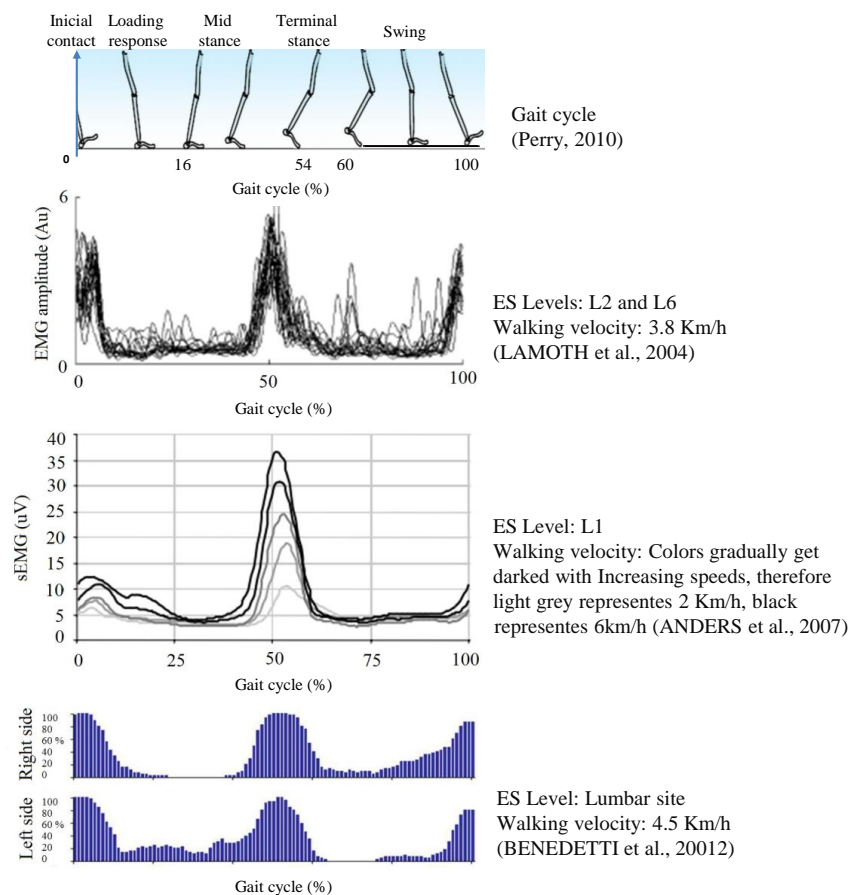
Figure 2.5: ES muscle activity during a gait cycle: healthy subjects.

Regarding gait differences between over-ground and treadmill walking, (MAZAHERI et al., 2016) have found that the patterns of sEMG activity of trunk and lower limb muscles during over-ground and treadmill walking are generally similar. However, the amplitude of sEMG

activity of trunk and lower limb muscles are greater in walking on the treadmill that overground walking (MAZAHERI et al., 2016), (NYMARK et al., 2005). On the other hand, the trunk posture in late stance phase was slightly more flexed on the treadmill than on overground (NYMARK et al., 2005). The localization of the electrode placement is difficult for the trunk muscles because of their multilayer structure and their mostly flat presence. However, researches conducted by (SèZE; CAZALETS, 2008) report that ES muscle activity can be recorded by skin electrodes in several locations of the posterior wall through a superficial muscle aponeurosis. At slower speeds, the interaction of the trunk and lower limbs may be different (NYMARK et al., 2005). For trunk electrodes displacement over the skin during sEMG signals acquisition are not reported (SWINNEN et al., 2012b).

Regarding post-stroke individuals, trunk function has been identified as an important early predictor of functional outcome after stroke. Based on sSEMG analysis, it was identified poor bilateral trunk muscles activity in individuals with stroke (KARTHIKBABU et al., 2012). However, the same study reports that trunk exercises given just after stroke could produce enhanced balance performance post-stroke.

(YAKIMOVICH; LEMAIRE; KOFMAN, 2006), In (BUURKE et al., 2005) a study to investigate changes in trunk muscle activation patterns in individuals with stroke, walking with and without aids was developed. Here, walking without an aid showed differences in timing compared to walking with a cane and with a quad stick. This same study reported that differences between walking with a cane and walking with a quad stick were small. When walking without an aid, the ES was almost continuously active throughout the gait cycle and a clear phasic activity was seen when walking with an aid. The average amplitude of the sEMG ($\simeq$ 100 μ) did not differ much between the three different walking conditions. This suggest that the information of sEMG during gait with and without assistive aid may be employed to gait intention detection or gait phase recognition due their phasic activity.

The next chapter describes the proposed controller to provide knee motion assistance using motion intention detection based on the ES muscle.

Chapter 3

Materials and Methods

3.1   Proposal

The materials used in this research include a robotic knee orthosis called ALLOR "Advanced Lower Limb Orthosis for Rehabilitation", developed at Federal University of Espirito Santo (UFES/Brazil) and a hierarchical control structure with a human motion intention recognition system (HMIR) taking place at a *high level*. For translation of the user's intent to a desired state for the robotic device, the controller includes a finite state machine at the mid level. Finally, a device specific controller responsible for executing the desired movement at the low level is employed. Figure 3.1 shows the generalized diagram of the control system proposed here.

The motion classes that are included in the controller are: 1) stand-up (SU); 2) sit-down (SD); 3) knee flexion-extension (F/E); 4) walking (W); 5) rest stand-up (RSU); 6) rest sit-down (RSD). The controller comprises the HMIR based on sEMG of trunk muscles and the HMIR system comprises two classifiers in order to recognize RSD-F/E-SU and RSU-W-SD motion class groups, respectively. Then, the user's motion intention is used to start the movement.

The *mid level* controller identifies mode transitions using a finite state machine (FSM), which determines suitable parameters for the low level controllers to execute F/E movements, assist
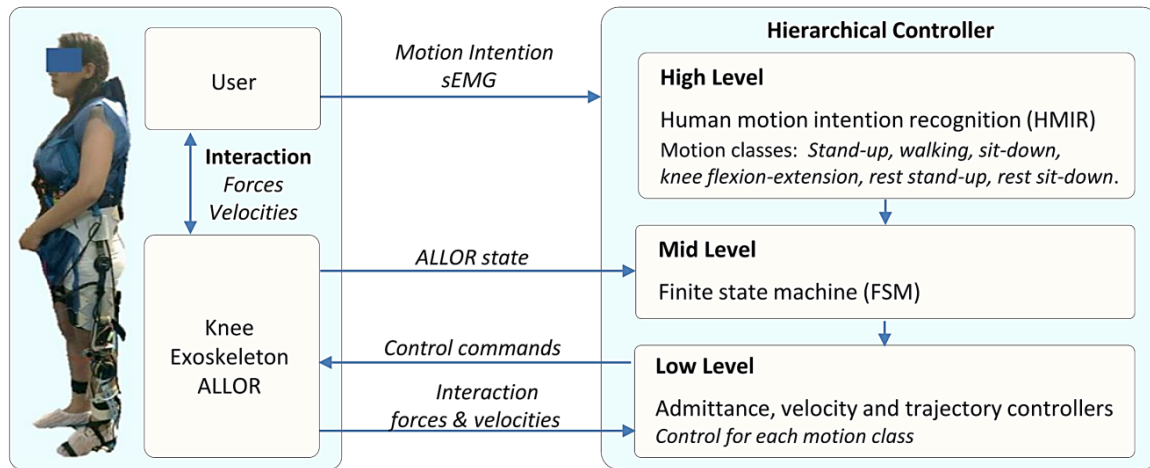
Figure 3.1: Block diagram of the proposed control

the knee joint during W, SD and SU states, and provide knee support during RSU position. Hence, this level sets the control strategy corresponding to each recognized motion class.

The *low level* controller sends commands to the actuators that move the structure of the robotic orthosis. This level includes an admittance, velocity and a proportional integral (PI) controller. Here and algorithm to generate a variable velocity path to guide the movement and a system for impedance modulation that allows a suitable assistance at the movements for each motion class are used. The following sections describe details of the components of the proposed system.

3.2 Robotic Knee Orthosis (ALLOR)

Figure 3.2 shows the robotic knee orthosis employed in this research and conceived for patients that require knee movement assistance or rehabilitation. Based on these purposes, the device was given the name of ALLOR, by the acronyms of "Advanced Lower-Limb Orthosis for Rehabilitation".

ALLOR is a two degree of freedom orthosis composed of an active knee joint and a passive hip, which moves in the sagittal plane during the walking. The hip joint has a manual flexion and extension angle regulator from 0 to 80 degrees. Although this joint is not active, its regulation,
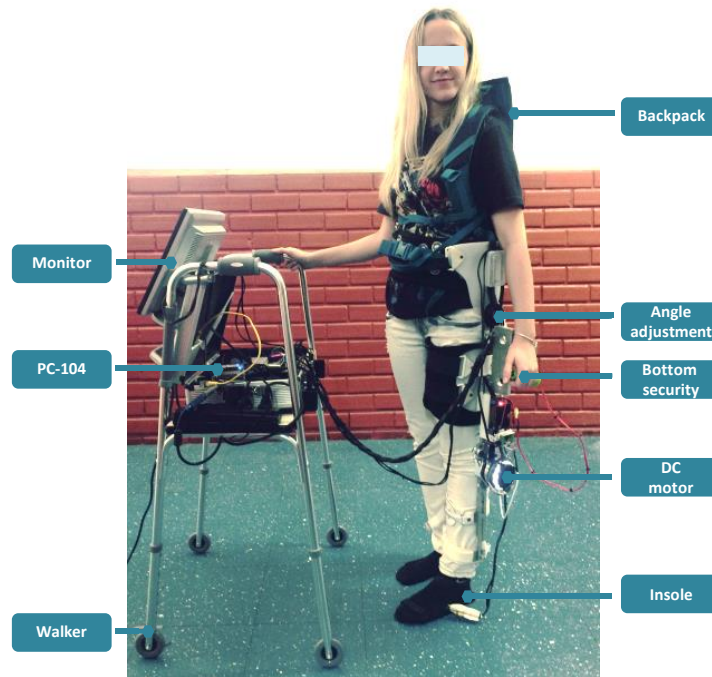
Figure 3.2: Advanced Lower Limb Orthosis for Rehabilitation (ALLOR) built for this research.

according to the user requirements, allows establishing a safe range of motion.

ALLOR is mounted on the left leg of the user with the axis of rotation of the orthosis' joint aligned with the axis of the user knee and hip joints. To ensure a correct alignment during operation, a backpack and rigid braces at the thigh and shank with velcro straps are used, such as as shown in Figure 3.2. The backpack was developed to alignment the active orthosis at the lower limb, and to sustain and redistribute the load of the orthosis structure. This setting was included after gaining experience during preliminary tests of gait with ALLOR. A single adjustment of the orthosis at user waist do not sustain the orthosis weight, due to usually after 10 minutes of test, a new alignment adjustment was needed.

The backpack consists of shoulder straps and a belt that wraps around the wearer's waist. The belt contains three arrays of four sew-on snaps (diameter: 30mm) that are adjusted at the hip joint to sustain the orthosis structure. The arrays allow adapt the adjustment at users with different waist size. In addition, the backpack was adapted for collocate the sEMG electrodes at trunk. This include a free space to access at the lumbar area of the user and a cover for the area during tests.

The weight of ALLOR is 3.4 kg, including 0.8 kg of the backpack. We considering that ALLOR has an acceptable weight for the purposes for which it is intended, compared with the prototypes shown in Figure 2.2. Most of them have adjustment in the hip, but do not have a necessary adjustment, such as the backpack of ALLOR.

ALLOR is adaptable to different anthropometric setups, which include heights of 1.5 to 1.85 m and weights from 50 to 95 kg. It provides both mechanical power to the knee joint and feedback information related to knee angle, interaction torque and gait phases. It was developed for knee rehabilitation in both sit position and during gait. In this last case, it is possible to use ALLOR without support devices, however clinical condition takes into account the need of using the orthosis plus the walker, or at least, canes, parallel bars or crutches. Due to the previous experience in our laboratory with gait assisted by walkers, this option was chosen. For gait assistance, the users must have good physical function of hip, due to the hip joint is a passive orthosis. In cases of loss of voluntary control of hip movements due to muscle weakness, it would be necessary to adjust the flexion and extension angles according to the user condition. For more critical cases, it would be necessary FES to assist this joint (HIROKAWA et al., 1990). On the other hand, cases of gait disorders due to weakness of the ankle dorsiflexors muscles, such as dropfoot, an ankle foot orthosis may be mounted to maintain foot clearance.

The components of the active knee joint are a brushless flat motor (model 408057), a Harmonic Drive gearbox (model CSD-20-160-2A-GR) and an analog pulse-width modulation (PWM) servo drive (model AZBH12A8). Additionally, ALLOR is equipped with a strain gauge arrangement (RS Pro Wire Lead Strain Gauge 3.5mm) in a Wheatstone bridge configuration, which measures the torque produced by its interaction with the user. A precision potentiometer (model 157S103MX from Vishay Spectrol) is used as an angular position sensor to measure knee angles. ALLOR also uses Hall Effect sensors inside the motor to compute angular speeds of the actuator. The computer used to implement the control software is a PC/104, which is a standard for embedded computers, in which the architecture is built by adding interconnected modules through an ISA (Industry Standard Architecture) data bus. The modules are a motherboard, power source, ethernet communication and an analog to digital (A/D) acquisition card, model Diamond-MM-32DX-AT (32 inputs of 16 bits, 4 outputs of 12 bits, with maximum
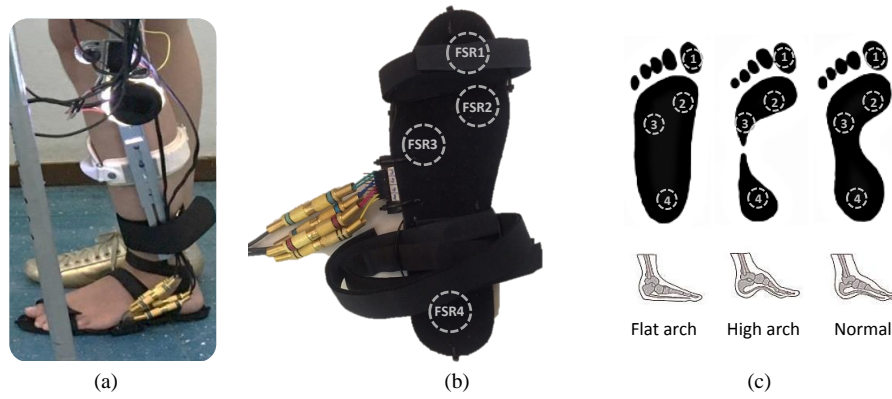
Figure 3.3: (a) Instrumented insole implemented at the active knee orthosis. (b) FSR locations. (c) FSR locations at flat arch, high arch and normal foot.

sampling frequency of 250 kHz). All sensors, acquisition and velocity driver are connected through the A/D card. The whole system requires 24V/12A DC power supply and uses a controller area network (CAN) bus running at 1 Mbps. The control software was developed in Simulink/Matlab and uses real-time target library. Safety conditions are incorporated at the ALLOR control system along with mechanical stops, which ensure that the actuator operates within the normal range of motion of the knee, allowing safe use.

ALLOR includes an instrumented insole built with four force sensing resistor (FSR) shown in Figure 3.3(a), in which four FSR are placed on the plantar surface of the foot. Figure 3.3(b) shows the sensor locations, which are defined in function of the peaks of the plantar pressure data reported in (WAFAI ALADIN ZAYEGH; BEGG, 2015) and (CALLAGHAN et al., 2011), corresponding to hallux bone (FSR1), 1st metatarsal (FSR2), 5th metatarsal (FSR3) and calcaneus (FSR4). These locations allow acquiring more relevant ground reaction forces generated during gait to recognize stance sub-phases, which are suitable to use in foot with normal arch, high arch and flat foot 3.3(c).

The FSR sensors are FlexiForce A401, with a sensing area of 25.4 mm and standard force range of 111 N. An electronic circuit was implemented to obtain output voltages proportional to the plantar pressure. To validate the insole data, a pressure sensitive gait mat (GAITRite Platinum, CIR Systems Inc., 9 m long) was employed. The signals of the insole were acquired with a DAQ USB-6009 (sampling frequency of 120 Hz) using the DAQExpress™ driver of National Instruments and Matlab software. The mat data were acquired at 1 kHz using the

PKMAS (ProtoKinetics Movement Analysis) software (LYNALL et al., 2017). The acquisition data were synchronized throughout an external pulse. Two subjects (men: 35 years; 1.72 m; 70 kg and women: 78 years, 1.75 m, 80 Kg) walked at a comfortable velocity on the mat using the insole with each subject completing 6 trials (each trial with 6 steps) and 36 gait cycles. A concordance correlation analysis was performed to estimate the reliability of the insole pressure signals in relation to the foot pressure measured by the mat.

3.3 High Level Controller

This level corresponds to the human motion intention recognition (HMIR) stage, which is proposed to convey control commands for ALLOR. HMIR is based on sEMG signals (from the trunk or lower limb muscles), in order to recognize the following motion classes: 1) Stand-Up (SU); 2) Sit-Down (SD); 3) Knee Flexion-Extension (F/E); 4) Walking (W); 5) Rest in Stand-Up position (RSU); 6) Rest in Sit-Down position (RSD). This way, two classification stages C1 and C2, shown in Figure 3.4, were used to recognize both class group: 1) Siting movements, which includes the sequence SU-F/E-RSD; 2) Standing movements, which includes the sequence RSU-W-SD. The classes SD and SU are taken into account to select the correspondent classification stage C1 and C2, respectively, hence, these are the states of transition between both classifiers outputs. Once detected the SD class, the three classes corresponding to the group 1 are recognized, while another group is recognized after detecting the SU class.

3.3.1 sEMG Signal Processing

The method for C1 and C2 is based on a feature extraction and pattern recognition. The raw sEMG are pre-processed to remove DC component. Feature vectors are extracted from sEMG, using window length of 80 ms, overlapped each 40 ms. This windowing function was agrees with the criteria reported in (JOSHI; LAHIRI; THAKOR, 2013) related to a good relation between controller delay and classification error during real-time control. In this stage, the following features are used: slope sign changes (SSC) with Thld = 0.001, zero crossing (ZC)
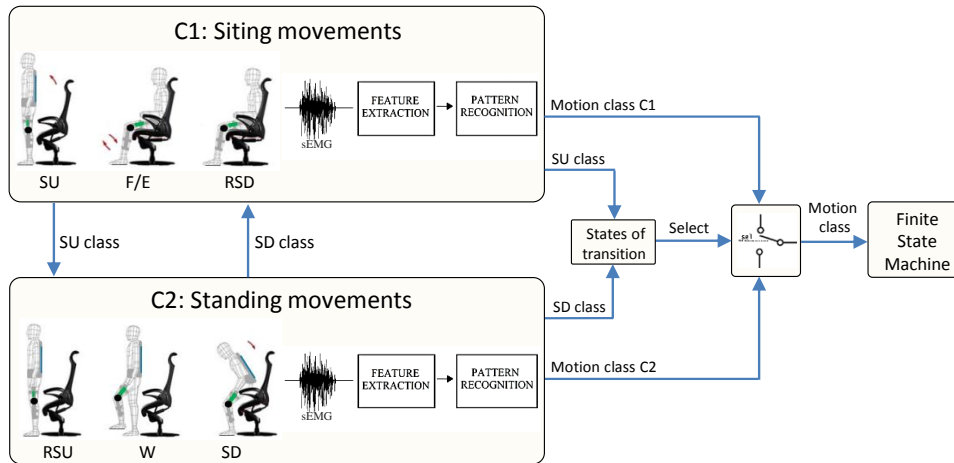
Figure 3.4: Configuration of classifiers for motion intention recognition.

with Thld = 0.0005, waveform length (WL), mean absolute value (MAV), variance (VAR) at time domain; and autoregressive (AR) coefficients of order 4 at frequency domain. These are common features used in literature for applications aimed controlling robotic assistive devices with sEMG signals (LEE et al., 2015b), (MAYOR et al., 2017). Each feature is normalized individually based on average and standard deviation values.

In this research, Linear Discriminant Analysis (LDA) and muti-class Support Vector Machine (SVM) are selected as classifiers, due to their high performance in classification problems and low computational cost (LEE et al., 2015b). The SVM configuration were used: one-against-one approach with polynomial kernel SVM-P of third order, and SVM with Gaussian kernel SVM-G (with C = 1 and $\gamma = 10$) (OSKOEI; HU, 2007). During the supervised learning, the classifier is trained through the first six trials from the sequential experiment, and four trials from the random experiment.

3.3.2   Experimental Protocol

Ten healthy subjects (males, 29.0 ± 4.0 years old, height 1.82 ± 0.07 m, weight 84.5 ± 15.3 kg) participated in the experimental protocol. Only subjects without lower limb injury or locomotion disorders were considered in this study. All volunteers were informed about the background of this study, which was approved by the Ethics Committee of UFES (214/10). All of them provided written informed consent prior to data collection.

A BrainNet BNT 36 acquisition equipment, with bandpass filter from 10 to 100 Hz, notch filter of 60 Hz, and sampling rate of 400 Hz was used to measure the myoelectric activity from trunk and leg muscles. sEMG data were acquired using pairs of bipolar sEMG electrodes (Ag/AgCl discs, 1 cm diameter, 20 mm inter-electrode distance).

The signals were measured from *rectus femoris* (RF), *vastus medialis* (VM), *biceps femoris* (BF), *semitendinosus* (SE), *gastrocnemius* (GC) and *erector spinae* (ES) at levels C7, T3, T7, T12 and L4, which are based on the study of trunk muscles during walking in healthy subjects (CECCATO et al., 2009). The anatomical electrode location for each level was identified according to the literature (SèZE; CAZALETS, 2008), as shown in Figure 2.4. These sEMG signals were measured on the right human body side. The placement of the electrodes and the motion classes during the protocol are shown in Figure 3.5. The locations for sEMG
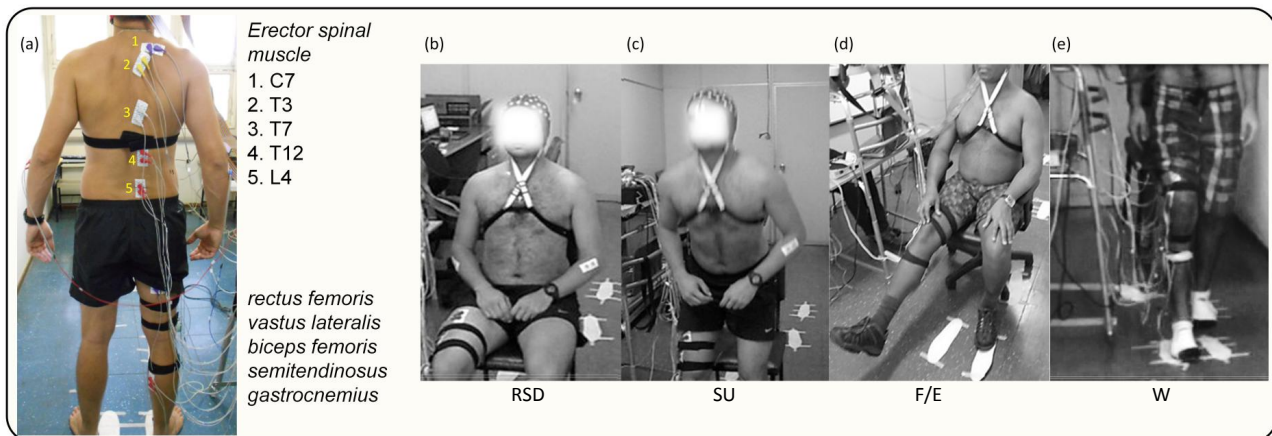
Figure 3.5: Electrodes placement and the execution of the motion classes during tests. (a) electrodes position at trunk and lower-limb. The electrodes on the trunk are marked at the picture with numbers. (b)-(e) are the motion classes during tests: Rest in Sit-Down position (RSD), Stand-Up (SU), knee Flexion-Extension (F/E), and Walking (W).

lower limb electrodes were guided by palpation based on dominant bone areas and prominences (KONRAD, 2005) and the reference electrode was fixed near of the right ankle. In the area of electrode placement, the skin was cleaned with alcohol. Ten muscles of the right side were measured, due to a limited number of available EMG channels at the equipment. A goniometer sensor and a footswitch insole were located on the right leg to measure the knee angle and foot contact signal, respectively.

The subjects were cued through visual and sound stimuli with a period of 10 s to execute the

following motor tasks: Stand-Up/Sit-Down (SU/SD), knee Flexion/Extension (F/E), one gait cycle in walking (W), and Rest Stand-Up/Sit-Down positions (RSU/RSD). The motor tasks performed were repeated into two different experiments. Initially, a defined sequence composed of ten trials for each motor tasks was performed. Afterward, a random order, including six repeated trials for each motor task, was proposed to enhance generalization ability due to the fluctuation of sEMG. Each experiment had three tests of 20 trials (60 trials total), with rest of 3 min. The acquisition hardware was attached to a mobile platform in order to follow the subjects during the test.

3.3.3   Evaluation

The database of sEMG acquired through the aforementioned protocol was employed to evaluate two stages: 1) gait sub-phases recognition; 2) motion intention recognition, in order to compare these two conditions for motion intention recognition of both muscular groups at lower-limb and trunk.

Gait Sub-phases Recognition: each gait cycle was segmented through the footswitch and angle signals by a trained specialist, in order to label the gait phases. For each segment only the steps with a good footswitch pattern were considered for the comparison (24 total steps for all the subjects, except one subject with 19 steps). The gait cycle was divided in two gait categories: (a) a the category termed 2ph (two phases: ST and SW); (b) a category 4ph (IC, MS, TS and SW phases), in order to analyze the effect of increasing classes to the classifier. After acquiring the periods of each phase, the trunk and leg sEMG signals were segmented based on these periods. Figure 3.6(b) shows the process of segmentation of signals with the purpose of gait sub-phases recognition.

Figure 3.6(a) shows the signals acquired during the aforementioned protocol.

Motion Intention Recognition: each motion class was segmented by a trained specialist through stimuli, footswitch, and angle signals. Figure 3.6(a) shows these signals considered for data segmentation.
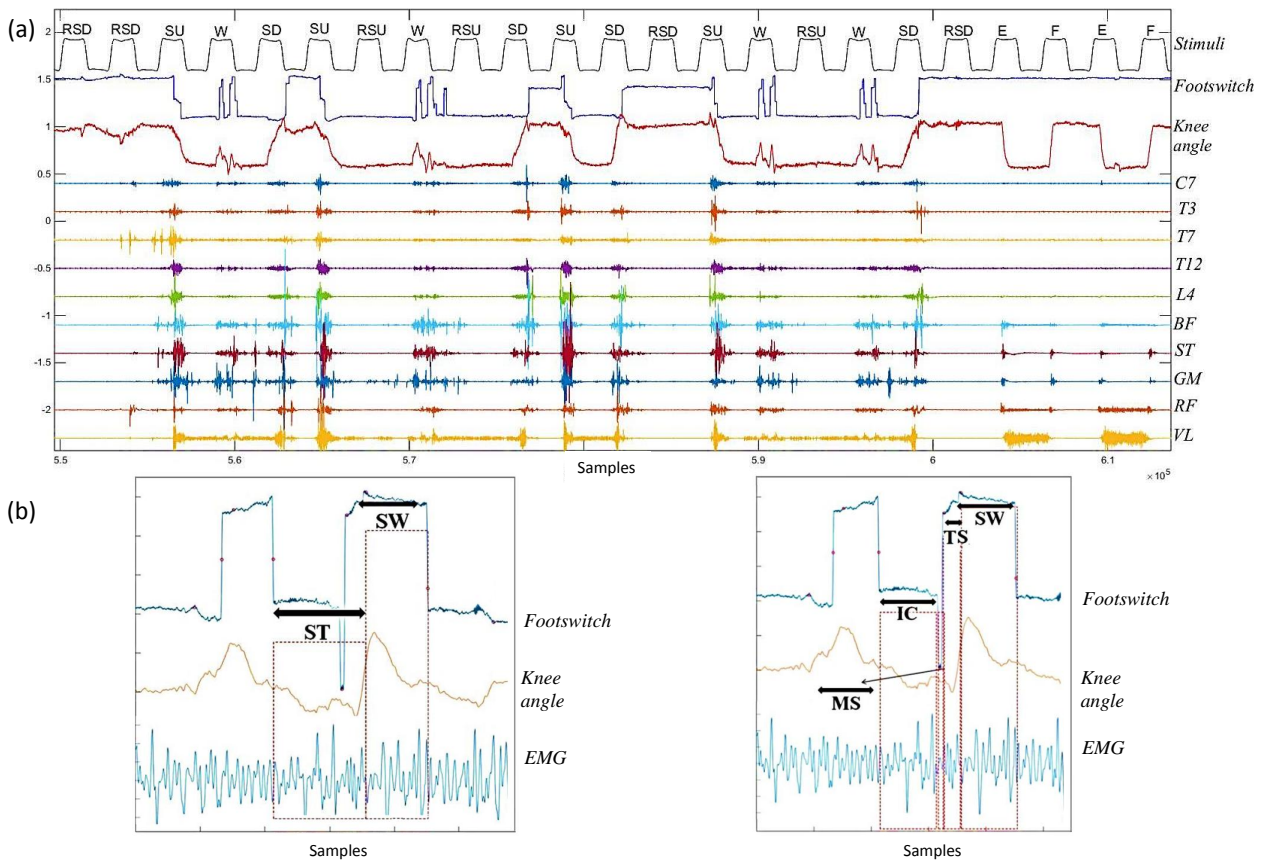
Figure 3.6: Signals acquired during the protocol. (a) Signals during the execution of motion classes indicated by the stimuli. (b) Segmentation data for gait sub-phase recognition 2Ph and 4Ph.

In both cases, after selecting the best set of features for the group of trunk and lower-limb related to their sEMG signals, each classifier was compared. For validation, the remaining four and two trials from the sequential and random experiments were considered, respectively. Analysis for each subject S1 to S10 was performed independently. To assess the effect of using muscular groups of the trunk to accurately recognize lower-limb motions, statistically significant difference between these two muscular groups were evaluated using the Wilcoxon rank sum test, as the data did not pass the normality test (one sample Kolmogorov- Smirnov). The threshold for statistical significance was adopted at $p < 0.05$. Wilcoxon rank sum test is a non-parametric statistical hypothesis method, which does not assume normality in the data, that is recommendable for a small sample size. The outcome of these tests was interpreted to establish if there was a statistically significance difference in accuracy of each muscular group related to the recognition. The features were evaluated for the subjects individually, for different number of channels (2, 3, and 5). After selecting the best set of features for

the 2Ph and 4Ph categories, the performance of each classifier was compared. In order to evaluate each classifier, accuracy (Acc) and Kappa coefficient (k) were obtained. The accuracy was determined using a five-fold cross validation, and the data were split randomly into five equal subsets. Four subsets were used for training, and the other one for testing. Finally, the average accuracy was computed from all results, following the same procedure. The Kappa coefficient was used, which is a parameter that represents the concordance between the targets and the prediction values (JAPKOWICZ; SHAH, 2011). Values between 0.61 and 0.80 indicate a substantial agreement, while values greater than 0.81 indicate an almost perfect agreement. Further, a matrix confusion was calculated to obtain the average accuracy for all classes. The sEMG data were processed off-line using the signal processing platform EMGTool (MAYOR, 2017) implemented in Matlab® 2014 showed in Figure 3.7.
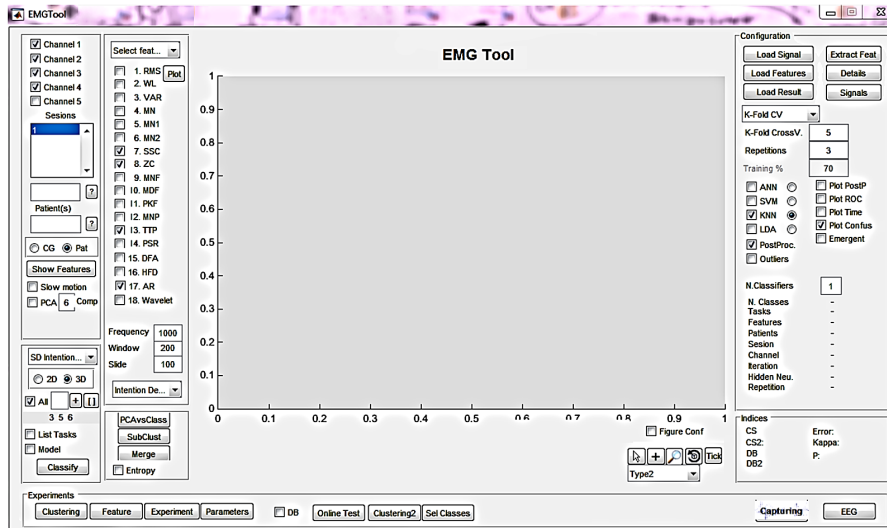
Figure 3.7: Signal processing platform EMGTool (MAYOR, 2017).

3.4   Mid Level Controller

A finite state machine (FSM) was used to establish a model for the transitions of the sequences: *siting movements* (SU-F/E-RSD) and *standing movements* (RSU-W-SD), according to the user's motion intention. Figure 3.8 shows the FSM configuration, which has two outputs: velocity $\dot{q}$ and admittance y. The objective is to activate the low level controller in order to

generate the control commands corresponding to the recognized motion class from the HMIR system.
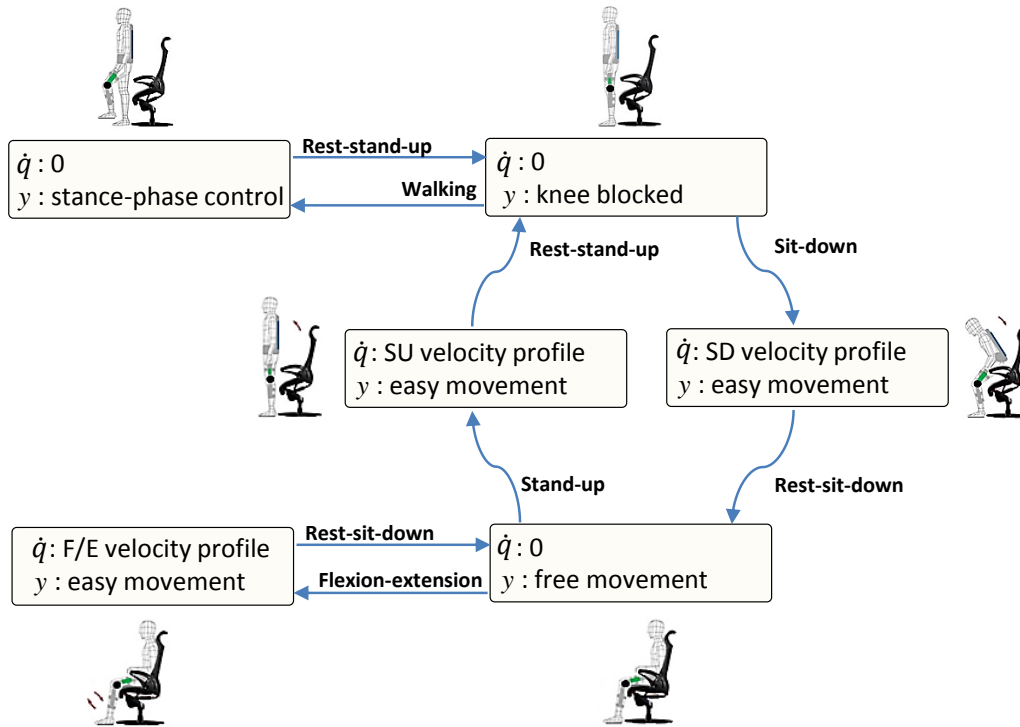
Figure 3.8: Finite state machine of the mid-level controller with two outputs velocity $\dot{q}$ and admittance y, which activate the modulation of admittance parameters and a velocity profile in the low level controllers in order to generate control commands corresponding to the recognized motion class recognized from the HMIR system.

Once the command of the HMIR is received, the FSM uploads the corresponding parameters of velocity $\dot{q}$ and admittance y to activate the low-level controllers, which include:

i) Admittance controller, which is employed to: 1) Assist the knee joint during W; 2) Provide knee support during RSU position; 3) Allow free knee movement in RSD position.

ii) Velocity controller, which is employed to execute F/E movements.

iii) Proportional integral (PI) controller, which is employed to execute movements in both SD and SU states.

Each action of control includes an output to define the end of the action, in order to resume the HMIR system. In each motion class recognized, the FSM is used as follows:

- For state W, y activates a modulation method to generate a stance control (SC) with admittance modulation over the gait cycle. Higher admittance values are desired when

the user performs gait sub-phases that has ground contact, while lower values are used during the movement of acceleration, such as the case of the leg movement during the swing phase. Here, as guided movement is not considered, $\dot{q}$ is equal to zero.

- For the states SD and SU, $\dot{q}$ activates a PI trajectory controller in order to let the joint execute the corresponding movement. As reference data, a recorded trajectory using ALLOR is considered.

- For the state RSU, y activates an admittance to block the joint, preventing movement. This way, ALLOR helps to both support the user's weight and prevent user's falls. $\dot{q}$ allows the controller guiding the movement, with a velocity path equal to zero.

- For the state RSD, y activates an admittance at the knee, in order to allow an easy knee movement, and $\dot{q}$ allows the controller guiding the movement.

- For the state F/E, $\dot{q}$ activates a path velocity to let the joint execute movements between $90°$ and $0°$. This includes a strategy to detect the user's intention, allowing stopping the movement when the user decides it.

The FSM model offers safety for the user, due to involves a logic sequence of movement, and because for the execution of the control, a suitable HMIR command is required. In this manner, the FSM guarantees that the system remains in a state and changes as long as the HMIR output follows the logical sequence of movements. For example, if the first HMIR output is SU and a second output is F/E, the FMS does not activate the F/E state, due to the knee extension movement is only executed in sit position. In such case, the FSM waits for a suitable HMIR output (W or SD after SU motion class), while the user is in a rest state. The FSM was developed in Stateflow® of Simulink/Matlab, which is an environment for modeling and simulating sequential decision logic based on state machines.

3.5   Low Level Controller

This level includes an admittance controller for the states W, RSU, RSD, a velocity controller for F/E, and a PI controller for the states SU and SD. This stage of control was implemented in a PC-104 embedded computer in Matlab/Simulink real time.

3.5.1   Admittance Controller

An admittance controller is one variation of impedance controller and its performance is determined by both the precision of force sensor and actuator position. Compared with impedance control, admittance behavior is often more easily implemented in hardware (BUERGER; HOGAN, 2004). Thus, a proper measure of the effectiveness of a system, which is meant to produce a rapid motion response to external forces, is the mechanical admittance Y (NEWMAN, 1992), defined as:

$$Y = v/F, \tag{3.1}$$

where v is the velocity of the controlled system at the point of interaction, and F is the contact force at that point. A large admittance corresponds to a rapid velocity induced by applied forces. The dynamic behavior for the interaction between the actuator and the environment (in this case the user during gait) can be expressed by the model shown in Figure 3.9.
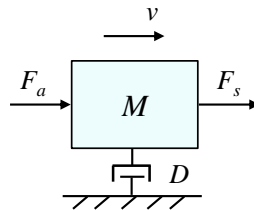
Figure 3.9: Schematic of one-mass dynamic system.

In this model, the plant parameters are assumed to have values M and D for the mass and damping, respectively, in which an actuator exerts a force F_a, and the environment a force F_s.

Then, the equation of motion for the system velocity is

$$M\dot{v} + Dv = F_a + Fs. \tag{3.2}$$

F_a and F_s can be measured with a force sensor in order to obtain an interaction force F, hence it can be considered $F_a + F_s = F$. In the Laplace domain, (3.1) can be expressed as

$$v(s) = F(Ms + D)^{-1}. \tag{3.3}$$

For the implementation, it is assumed the use of a velocity controller in the active knee orthosis. Based on (3.1) and (3.3), the desired admittance can be expressed as:

$$Y(s) = (Ms + D)^{-1} \tag{3.4}$$

The gain pattern to modulate the inertia and damping is applied to the relation of M and D, maintaining a ratio $r = 0.2$ without considering units, where r was experimentally obtained here and expressed as:

$$r = M/D, \tag{3.5}$$

with $M > 0$ and $D > 0$.

The admittance controller shown in Figure 3.10 includes an algorithm for impedance modulation to assist the knee joint during the motion classes recognized by the HMIR. As previously mentioned, the outputs y and $\dot{q}$ from FSM define the performance of the controller.
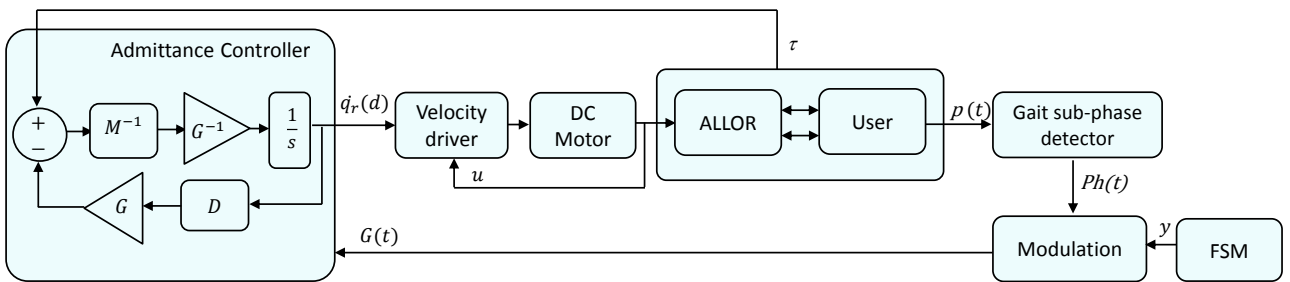
Figure 3.10: Admittance controller used in this research

3.5.2 Knee Impedance Modulation

In order to implement the control for the motion classes RSU, RSD and W with the admittance controller, a modulation through a variable gain G to increase or decrease the impedance components was proposed.

RSU: For the state RSU, a high G to increase the knee admittance and support the user weight is required. The value of G depends on the user condition and should guarantee at least 50% of the user's weight (UW) to avoid falls.

RSD:For the state RSD, a low G to decrease the knee admidtance and allow an easy movement is required.

W: For the state W, a variable G must be according to the gait sub-phases to adapt the knee joint admittance during gait. Here, the objective is to assist the knee with a stance control. According to the description of the SC principle, during gait it is necessary that the knee impedance variation allows both body support and free movement of the leg. This dynamic requires high resistance at the movement, which can be defined using a system with force feedback. In this sense, an admittance controller is stable in high stiffness conditions, therefore it is more suitable for implementation of a stance control, due to the high and stable stiffness needed to avoid knee collapse during stance phase (ESPINOSA, 2013). Thus, in order to implement the SC control strategy with the admittance controller, a modulation through a variable gain G to increase or decrease the admittance components was used, which must be according to the gait sub-phases to adapt the knee joint admittance during gait. The gait phases considered was the following: IC, MS, TS and SW as shown in Figure 3.11 (a).

This sequence offers information to develop an impedance modulation for an on-line variation of the knee joint impedance. The objective is to block the knee joint only in the stance phase to resist the knee flexion and allow both free knee extension and free knee motion in the swing phase (IR; AZUAN, 2015), (YAN et al., 2015), in order to achieve, during gait, the knee angle, moment and velocity, as shown in Figure 3.11 (d), (e) and (f).

For that, a different value of G for each sub-phase must be defined and vary smoothly. Figure
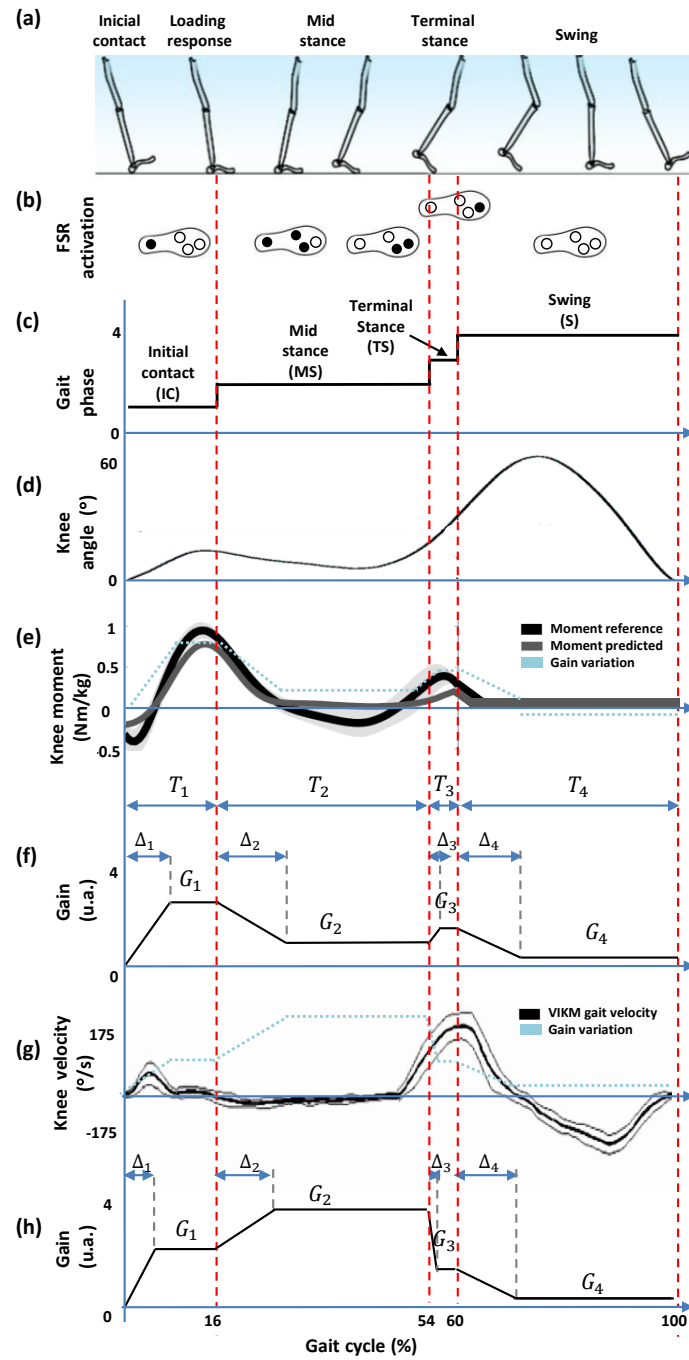
Figure 3.11: Events related to gait phases. (a) sub-phases of the gait cycle: initial contact (IC), mid-stance (MS), terminal stance (TS) and swing phase (SW); (b) on-off sequence of force sensing resistors (FSR) throughout the gait cycle; (c) footswitch signal generated by the instrumented insole to identify gait phases; (d) knee angle throughout the gait cycle; (e) knee moment during gait, correspondent to the reference and predicted values of (SARTORI et al., 2015); the gain variation was considered to define the gait pattern for knee impedance modulation during gait; (f) gain pattern P_1 based on the knee moment to decrease/increase gain values during gait phases for stance control; (g) knee velocity during gait using the variable impedance knee mechanism (VIKM) (BULEA; KOBETIC; TRIOLO, 2011); (h) gain pattern P_2 based on the the knee velocity to decrease/increase gain values during gait phases for a stance control.

3.11 (f) and (h) show two examples of variation of G in a gait cycle. In both cases, the value for each sub-phase is G_1 for IC, G_2 for MS, G_3 for TS, and G_4 for SW, which requires suitable times to increase/decrease G during the gait cycle, defined as: Δ_{t1}, Δ_{t2}, Δ_{t3} and Δ_{t4}. Considering that the weight and the gait velocity are the two major parameters that affect the mechanical parameters of the knee (SHAMAEI; DOLLAR, 2011), the stiffness, angle of engagement, and amount of rotation of an assistive device for the knee should be based on the gait speed and the pilot/robot weight. For this reason, both weight and the gait velocity are considered here to define the corresponding G and Δ_t for knee impedance modulation.

The first example of variation of G, termed *pattern* 1 (P_1), shown in Figure 3.11 (f), corresponds to a pattern based on the knee moment variation shown in Figure 3.11 (e), which is the knee moment reported in a study of a model of a neuromuscular mechanism to regulate knee joint impedance during human locomotion (SARTORI et al., 2015). Here, P_1 is adapted at the knee moment tendency throughout the gait sub-phases, in which G_1 has the highest values in the IC phase when the knee generates the first flexion. In sub-phase MS, G_2 decreases with a little increment in TS.

The second example of variation of G shown in Figure 3.11 (h), termed *pattern* 2 (P_2), is a pattern obtained from a tendency marked in Figure 3.11 (g), which shows the knee velocity during walking using the variable impedance knee mechanism of a SC orthosis (BULEA; KOBETIC; TRIOLO, 2011). In this case, the highest value of G_2 is generated in the sub-phase MS, when the knee maintains the angle but the knee torque decreases. In both cases, an impedance modulation using P_1 and P_2 can generate a knee impedance that allows a shock damping during the weight acceptance stage (sub-phases IC and MS) where the knee applies a large moment.

For both patterns, the increase/decrease of G can be executed in times Δ_1, Δ_2, Δ_3 and Δ_4 for IC, MS, TS and SW, respectively. Hence, values of Δ depend on the period of duration of each sub-phase of the gait cycle. Then, considering i as the phase number assigned as follows: i=1 for IC, i=2 for MS, i=3 for TS and i=4 for SW, the duration of each sub-phase can be expressed as

$$T_i = t_{GC}(Q_i/100)f_s, \tag{3.6}$$

where T_i is the duration of each sub-phase in seconds, t_{GC} is the time of the gait cycle in seconds, Q_i is the percentage of each phase with respect to the gait cycle, and f_s is the sampling frequency in samples per second. As shown in Figure 3.11 (f), a suitable Δ_i does not have to exceed the corresponding T_i. According to gait studies (ARNOS, 2007), t_{GC} can be estimated through Equation 3.7.

$$t_{GC} = SL/v_u, \tag{3.7}$$

where SL is the stride length in meters, and v_u is the user velocity in meters per second. SL can be estimated from the users height H in meters multiplied by the constant 0.826 (ARNOS, 2007). Hence, T_i can be expressed as

$$T_i = 0.826(HQ_if_s)/100v_u. \tag{3.8}$$

Experimental tests to validate Q_i with the instrumented insole were conducted, obtaining the following percentages for each phase (mean and standard deviation): 16 (4)%, 38 (6)%, 6 (0.8)% and 40 (4)% for IC, MS, TS and SW phases, respectively, as shown in Figure 3.12 (a).
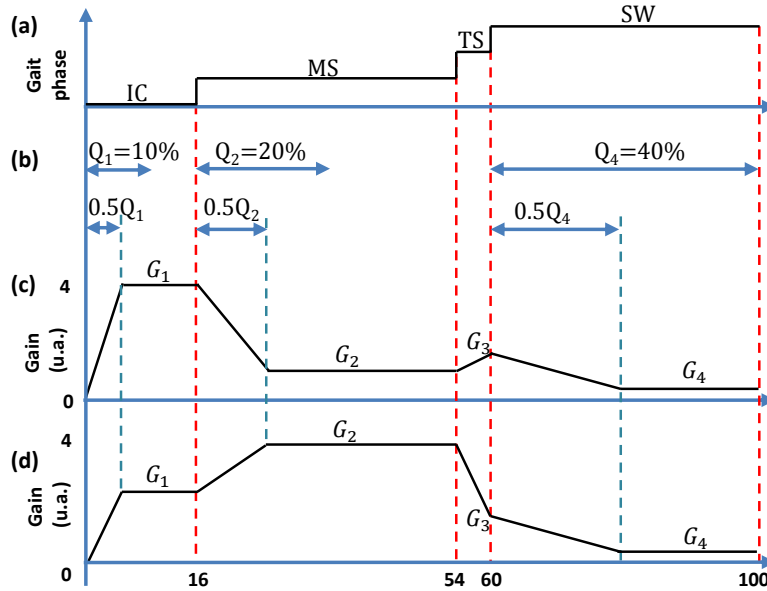
Figure 3.12: (a) gait phase recognition based on information of the instrumented insole. (b) percentage of each phase respect to the gait cycle taken into account in this approach. (c) gain pattern P_1 based on the knee moment; (d) gain pattern P_2 based on the the knee velocity .

Based on the knee moment and velocity shown in Figure 3.11 (e) and (g), IC and MS are the more critical phases, which occur when a knee support is required. In this case, Δ_t should

allow a time of stabilization in order to sustain the knee with a G constant for each phase. Therefore, for this method, values of Q_i were defined as: $Q_1=10\%$ and $Q_2=20\%$ for IC and MS respectively as shown in Figure 3.12 (b). This consideration allows having a minimum period of time to increase or decrease the corresponding G, which applies for the gain patterns P_1 and P_2 (knee moment and velocity) as shown in Figure 3.12 (c) and (d). In relation to the sub-phase *TS*, the experimental tests result in 6 (0.8)% of the gait cycle as shown in Figure 3.12 (a). It has short duration respect to other phases, and does not allow a suitable time for stabilization of G for both patterns. For that reason, in order to simplify the method, 30% was chosen as a suitable percentage for Q_3. For SW phase, the percentage $Q_4=40\%$ was chosen, which allows a period of time for decrease G.

Considering that Δ_i represents 50% of its corresponding T_i, to obtain a smooth switching between the levels of G, Equation 3.9 is used.

$$\Delta_i = (0.0413i/v_u)Hf_s. \tag{3.9}$$

Figure 3.13 shows the flowchart of the algorithm implemented in Simulink/Matlab for online gain pattern generation, where *Phd* is the default phase from which the pattern G begins to be generated; *Phs* is the current phase recognized through the insole, and δG is the gain increment for each phase.
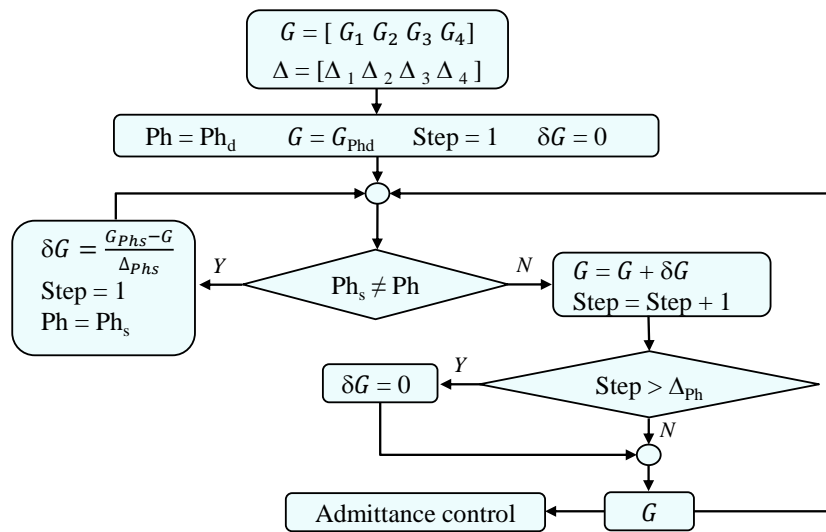
Figure 3.13: Flowchart of the algorithm used to generate the pattern G, where *Phs* is the output of the gait phase detector, and *Phd* is the default phase (recommended sub-phase MS).

Using the gain patterns P_1 and P_2, the modulation of M and D in each gait sub-phase during the gait cycle can be expressed as

$$M_i = M_d G_i, \tag{3.10}$$

$$D_i = D_d G_i, \tag{3.11}$$

where M_d and D_d are the inertia and damping default values, respectively, according to (3.5). For gait sub-phases detection, an algorithm based on the plantar pressure of the instrumented insole (Figure 3.3) during gait was programed in Matlab Simulink. The signals were acquired through a Diamond-MM-32DX-AT Analog I/O Module of a PC-104 computer, sampled at a frequency of 1 kHz, and conditioned through a low-pass filter Butterworth of 5th-order, with cutoff frequency of 10 Hz. After, the signals were compared to a threshold of 0.5 V in order to obtain contact information (on-off) from the footswitch. In order to recognize the gait sub-phases IC, MS, TS and SW, the combinations shown in Figure 3.11 (b) were considered. Then, a truth table implemented in Simulink/Matlab, which includes these combinations, was used to obtain a logic scheme to generate the footswitch signal shown in Figure 3.11 (c).

3.5.3   Velocity Controller

Figure 3.14 shows the diagram of motion class F/E controller. Here an algorithm is activated to generate a velocity path to execute the movements.

The algorithm requires the inputs *qmin* (limit of extension), *qmax* (limit of flexion), *downtime* (time in which the leg stays in extension) and *uptime* (time in which the leg stays in flexion). The periods of time (t) are in seconds. The algorithm was adapted from the research carried out by (BOTELHO, 2017). Additionally, at the motion class F/E, a strategy to detect the user's intention of stopping was included, employing the following hyperbolic function defined by the following Equation (3.12).

$$A = 1 \pm \tanh(k\tau), \tag{3.12}$$

where k is a constant that represents the level of force that the user requires to stop or accelerate
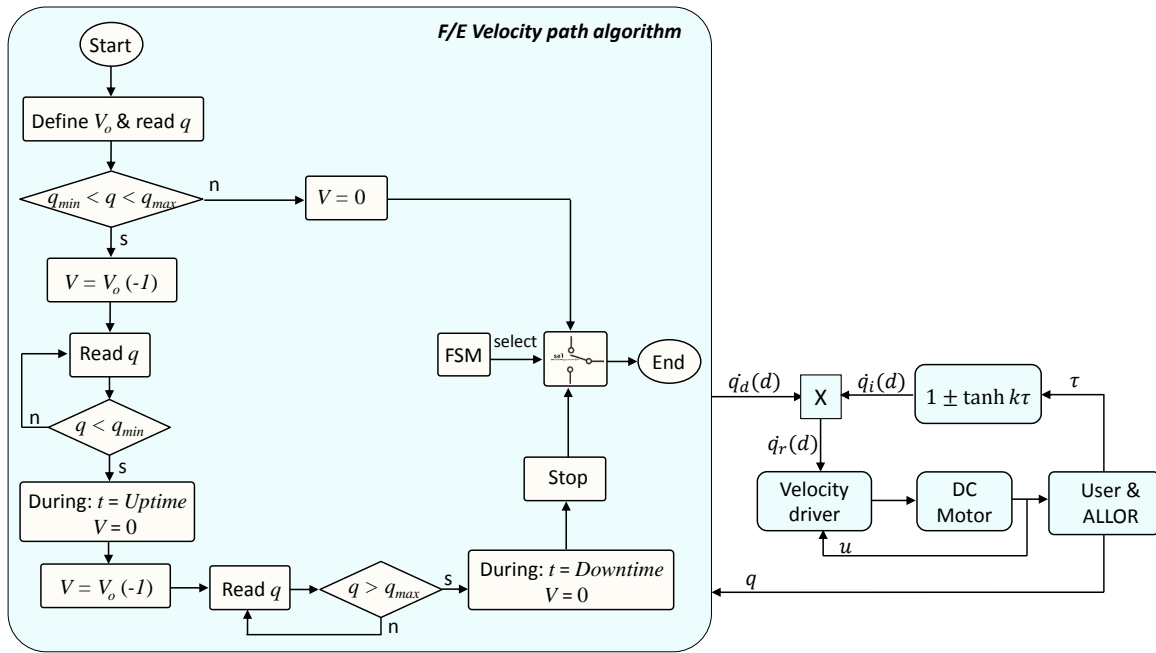
Figure 3.14: Diagram of motion class F/E control. The knee angle (q) is required to generate a velocity path, and a hyperbolic tangent function is applied in order to allow stopping and resuming the movement according to the user's intention.

the movement, and τ is the interaction torque between the user and ALLOR. The hyperbolic tangent function with offset $= 1$ produces a gain in absence of motion intention and does not change the programmed velocity path. This function allows increasing the gain in order to accelerate or decelerate the movement. On the other hand, if the user has an intention of stopping, the gain approaches to zero, stopping the movement.

The value of k is determined empirically and individually, as the torque generated by each subjects is different. Once determined, it is kept constant tests for specific subject.

3.5.4 PI Controller

Figure 3.15(a) shows the diagram of the PI controller for the motion classes SU and SD. For recording the trajectories, the controller in Figure 3.15(b) is used. The admittance parameters allow a smooth movement to record trajectories of movements of the knee joint and provide predefined trajectories for the exoskeleton.
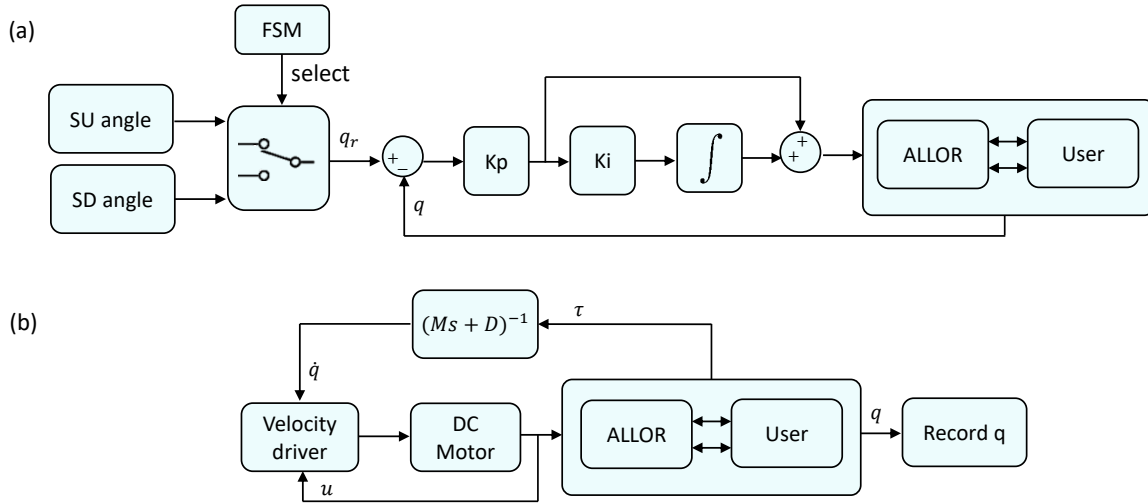
Figure 3.15: (a) PI controller for SU and SD motion classes; (b) admittance controller to record trajectories of movements of the knee joint.

3.6   Experimental Validation

A experimental protocol for each stage of the controller was developed, which is described below.

3.6.1   Stance Control Evaluation

In order to evaluate the proposed method, the following protocols were conducted with AL-LOR and healthy and post-stroke patients. Written informed consent was obtained from each subject before participation. The Ethics Committee of the Federal University of Espirito Santo approved this protocol, with number: 64801316.5.0000.5542.

Health Subjects

Three healthy subjects, female (26±5.13 years; height 1.62±0.03 m; weight 56±8.75 kg) without lower-limb injury or locomotion deficits participated of the tests. At the beginning of the test, the subjects were asked to perform a trial with the walker and without ALLOR, walking a distance of 10 m at comfortable speed for each one. Then, the gait velocity was calculated to obtain the reference value v needed to adjust G

ALLOR was mounted on the subject to perform three level-ground walking trials in a distance

of 10 m with the following patterns for G: (1) knee moment based-pattern shown in Figure 3.12 (a), termed P_1, with $G_1 = 0.7UW$, $G_2 = 0.2UW$, $G_3 = 0.3UW$ and $G_4 = 0.1UW$; (2) knee velocity based-pattern shown in Figure 3.12 (b), termed P_2, with $G_1 = 0.4UW$, $G_2 = 0.7W$, $G_3 = 0.2UW$ and $G_4 = 0.1UW$; (3) pattern termed P_3 to perform a gait without knee modulation, maintaining G_4 corresponding to SW phase in all the gait cycle, hence $G_1 = G_2 = G_3 = G_4 = 0.1UW$, where UW is the user's weight.

For the three patterns of G, the impedance parameters M and D were set as 0.5 Kg and 2.5 N/(m/s) respectively, which were obtained experimentally from gait tests with ALLOR. The trials were carried out at slow speed, determined by the subject, and were performed with the acquisition hardware attached to a four wheel walker, as shown in Figure 3.2, in order to have a mobile platform during the tests. Three trials with each pattern G were performed. The patterns (P1, P2 and P3) were randomly applied to the controller in order to not influence the perception of the user regarding the effects introduced by each modulation pattern. During these experiments, the subjects were asked to accomplish their normal gait patterns, considering the imposed system (ALLOR and walker) and a slow speed. The use of a walker in this study for healthy subjects was with the goal of emulating the same conditions of patients or subjects with disabilities, which will need the walker to improve their stability and ambulatory ability themselves, in order to feel safety during gait.

A sequence of a healthy subject performing this protocol is illustrated in Figure 3.17.

Post-stroke Patients

Three post-stroke patients (1 female and 2 males, 54.67±3.06 years) from a rehabilitation institution of Espirito Santo state (Brazil), volunteered for the experiments. Eligibility criteria for inclusion in this study were:

- Hemiparetic gait of left side

- Cognitive skills and language to follow the experiment instructions

- Volunteers without some type of cardiorespiratory disease that interfered with the protocol

- Volunteers without additional neurological or orthopedic disease that hinders ambulation
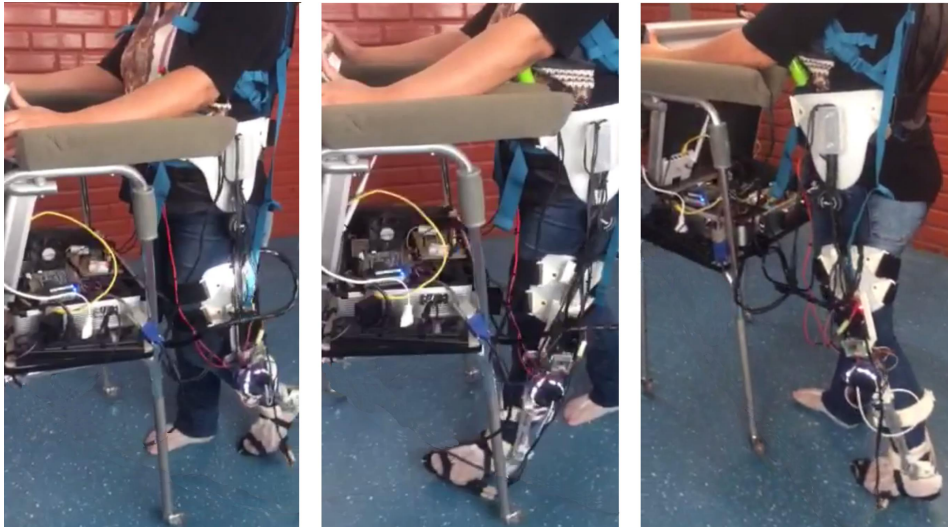
Figure 3.16: Sequence of an experiment conducted at 0.2 m/s by a subject wearing ALLOR, with the SC controller using the knee impedance modulation based on the knee moment during gait.

- Volunteers without alteration of the balance based on the Berg Balance Scale (BBS) (MAEDA; KATO; SHIMADA, 2009)

- Volunteers without detectable cognitive alterations based on the Mini Mental State Examination (MMSE) (LOURENÇO; VERAS, 2006)

- Height range between 1.5 to 1.85 m and maximum weight of 95 kg (ALLOR adjustment limitations)

ALLOR was mounted on the subject to perform three level-ground walking trials in a distance of 10 m with the following patterns for G: (1) knee velocity based-pattern shown in Figure 3.12 (b), termed P_2, with $G_1 = 0.4UW$, $G_2 = 0.7W$, $G_3 = 0.2UW$ and $G_4 = 0.1UW$; (2) pattern termed P_3 to perform a gait without knee modulation, maintaining G_4 corresponding to SW phase in all the gait cycle, hence $G_1 = G_2 = G_3 = G_4 = 0.1UW$.

For the three patterns of G, the impedance parameters M and D were set as 0.5 Kg and 2.5 N/(m/s) respectively. The trials were carried out at speed determined by the subject, and were performed with the acquisition hardware attached to a four wheel walker. Two trials with each pattern G were performed. The condition of the study with the post-stroke patients is illustrated in Figure 3.17.

Figure 3.17: Post-stroke patients wearing ALLOR during the experiments. A walker as a balance assistive device was used.

3.6.2 Mid and Low-level Control Evaluation

Two healthy female subjects (25 years; height 1.60 m; weight 72 kg and 22 years; height 1.69 m; weight 70 kg) without lower limb injury or locomotion deficits were selected to participate. At the beginning of the experiments, the subjects were given 5 to 10 min to familiarize with the exoskeleton. The recording of the trajectories SU and SD was performed at the beginning of the experiment executing the motion class SU/SD with the controller of Figure 3.15(b).

The velocity profile F/E was generated by the algorithm previously shown in Figure 3.14, with $qmin$=20°, $qmax$=75°, $downtime$=0.5 s, $uptime$=0.5 s. To assist the gait, the gain G for initial contact, mid-stance, terminal stance and swing gait phases were: G1= 0.4 UW, G2 = 0.7 UW, G3 = 0.2 UW and G4= 0.1 UW, respectively, where UW is the user' weight in Kg.

A sequence of the motion classes was conducted to demonstrate the ability of the controller to perform the movements. Three trials were performed with the acquisition hardware attached to a four wheel walker, in order to have a mobile platform during the test. To assess the effect of using ALLOR during gait, data from the subjects, related to knee angle, torque, admittance modulation, gait cycle duration, stance phase percent and maximum knee flexion in swing phase were analized.

3.6.3   Statistical and User's Satisfaction Analysis

For statistical analysis, data from the subjects that participated in the test of the SC evaluation, related to speed of walking, cadence, stance phase percent and maximum knee flexion in swing phase were used. Friedman test (non-parametric statistical test) was used to compare the three gain modulation patterns. The level of significance was set at $p < 0.05$. Finally, a survey to measure post-stroke patients satisfaction with the use of assistive technology, the adapted Quebec User Evaluation of Satisfaction with Assistive Technology (QUEST 2.0), was used (CARVALHO et al., 2014). QUEST 2.0 may be used to evaluate the user satisfaction through 12 questions separated in two items: assistive technology and services.

In this study only the issues related to assistive technology (dimensions, weight, adjustments, safety, durability, simplicity of use, comfort, and effectivenes) were evaluated, since it is a non-commercial product in phase of controlled tests. The score for each question ranges from 1 to 5 (1 "not satisfied at all"; 2 "not very satisfied"; 3 "more or less satisfied"; 4 "quite satisfied"; and 5 "very satisfied"), and, finally, an average score is taken for the number of valid questions answered. The subjects were asked to select the three most important items.

Chapter 4

Results and Discussion

Initially, in this chapter, the HMIR results are presented. The comparison between sEMG signals from trunk and lower-limb as information to recognize gait sub-phases and motion intention was conducted. Following, a comparison of the results obtained with different number of channels for the trunk sEMG signals was realized, in order to define the most appropriate arrangement for motion intention recognition. In the subsequent section, the mid-level and low-level controller are evaluated. First the results of the stance control during gait, and then the results of a test considering all the motion classes executed with ALLOR are presented.

4.1 Human Motion Intention Recognition (HMIR)

4.1.1 Gait Phase Detector Evaluation

The features SSC, ZC, WL, MAV, VAR and AR were evaluated individually and in groups for all the possible combinations. For trunk (TR) and lower limb (LL) muscles, the average classification accuracy (unit: %) and Kappa's coefficient for 2ph and 4ph phase categories, with data from eight subjects, considering different five channels, are presented in Table 4.1. The performance of the classifiers and Kappa's coefficient were better for leg muscles than for trunk muscles. However, the accuracy for both trunk muscles presents good results for ST and SW

of the 2ph gait category, and for MS of the 4ph category. Analyzing the difference between
(TR) and (LL) muscles, based on Wilcoxon rank, in the classification with LDA, the trunk
muscles did not have a significance difference in relation to lower limb muscles for ST (ρ<0.27),
but they had a significant difference with SW (ρ<0.007). On the other hand, trunk muscles
presented a significant difference with lower limb muscles for ST (ρ<0.049) and SW (ρ<0.002)
for SVM-P.

Table 4.1: Average classification accuracy (%) and Kappa's coefficient (mean and standard
deviation) of 2ph and 4ph phase categories for trunk (TR) and lower limb (LL) muscles with
data from eight subjects and considering different array of 5 channels.

Muscular Group	Phase Category	Phase	LDA Acc(%)	Kappa	SVM-P Acc(%)	Kappa
LL	2ph	ST	89.85 (05.53)	0.72 (0.13)	86.25 (06.09)	0.69 (0.09)
		SW	83.95 (08.69)		83.75 (04.58)	
	4ph	IC	38.25 (22.86)	0.66 (0.17)	44.05 (14.91)	0.63 (0.15)
		MS	80.60 (07.96)		82.40 (07.52)	
		TS	69.60 (13.08)		62.65 (13.49)	
		SW	65.20 (24.73)		52.25 (26.06)	
TR	2ph	ST	82.25 (06.21)	0.45 (0.13)	77.65 (06.62)	0.53 (0.09)
		SW	67.50 (11.99)		73.50 (04.87)	
	4ph	IC	29.30 (16.76)	0.36 (0.10)	28.75 (15.30)	0.32 (0.11)
		MS	72.05 (06.80)		68.80 (07.35)	
		TS	55.60 (13.24)		54.65 (15.54)	
		SW	40.70 (23.03)		38.85 (25.64)	

For both classifiers, the phases ST and SW of the 2ph category presented better accuracy than
the phases of the 4ph category. Then, the analysis of the trunk muscles was performed for the
2ph category. For this, the five channels of the trunk were named as TR1, TR2, TR3, TR4
and TR5, corresponding to C7, T3, T7, T12 and L4 levels, respectively. For trunk muscles,
the average classification accuracy (unit: %) and Kappa's coefficient of 2ph category, with data
from eight subjects (S), considering different number of channels, are presented in Table 4.2.
For ST, the LDA classifier had the best performance in relation to SVM-P for all number of
channels. For SW, the SVM-P had the best performance in relation to LDA for all number
of channels. However, the standard deviation for SVM-P is smaller than for LDA. Although
the Kappa value was lower than the substantial agreement range, SVM-P is better than LDA.

Table 4.2: Average classification accuracy (%) and Kappa's coefficient (mean and standard deviation) of 2ph category with data from eight subjects and considering different array of channels.

Channel	Phase	LDA		SVM-P	
		Acc (%)	Kappa	Acc (%)	Kappa
TR1 to TR5	ST	82.25 (06.21)	0.45 (0.12)	77.65 (06.62)	0.53 (0.09)
	SW	67.50 (11.99)		73.50 (04.87)	
TR3 TR4 TR5	ST	83.50 (08.97)	0.31 (0.12)	69.00 (08.26)	0.42 (0.09)
	SW	55.85 (19.69)		75.20 (04.11)	
TR4 TR5	ST	80.25 (19.69)	0.33 (0.14)	55.85 (11.72)	0.33 (0.13)
	SW	54.10 (22.20)		83.90 (04.67)	

This can be explained because SVM requires fewer assumptions about the data and it does not assume normality and continuity, as its performance does not depend on the size of the sample. Thus, SVM-P, in this case, has better performance, with a limited amount of data, in contrast to LDA. These results show that the trunk sEMG signals can be used to recognize two gait phases (2ph category). With both classifiers, the best accuracy was obtained for the phases ST and SW belonging to the 2Ph phase category. This is believed to be due to the 2ph phases last longer compared to category 4Ph, in which phases IC, MS and TS are shorter. The SVM-P classifier shows the best performance for the trunk muscles, due to its accuracy above 73% for ST and SW phases, and lowest standard deviation than LDA. Thus, SVM-P may be used to recognize gait phases with acceptable accuracy, while others configurations of SVM, such as SVM-L (SVM Linear Kernel) and SVM-RBF (SVM Radial basis function) can be explored to improve the performance. Additionally, other features and methods of feature selection need to be tested, in order to improve the accuracy. In general, recognizing the SW phase is the biggest challenge in relation to ST, due to the back lower trunk muscles have low amplitudes in SW. A bilateral study is required to analyze the response of the classifiers with patterns from both sides. Regarding the number of channels, five is the number of arrays with better accuracy for both classifiers. However, an array of two channels can be considered an option, in order to use low number of channels. On other hand, the results show that the class IC of the 4ph category is the most difficult to recognize which can be related to uncertain and high variability of the subject' response in this gait phase.

4.1.2   Motion Classes Recognition

From the HMIR overall results, it was found that SVM showed the best performance in relation to LDA, for both muscular groups and for both sets of motor tasks. Results from SVM can be summarized in Table 4.3.

Table 4.3: Classification results (mean and standard deviation) using SVM for motion intention recognition of motor tasks: sitting (C1) and standing (C2) movements, for both lower limb (LL) and trunk (TR) muscles.

Subject	C1-LL	C1-TR	C2-LL	C2-TR
1	74.2 (8.3)	66.9(39.4)	79.7 (11.6)	84.4 (11.3)
2	80.9 (11.8)	71.3 (15.3)	75.7 (9.0)	82.1 (13.9)
3	86.0 (8.7)	77.7 (17.9)	77.4 (4.3)	83.7 (14.5)
4	73.3 (16.9)	62.8 (40.9)	70.7 (9.2)	80.0 (16.6)
5	89.1 (5.6)	79.9 (9.0)	73.0(4.9)	69.6 (6.0)
6	92.9 (4.5)	88.4 (8.3)	82.5 (15.5)	76.1 (18.8)
7	77.5 (4.3)	66.6 (27.1)	78.0 (13.3)	77.4 (13.9)
8	83.6 (9.6)	59.7 (14.8)	69.5 (7.8)	77.8 (17.3)
9	89.4 (2.2)	80.0 (9.1)	77.5 (14.1)	71.2 (6.5)
10	84.7 (9.4)	56.5 (31.7)	77.8 (7.9)	65.6 (14.9)
Mean	83.2	71.0	76.2	76.8
Standard deviation	(6.3)	(9.7)	(3.8)	(5.9)
Median	84.2	69.1	77.4	77.6
Range	[73.3-92.9]	[56.5-88.4]	[69.5-82.5]	[65.6-84.4]

The average accuracy of classification using LL muscles for siting movements (C1) was 83.2% ± 6.3 for all subjects, while for standing movements (C2) was of 76.2% ± 3.8. On the other hand, using TR muscles, the average accuracy was 71.0% ± 9.7 and 76.8% ± 5.9 for sitting and standing movements, respectively. It can be noted a difference between results for LL and TR muscles, for sitting movements, while for standing movements, average accuracies were very similar, with 0.6% of difference. In particular, for sitting movements, most of subjects showed a slightly better classification using LL muscles, with difference from 4% up to 10% in comparison with TR muscles, except subjects S8 and S10, whose differences were of 25% approximately. Subject S6 showed the highest accuracy for TR muscles, with 88.4% ± 8.3, followed by S9 and S5, with 80.0% ± 9.1 and 79.9% ± 9.0, respectively. Subjects S1-S4 showed

the best performance using TR muscles, with accuracy $\geq 80\%$. The lowest accuracy (65.6% $\pm 14.9\%$) was obtained for subject S10. The confusion matrix for S6 is shown in Figure 4.1. From this figure, it can be noted the confusion between rest sit-down (RSD) and stand-up (SU) classes, with 18.3% of false positives for SU.
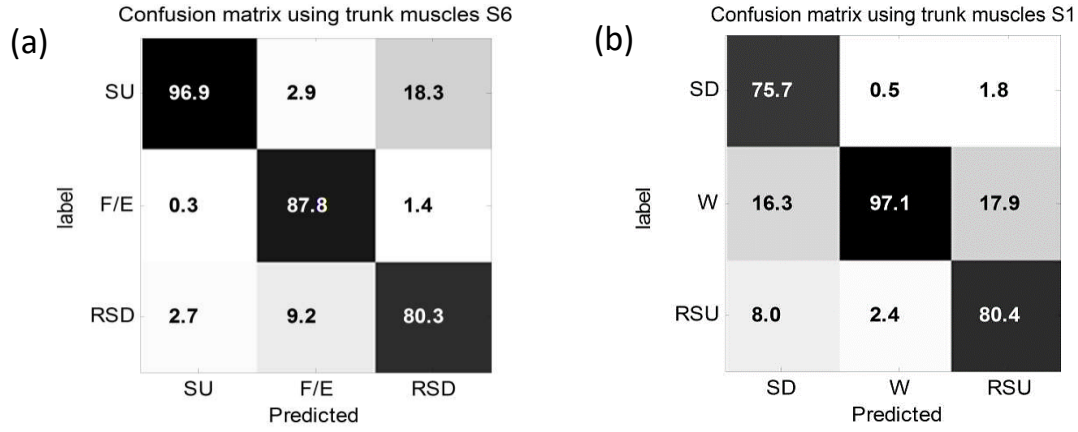
Figure 4.1: Confusion matrix using trunk muscles. (a) subject S6 for sitting movements; (b) subject S1 for standing movements.

On the other hand, for standing movements, it was found that five subjects showed and improvement in accuracy using TR muscles, with up to 9.3% of differences in relation to LL muscles. Subjects S1 achieved the highest accuracy ($84.4\% \pm 11.2$). From this Figure, it can be noted the tendency of classes Sit-Down (SD) and Rest from Standing-Up (RSU) to be confused with walking (W), with false positives above above 16%.

Figure 4.2 shows the accuracy dispersion among all subjects for each one of the motion class considered in this study, using both TR and LL muscles.

These results showed similar tendency to recognize most of motor tasks for both muscular groups. However, the performance using LL muscles was better than TR muscles. In both cases, the motor tasks RSD showed high dispersion in comparison with other tasks. RSU and SU showed the best performance, with median of 93.05% and 88.27%, respectively. However, the median of RSD for TR muscles (50.43%) was the lowest in relation to the other classes, being that S1 and S4 showed the lowest accuracies among other subjects (21.5% and 16.2%, respectively). A comparison between trunk and lower limb muscles was also carried out, and it was observed no significant difference between lower limb and trunk muscles for both C1 (p
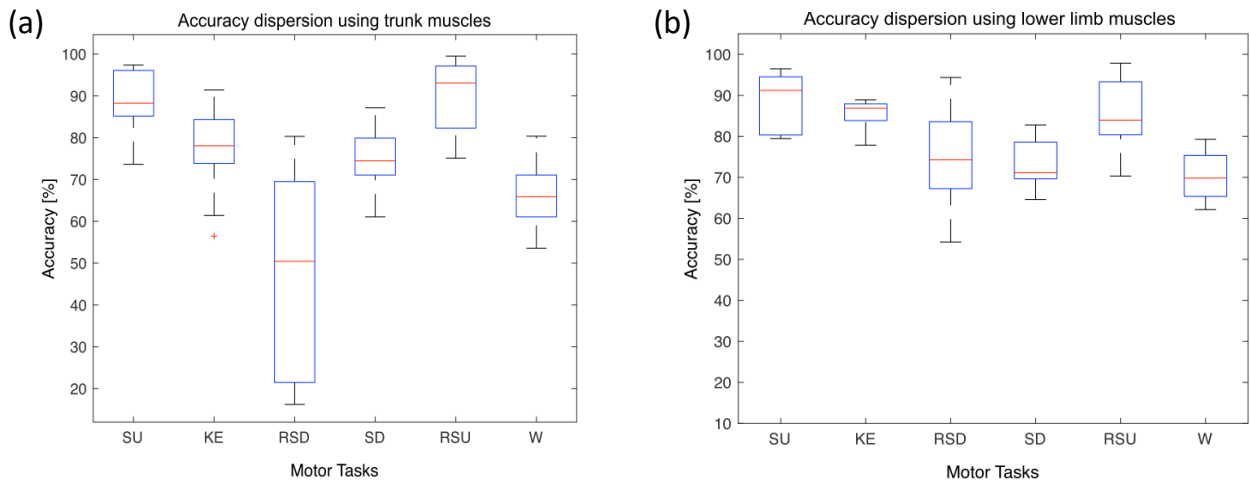
Figure 4.2: Accuracy dispersion among all subjects for each motion class. (a) using trunk muscles; (b) using lower-limb muscles.

$= 0.0757$) and C2 ($p = 0.6776$), for all subjects.

Figure 4.3 shows the relation between accuracy and results for both classifiers (C1 and C2), and both muscular groups: trunk and lower limb.
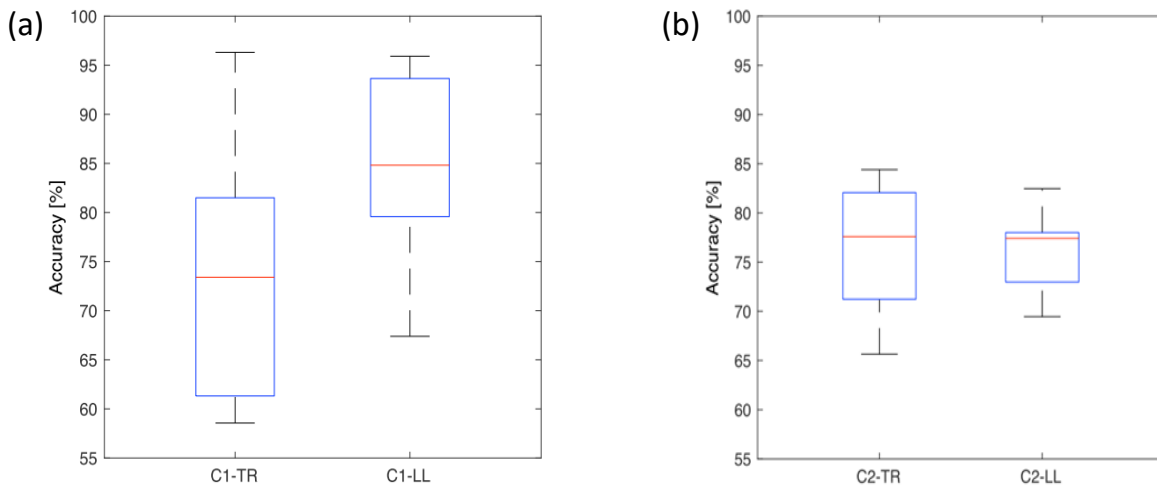
Figure 4.3: Accuracy (%) of dispersion for the classification for trunk (TR) and lower-limb (LL) muscles. (a) sitting (C1) movements; (b) standing (C2) movements. Boxplot depicts the median (red line), interquartile range (blue box) and maximal/minimal values (whiskers).

On the other hand, a comparison of the muscular groups in relation to each one of the motor tasks was performed. From these results, it was observed no significant difference for the motor tasks SU, SD, W and RSU ($p > 0.2890$). The motor tasks F/E and RSD showed a significant difference ($p < 0.0451$) when using both muscular groups.

4.2 Low-Level Controller

4.2.1 Instrumented Insole

Such as aforementioned, an instrumented insole is used to acquire plantar pressure data. Figure 4.4 shows the insole pressure data during a test with subject 1, in which 77 step were collected. The pressure data from the insole presented acceptable values of precision ($r > 0.92 \pm 0.02$) respect to a mat pressure (GAITRite Platinum, CIR Systems Inc.), which has accuracy (mean and standard deviation) of $Cb > 0.82$ (0.02), and acceptable reproducibility due $pc > 0.89$ (0.03).

Although the pressure data presented differences in the first sub-phases of stance phase, as shown in Figure 4.4, the insole showed a good response to recognize stance and swing phase. Hence, the algorithm used in this research to determine the gait phases uses data from the insole.
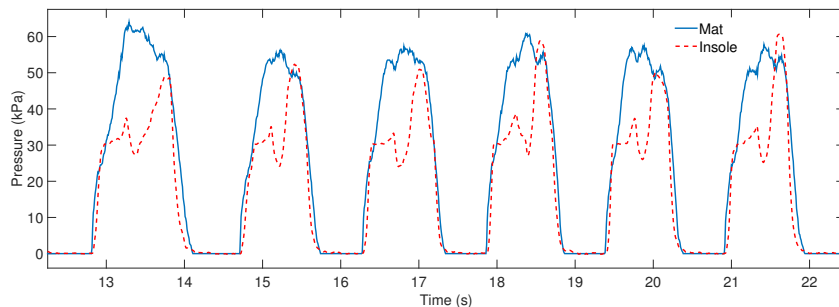
Figure 4.4: Insole plantar pressure data during six steps compared with data from a commercial pressure sensitive mat.

4.2.2 Stance Control Evaluation

Two gain patterns for knee impedance modulation were used to control the knee orthosis: the first based on the knee moment during gait P_1 and, the second based on knee velocity P_2. For purposes of comparison with both knee modulation patterns, a third pattern P_3 was also used to develop a free gait without knee impedance modulation. This evaluation were applied in a study with healthy subjects and post-stroke patients.

Healthy subjects: Results are shown in Figure 4.5 to demonstrate the efficiency of the knee modulation proposed for SC assistance, where it is possible to see the variation of the knee angle during gait using patterns P_1 and P_2. Here, the variation of the knee angle in time shows that the subject walked approximately with the same velocity, with the knee angle showing similar amplitudes for both patterns. Even though the footswitch signals presented an incorrect value in a period of the sub-phase TS (between 773.5 s and 773.75 s) as shown in Figure 4.5 (a), the method may adapt the modulation of the gain G in this period and maintain the expected value of G.
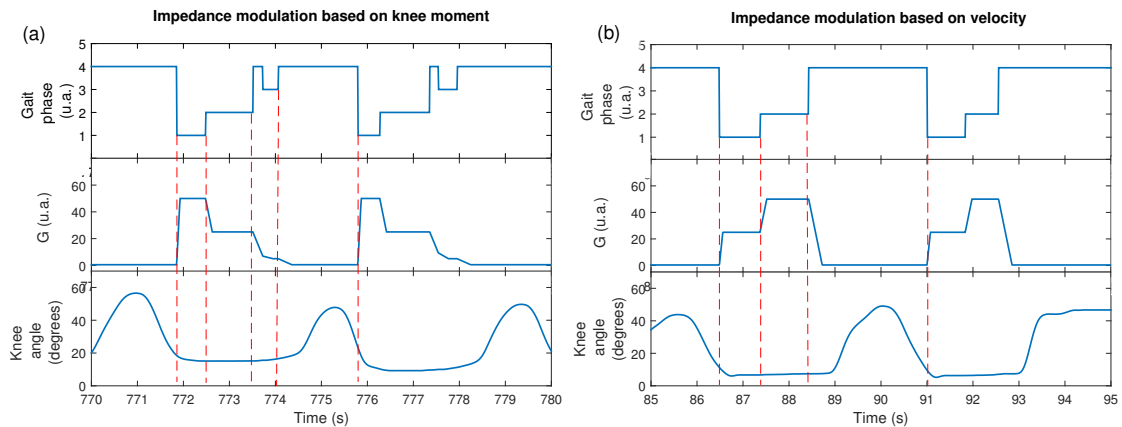
Figure 4.5: Footswitch signal, gain variation and knee angle during gait with impedance modulation. (a) modulation obtained from the pattern P_1 based on normal velocity; (b) modulation obtained from the pattern P_2 based on the knee moment.

For the pattern G based on velocity P_2, Figures 4.6 (a), (b), (c) show the variation of G during the gait. Here, during gait was generated different footswitch signals at different walking speeds. The FSR signal showed a good recognition of stance and swing phases in Figure 4.6 (a) and (c), then the footswitch signal of the instrumented insole showed good performance to measure the four gait sub-phases considered for the impedance modulation. For the case (b), the user generates the two principal gait sub-phases. Here the gait pattern was different as shown in Figure 4.5, which is considered common due the gait dynamic.

These examples demonstrate that a specific subject does not present a single characteristic gait cycle. It is reported in literature that the percentage of atypical cycles in healthy adults is from 1% to 3% (AGOSTINI; BALESTRA; KNAFLITZ, 2014). Despite this, the modulation method proposed here was able to generate a pattern G to obtain a SC performance even with

a non ideal footswitch signal, as shown in Figure 4.6.
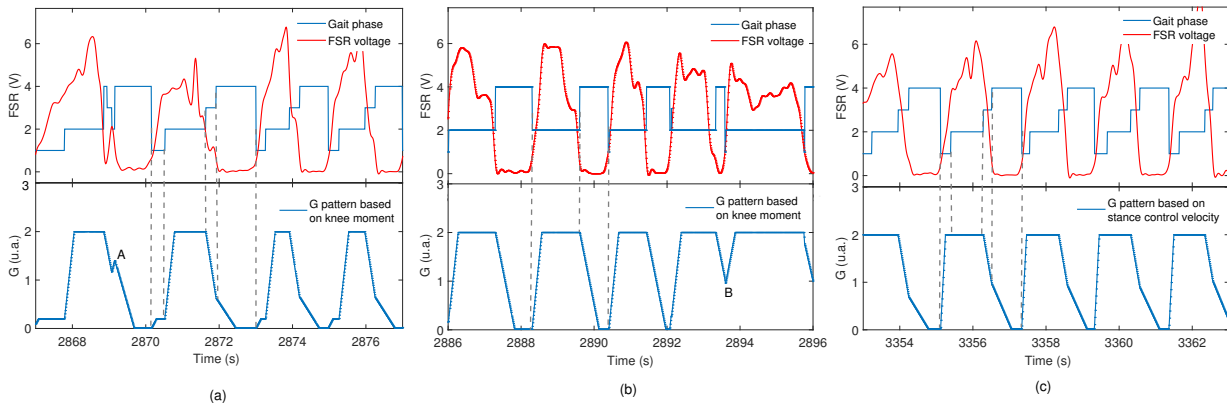
Figure 4.6: *G* variation during gait cycle. (a) variation of footswitch during a gait test, which generates four sub-phases: initial contact (IC), mid-stance (MS), terminal stance (TS) and swing (SW); (b) example with three sub-phases; (c) example that shows the variation of G during a gait cycle with noise.

Figure 4.7 shows the knee angle and knee torque of subject 1, with impedance modulation patterns P_1, P_2, and P_3 during the gait.
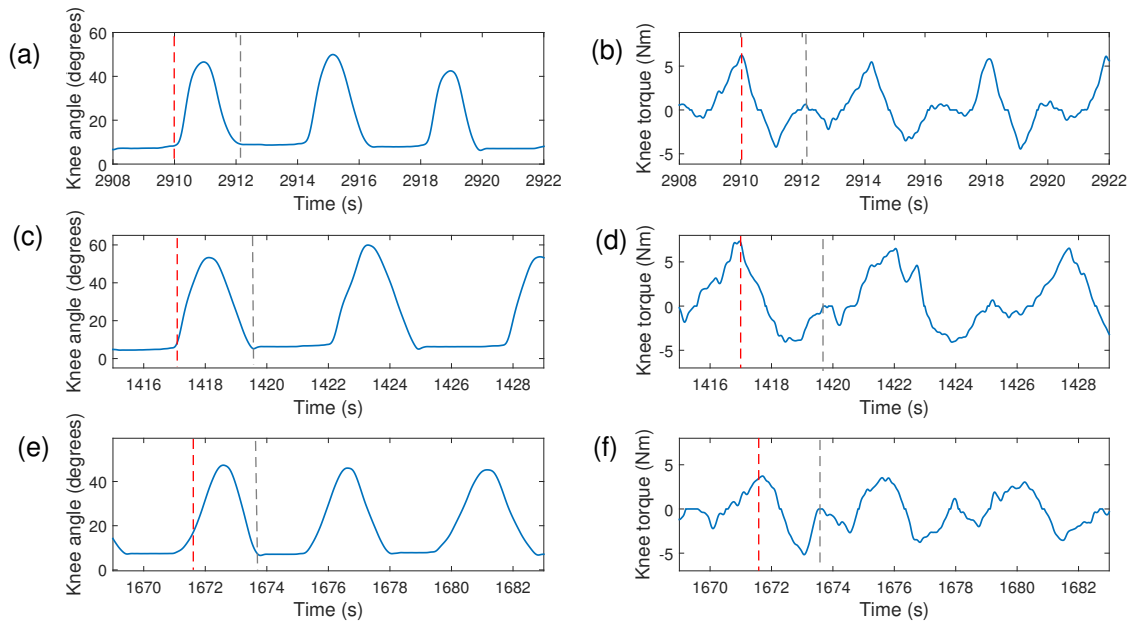
Figure 4.7: Knee angle and knee torque during knee impedance modulation with patterns G: P_1 (a) and (b); P_2 (c) and (d); P_3 (e) and (f).

Here, the maximum torque is presented at the beginning of the knee flexion (marked with red dashed line) for P_1 and P_2. Another increment of knee torque was obtained at the beginning

of the stance phase (marked with gray dashed line) for the three patterns.

In (FIGUEIREDO et al., 2017), a gait analysis with an active knee orthosis without walker was conducted, in which the torque with a position control at 0.28 m/s was approximately ± 5N.m. In addition, this study reported that the torque with an adaptive impedance control at 0.28 m/s and 0.44 m/s may have values of ± 10 Nm. In our work, walking with ALLOR and the walker at 0.2m/s implies an interaction torque of ± 5 Nm, as shown in Figure 4.11. In this sense, the new method for knee impedance modulation proposed here presents less knee torque than the torque presented in (FIGUEIREDO et al., 2017), with both position control and knee impedance modulation. Hence, the method based on FSR sensors for gait phase segmentation may be used to modulate knee impedance without demanding additional knee torque at the user during walking.

Table 4.4 shows the temporospatial and kinematic information of the subjects when walking using the three G patterns P_1, P_2 and P_3.

Table 4.4: Mean and standard deviation for temporospatial parameters, and maximum flexion during swing phase for subjects wearing ALLOR controlled by the SC strategy using three types of impedance modulation patterns.

	Gait velocity (m/s)	Cadence (steps/min)	Stance phase (%gait cycle)	Maximum flexion in swing phase (°)
P1	0.18 (0.07)	29.86 (8.42)	49.73 (7.87)	36.44 (9.56)
P2	0.14 (0.05)	23.17 (2.86)	46.19 (9.04)	39.92 (12.40)
P3	0.18 (0.04)	26.79 (6.84)	44.51 (7.75)	39.0 (10.61)
p-value	0.0670	0.0381	0.4493	0.1534

P1, Gain pattern based on knee moment
P2, Gain pattern based on knee velocity
P3, Gain pattern for gait without knee support in the stance phase

For the three subjects, the results shown in Table 4.4 demonstrate no significant difference in gait velocity ($p = 0.067$), cadence ($p = 0.0381$), percentage of ST phase of the gait cycle ($p = 0.44$) and maximum flexion in SW ($p = 0.153$) between P_1, P_2 and P_3.

Considering both modulation patterns, the pattern G that presents better temporospatial parameters was the knee moment based on pattern P_1, which reported highest walking speed, cadence and stance phase percentage of the gait cycle compared with P_2. However, regarding

the kinematics, the maximum knee flexion was increased ($39.92° \pm 12.40°$) using the pattern P_2 based on knee velocity.

In addition, the duration of the swing phase during walking generally represented 50% to 56% of the gait cycle, as shown in Table 4.4. A study that describes gait analysis using an exoskeleton with walker (KANG et al., 2007) reports a swing phase around 37% of the gait cycle with healthy subjects. On the other hand, in (TO et al., 2011), a gait analysis with an hybrid neuroprosthesis for SC is performed, which reports that the swing phase during evaluation with nondisabled subjects represents 36% to 51% of the gait cycle. Then, the swing phase percentage obtained during gait with the proposed method agrees with a gait analysis that considers SC. Furthermore, a study of gait analysis with assistive devices tested with pathological cases, such as spinal cord injury (TO et al., 2011), reports that the swing phase represents 25% of the gait cycle. In (ARAZPOUR et al., 2016), other research of a gait analysis using a knee-ankle-foot orthoses with a powered knee joint is reported, whose swing phase during evaluation with poliomyelitis subjects represents 36% to 51% of the gait cycle. Then, in this sense, an important future task is to analyze the real-time adjustment of knee impedance in pathological gait.

Walker assisted gait with healthy subjects has reported values between 0.17 m/s and 0.29 m/s depending on the body weight bearing patterns of the leg (BACHSCHMIDT; HARRIS; SIMONEAU, 2001). In (LOTERIO et al., 2017) a gait assisted by a smart walker without orthosis in post-stroke subjects showed gait velocity values between 0.23 m/s and 0.44 m/s. Then, for the three patterns used here, the walking velocity is within that range of the first case, which means that the effect of ALLOR with knee impedance modulation does not produce a significant speed reduction in walker-assisted gait. Also, this value indicates that the incorporation of a smart walker can be considered for tests with post-stroke subjects.

Regarding the maximum knee flexion during swing phase, the three patterns present similar values, agreeing with (KANG et al., 2007), where the walking speed using a powered gait orthosis with a walker has been reported as being $48° \pm 10°$. Here, it should be made clear that during walker assisted gait the gait velocity and knee flexion in phase SW are lower than a normal gait.

The experience with healthy subjects presented in this section aimed to verify the functionality

of the impedance modulation method for a stance control during gait. This in order to adapt and test the protocol to be used with post-stroke patients in pilot clinical tests.

Post-stroke patients: No dangerous situation and no adverse effects were reported during or after the experiments and all subjects completed the experiment. To illustrate the ALLOR operation, results are shown in Figure 4.8 to demonstrate the efficiency of the knee modulation proposed for SC assistance in patient 1.
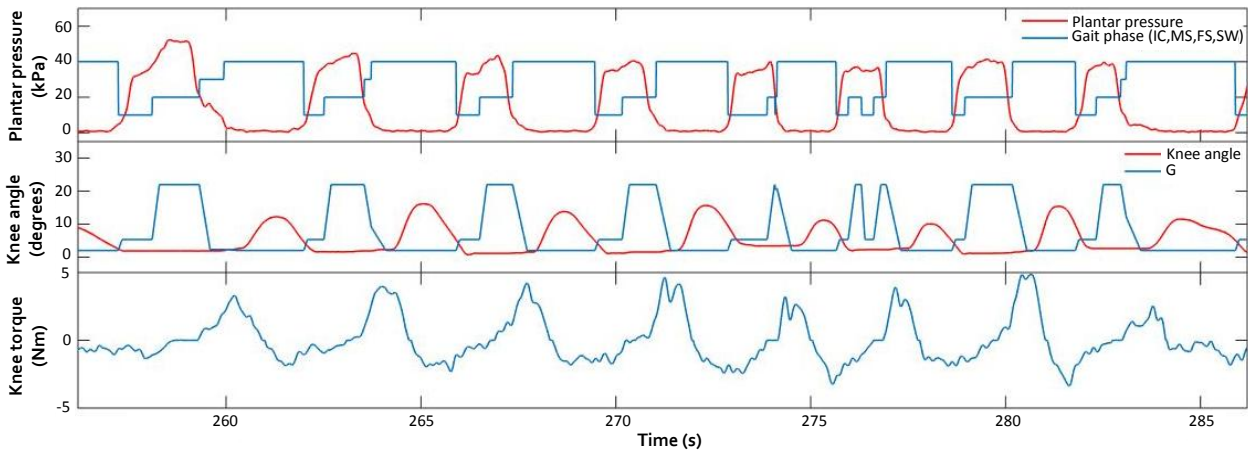
Figure 4.8: Plantar pressure, footswitch signal, gain variation, knee angle and knee torque during gait with impedance modulation obtained from the pattern P_2 based on the knee moment for the post-stroke patient 1.

Figures 4.9 and 4.10 shown the results during the experiment with patient 2 and patient 3 respectively.
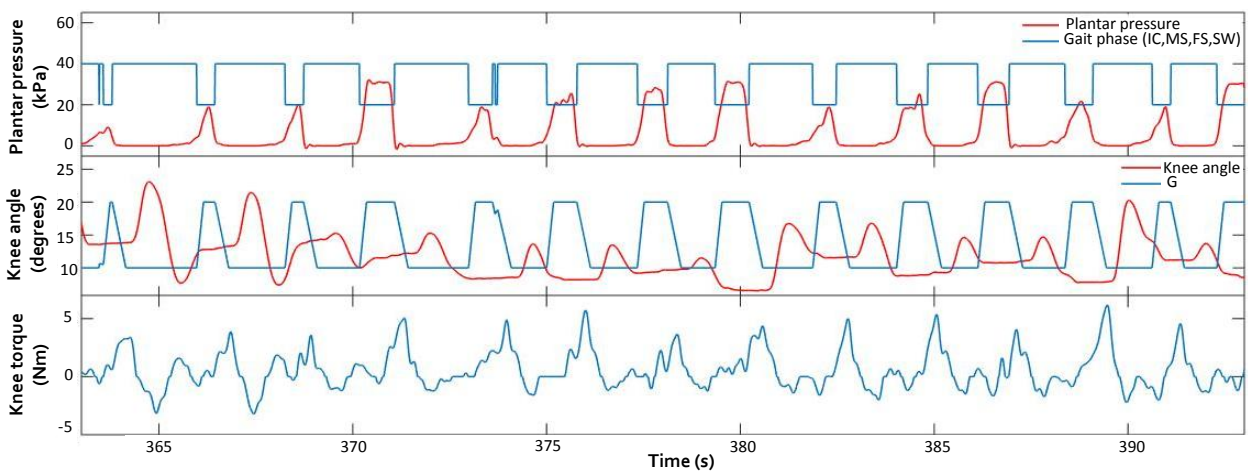
Figure 4.9: Plantar pressure, footswitch signal, gain variation, knee angle and knee torque during gait with impedance modulation obtained from the pattern P_2 based on the knee moment for the post-stroke patient 2.
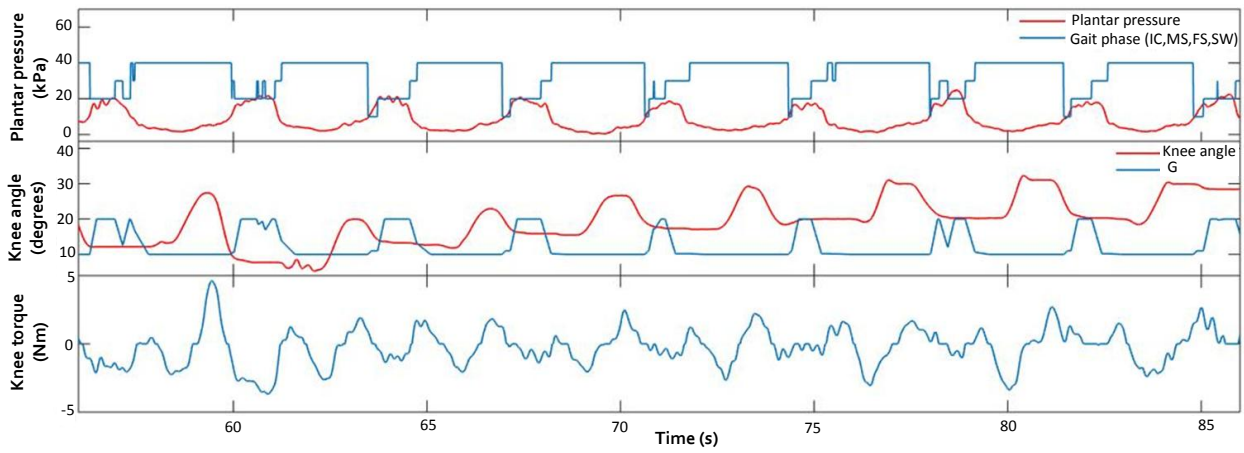
Figure 4.10: Plantar pressure, footswitch signal, gain variation, knee angle and knee torque during gait with impedance modulation obtained from the pattern P_2 based on the knee moment for the post-stroke patient 3.

The figures show the plantar pressure, gait phase pattern, knee trajectory, knee impedance modulation and knee torque. It can be observed from the results that the stance control with ALLOR can successfully support the knee joint during stance phase of gait. Transitions amongst stance and swing phase were similar as reported in healthy subjects. For all the cases, the gait phases were recognized according to the plantar pressure and knee torque did not exceed 5 Nm. As in the results with healthy subjects, the gait phases present different sequences of gait phases.

Table 4.5 shows the temporospatial and kinematic information of the patients when walking using ALLOR.

Table 4.5: Mean and standard deviation for temporospatial parameters, and maximum flexion during swing phase for post-stroke patients wearing ALLOR controlled by the SC strategy using impedance modulation with pattern P2.

Patient	Cadence (steps/min)	Stance phase (%gait cycle)	Maximum flexion in swing phase (°)
1	34.72	46.35 (7.18)	13.82 (3.30)
2	37.07	28.19 (9.26)	8.61 (5.78)
3	33.68	51.81 (5.72)	15.21 (1.60)

For the three subjects, regarding cadence, the results demonstrate better performances in patients compared to healthy subjects. The percentage of ST phase of the gait cycle was proximal at healthy subjects for patient 1 and 3. The opposite for patient 2 who decreased the stance

phase. Regarding the kinematics, the maximum knee flexion were lowest for the three cases respect results with healthy patients.

Regarding the QUEST survey, the user satisfaction with ALLOR (mean and standard deviation) controlled by the proposed approach was scored for post-stroke patients as: dimensions: 3.91(0.00), weight: 3.91(0.82), adjustment: 4.22(0.94), safety: 4.64(0.47), durability: 3.91(0.82), ease of use: 5.00(0.00), comfort: 4.31(0.47) and effectiveness: 3.91(0.82), in a range of 0 to 5.

Based on the experience after and during this study, it was verified that the use of our system requires a therapist or assistant to mount the orthosis on the user. The total time required to this task is approximately 8 minutes with subjects familiarized with ALLOR. When it is being used for the first time, more minutes are required, in order to adjust the length of leg and thigh segments along with hip angle adjustment. In this case, the total amount of time is from 20 to 25 minutes.

4.2.3   Mid and Low-Level Control Evaluation

Figure 4.11 shows the knee angle, knee torque and gait phase of subject S1 during the execution of the sequence RSU-SD-SU-W-RSU-SD-F/E-SU of motions classes (dashed line in red) using ALLOR.

From Figure 4.11, during F/E (204s < t < 247s) the movement is executed according to the trajectory, except in the two points marked with k where the arrows are located. In these points, the user's intention seems stopping the movement, and an increment of the knee torque was obtained, such as expected. The third arrow, termed non-sequence, in the RSU motion class (247s < t < 260s) indicates a motion class that is not possible to be executed, due to not follow the motion class sequence after F/E. Here, the user finished the knee flexion and waited in SD position until a SU motion class activates the corresponding controller. This demonstrates the performance of the FSM controller to guarantee safety for the user. The maximum torque is presented, during walking, at the beginning of the knee flexion. During RSU and SD, the
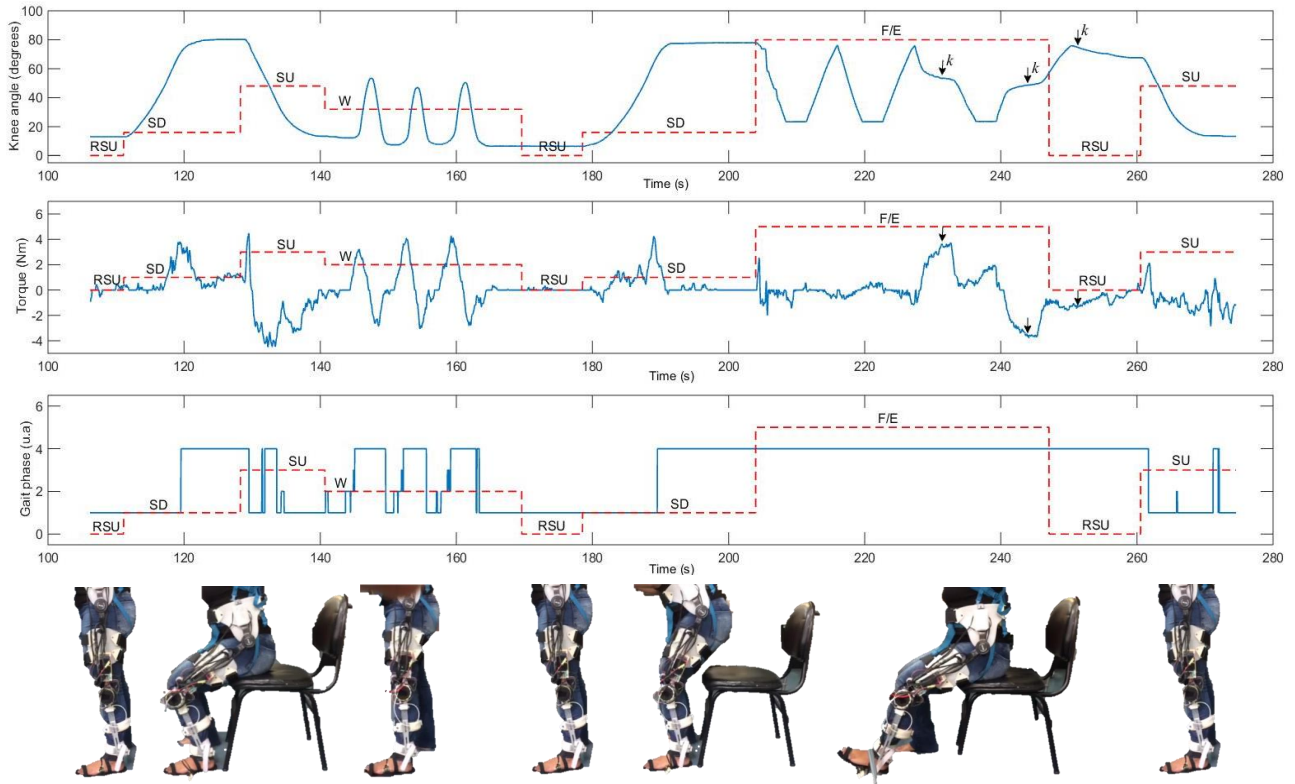
Figure 4.11: Experimental results of the mid-level and low-level controller. Knee angle, knee torque and gait phase of subject S1 during the execution of motion classes (dashed line in red). During the period of time when F/E is executed, the user's intention of stopping the movement is marked with k where the arrows are located. The last motion class RSU cannot be executed after F/E due it non corresponds at a motion class sequence.

knee torque is approximately zero. On the other hand, to execute the sequence SU (128s < t < 140 s), the torque is around 4 Nm. Regarding the gait phase information, the footswitch signal shows a consistence during the motion classes RSU, SD and F/E. In SU, the gait phase presents a different pattern, and during W the signal allows recognizing 4 sub-phases. Table 2 shows the knee angle, torque and gait parameters obtained for subject S1.

Table 4.6: Gait parameters: angle and torque for the left knee joint while motion classes are performed with ALLOR for subject S1 (mean and standard deviation).

Motion class	Max angle (°)	Max torque (Nm)	Stance phase (%gait cycle)	Gait cycle duration (s)
RSU	9.17 (4.59)	0.04 (0.09)	100.00 (0.00)	-
SD	78.99 (1.70)	3.00 (0.33)	84.76 (12.62)	-
SU	13.48 (0.23)	3.00 (1.76)	84.76 (2.25)	-
W	40.96 (1.60)	6.69 (0.64)	48.89 (1.44)	7.38 (1.80)
F/E	23.40 (0.13)	0.34 (0.03)	0.00 (0.00)	-

4.3   Discussion

HMIR

Leg muscles have specific functions that provide movements of lower limbs, such as knee flexion-extension, ankle flexion and extension, walking, jump, among others. On the other hand, trunk muscles play an important role to control the posture in order to maintain the equilibrium during walking. ES muscles specifically have an active participation during lower-limbs movements. Thus, this behavior of ES muscles may be a challenge to recognize lower-limb movements. Unlike lower limb muscles, trunk muscles may be preserved in neurological cases, such as spinal cord injuries and post-stroke patients. Therefore, these muscles may be exploited in a recognition system, in order to convey control commands for the knee exoskeleton. We showed that leg and trunk muscles may be interchangeable to recognize some conditions as SU, RSU and W. However, different results were obtained for other conditions, such as knee flexion-extension and sitting.

The proposed system here for trunk muscles was able to obtain higher values of standard deviation, which shows a low participation of these muscles for the aforementioned conditions. However, an acceptable performance was obtained for three subjects: S5, S6 and S9 (Acc $\geq$ 79.9%). Thus, we consider that trunk muscles may be used as an alternative to convey control commands for our exoskeleton ALLOR. Furthermore, other techniques will be explored to improve the feature selection/extraction, and in addition, the classifier setup can be optimized to increase the performance. We consider that the main finding of this study is that the trunk muscles provide enough information to recognize the following motion classes: stand-up, rest in stand position and walking. The results of this study also indicate that HMIR can be used to control a knee exoskeleton although on-line tests were still not developed.

Based on our experience obtained during the development of this protocol, the use of trunk muscles as myoelectric sources was more suitable than leg muscles, due to trunk signals were more comfortable to acquire.

During acquisition trials and tests, trunk muscles signals do not showed additional perturbations respect lower limb sEMG signals and the electrodes did not move from their place contrary to

the electrodes located in the lower limb. Based on users comments, the electrodes located in the trunk result more comfortable to study motion intention due to the users do not see wires and electrodes and also because the action of placing the electrodes is fast. Thus, this system based on trunk muscles may be an alternative to control exoskeletons in cases where the lower limb muscles are affected.

We consider that this study opens the research to develop other methods to be incorporated in rehabilitation protocols for patients with weakness and/or spasticity in their lower limb muscles. As future work, it remains to be verified whether the system effectively assists post-stroke patients with residual physical functions to generate commands of motion intention.

Mid and low-level control

Regarding the mid and low-level control, the development of a strategy that allows assisting movements related to knee joint based on motion intention recognition was presented here. The control of the exoskeleton ALLOR was developed and validated through the execution of the sequences sit-down, stand-up, walking and knee flexion-extension movements, which were synchronized with a motion intention indicated by the user. A pilot test was undertaken, which confirmed the validity of the methodology.

The experimental results showed that the proposed controller can execute the movements of ALLOR commanded by the user's intention. We confirmed also that the controller provides reference pattern for the motion classes SD, SU and F/E, and a proper torque for the motion classes considered here. The motion SD results in a lower support torque for the knee compared with the motion SU, such as expected, which is also reported in previous studies (FLEISCHER et al., 2006), (CHEN et al., 2015), which is due to the reduction of muscle activation during sit-down position. Therefore, this controller can be used to help patients to re-learn motion patterns, such as the cases of the movements SD, SU and F/E. For F/E, the controller allows stopping the movement with the user motion intention detected by force sensors, providing a simple solution to incorporate tasks with direct user's interaction. Also, it is possible to incorporate variable knee resistance in the training, once the user has reached a certain level of progress when using the admittance modulation. The controller also reduces the risk of falls by assisting the knee in rest in stand position, by blocking the joint to sustain the user's weight.

SC control

Regarding the SC, this work evaluated the effect on walking with an active knee orthosis (ALLOR) while using two knee impedance modulation patterns: P_1 (based on knee moment) and P_2 (based on knee velocity), which incorporates a SC strategy. The main functional purpose of the SC strategy is to provide free movements in swing phase and provide a support to knee joint during stance phase.

The three patterns presented no significant difference in walking speed, stance phase percentage of the gait cycle, and maximum flexion during swing phase, as indicated in Table 4.4. The results of our study demonstrated that the proposed patterns P_1 and P_2 could be used to improve the knee support in stance phase. The methodology do not allow to determine the more suitable pattern to modulate the knee impedance. More tests with a larger sample are required to conclude if both gain patterns are suitable to modulate the knee impedance and assist the knee joint under the SC strategy using an admittance controller.

Regarding the gait velocity, the results indicates lower walking speeds, fact according with the literature. It is reported that using an orthosis with a stance control is required a small knee extension moment to disengage knee joint locking in late stance (RAFIAEI et al., 2016a). With ALLOR is required a time until the user feels the more lower knee impedance. Also is reported that the experience of users during walking with this stance control must be increased over time to provide more ability in controlling the orthosis (RAFIAEI et al., 2016a). During our test, it was possible to notice that the users feel more comfortable and safe after some trials walking with ALLOR. The variation of the knee impedance was performed considering two implications for the design of orthosis with stance control: walking speed and weight. In fact, literature shows that the following parameters: stiffness, knee flexion and extension, and maximum moment change their values with gait speed (SHAMAEI; DOLLAR, 2011). On the other hand, it is also reported that the stiffness of the parallel assistive device should be modified as the load or pilot weight changes (SHAMAEI; DOLLAR, 2011). In this sense, both patterns G change the impedance at knee during gait cycle, increasing or decreasing it, according to both weight and velocity of the subject. Then, the approach proposed here may also be considered to evaluate the knee impedance variation to design efficient assistive devices.

The weight percentage considered for each gait phases was due to the characteristics of the subjects during tests. For this study, gait assisted by a walker was chosen due to it allows offering safety to the users. It is worth to mention that parallel bars, crutches or canes can be also used as support element instead of the walker. For future tests with patients and subjects with disabilities, the total weight of the user will be considered, according to recommendations for the design of parallel assistive devices (SHAMAEI; DOLLAR, 2011).

The data analyzed shown for the ST phase in the gait cycle a value around 50% and do not 60% as the literature indicates in cases of normal gait. Some studies of gait using lower limb exoeskeletons report similar values (TO et al., 2011), (ARAZPOUR et al., 2016). In this sense, is clear that the use of an assistive device presents influence in the gait phases percentages. In order to improve the adaptation of the user and offer a user velocity value adapted at the user gait to modulate the knee impedance, the time of a previous gait cycle together with the user height data can be used. In the proposal here presented, the ST gait phase segmentation for impedance modulation was considered due to this phase presents the maximal variation of impedance and minimum movement variation. For that reason an instrumented insole was built. However, a technique to identify the swing phase also can be explored to improve the adaptation of the user during gait with ALLOR.

For post-stroke patients the results demonstrate that the modulation allows developing the gait under the stance control strategy. The three patients were able to finish the tests. Patient 1 and 3 demonstrate better percentage of ST phase during test respect patient 2. For all the cases, lower flexion in swing phase were obtained during gait. In order to improve the range of knee flexion, a position control, at the beginning of the swing phase, can be implemented. The use of ALLOR in patients did not demand knee torque greater than for healthy subjects. For gait phase recognition in pathological cases with foot drop problems, which present different footswitch signals (percentage of atypical cycles from 11% to 100% in pathological subjects) (AGOSTINI; BALESTRA; KNAFLITZ, 2014), an alternative for gait phase detection might be necessary. Therefore, an individual study to define if either it is recommended to design an insole with additional sensors or program a gait-phase detector for each case must be conducted. Also data fusion techniques may be needed, taking into account the knee angles acquired

by goniometers or inertial measurement units (IMUs). The inclusion of angle information in the swing phase can support the implementation of a position control in cases where the lower limb can not execute required flexion-extension in this phase. Based on the experience and participants' comments (healthy and post-stroke patients), the instrumented insole was comfortable to use. In future works, the insole will be used to study plantar pressure in order to detect alterations in gait, and allow comparing stroke survivors with healthy people, as stroke survivors usually adopt walking strategies, such as heel walking, planar stride or low heel pressure. These gait alterations can evolute to more complex musculoskeletal disorders, which influence in functional activities. Plantar pressure can inform about these alterations, calculating the gait variability over time (MUNOZ-ORGANERO et al., 2016), and therapists can use this data as feedback to propose different strategies for rehabilitation avoiding the evolution of gait disorders.

User satisfaction

In relation to user satisfaction, results show that the lowest score (3.91) was related to "dimensions", "weight", "durability" and "effectiveness", while questions on "adjustment", "safety", "ease of use" and "comfort" received values over 4.22 on the QUEST score. In this sense, some hardware adjustments are needed to obtain a more robust system and improve the "weight" item, such as new materials to decrease the structure and the hardware weight. The comfort is associated with adjustment of actuators and mechanical to the human body, which must be taking account. Some factors such as sensors, straps and weight also affect the gait, causing more energy cost (HUO et al., 2016). Physiological theories have been developed to address these limitations in wearable robots (LI et al., 2015), but it is necessary more clinical trials with a larger sample to determine how theses adjustments influence in normal and pathological gait, turning these exoskeletons more easy to use in daily activities. It is worth noting that participants in this study used for first time the system. Based on their comments after the experimental protocol, the time required to adjust the device will be improved.

Regarding the "effectiveness", a clinical protocol with a therapist is important to address this issue in practice, in order to evaluate ALLOR with knee impedance modulation and its effect in patients for long-term. With this purpose, a previous graphical user interface (BOTELHO,

2017) will be adapted for the therapist who accompanies the rehabilitation, in order to facilitate the programing and monitoring of variables, such as: knee angle and torque, plantar pressure, number of steps and to choose the pattern G for knee impedance modulation.

As our control method constitutes an approach to assist knee movement in stance phase, future works will focus on implementing a position controller for swing phase, or using functional electrical stimulation (FES), in order to apply force to advance the user's leg. In addition, future efforts will investigate correlations between the FSR activation and the knee joint impedance during walking on treadmill and stair climbing. Based on the results and with professional consulting of the therapist who accompanies the process, a protocol is proposed in Appendix B to pilot tests using ALLOR with the system described in section 3.1.

Chapter 5

Conclusions and Future Work

This chapter summarizes the main conclusion and contributions of this work and also describes the future works that can give continuity to the researches presented here, which are the design of new control approaches for ALLOR (Advanced Lower-Limb Orthosis), and the integration with the UFES's Smart Walker for rehabilitation tasks.

5.1   Conclusions

Strategies to provide the user with the ability to control a lower-limb active orthosis through voluntary movements was the main motivation for this research. The main goal was to develop and validate a controller for a robotic knee orthosis in order to assist the joint based on the user's motion intention, and explore the possibility of acquiring this information from trunk muscles as a new approach to robotic rehabilitation robotics. Several research activities were conducted towards the development of hardware and control methods to face this challenge. Three objectives were proposed in section 1.4, which were accomplished with the methodology and results presented in Chapters 3 and 4.

The first partial objective of this thesis was achieved through the proposal of a protocol to acquired a database of sEMG signal from lower-limb and trunk. After that, sEMG signals were

acquired, processed, and a new protocol was defined, which included the correct positioning of electrodes to obtain a database oriented to lower-limb motion analysis. The experience showed that our protocol to acquire sEMG signals is safe, fast and can be employed in clinical environments.

The second partial objective was achieved through the sEMG signal processing and analysis in order to get suitable features and classifiers to obtain information from lower-limb motion intention. Two applications of motion recognition were analyzed: gait sub-phases and motion intention in daily life movements, such as: stand-up, sit-down, knee flexion-extension, walking, rest in stand-up position and rest in sit-down position. The information provided by trunk muscles presented better performance to recognize stance phase when using LDA classifier. On the other hand, to recognize the motion classes, a SVM with Gaussian kernel classifier showed the best performance. Results suggest that trunk muscles can be considered to obtain information of lower-limb motion intention to be used in robotic assistive devices. As was mentioned, trunk muscles may be preserved in neurological cases (spinal cord injuries and post-stroke cases) In this research, the trunk sEMG signals demonstrate good potential to recognize motion intention related to knee joint. In addition, during acquisition tests, trunk muscles signals do not showed additional perturbations respect lower limb sEMG signals and the electrodes did not move from their place, contrary to the electrodes located in the lower limb. Finally, for the users, the electrodes located in the trunk result more comfortable to study motion intention due to the users do not show wires and electrodes and also because the action of placing the electrodes is fast. With respect to the third partial objective, this work proposed mid-level and low-level control strategies to establish a system that provides the user with the ability to modulate the behavior of the robotic knee orthosis through voluntary movements using their residual motor skills. For this purpose, our robotic knee orthosis (ALLOR) was adapted to be used to assist the knee during the execution of the movements considered in the high-level control stage. In order to execute the motion class desired by the user, a suitable selection of admittance, velocity and position controllers through a finite state machine was achieved.

For the walking state, a stance control strategy based on the modulation of admittance pa-

rameters along the gait cycle was implemented and validated. For this, an instrumented insole was used to identify the gait phases. Velocity, gait phases and user height are used to calculate suitable times to increase or decrease admittance parameters. The admittance modulation method proposed here may also be considered to evaluate knee impedance variation during gait. For stand-up and sit-down states, the low-level controller includes a PI controller to execute movements, and an admittance controller is used to record the trajectories of the user. For flexion-extension movements, a velocity controller and a function to detect motion intention were employed. The control system was designed, implemented and preliminary validated with healthy subjects. The results suggest that the active knee orthosis ALLOR can be used to assist the knee joint during gait, sit-down and stand-up movements. For knee flexion-extension movements, a stage of the controller allows programing the allowed range of movements, with the option of stopping when the user decides employing force information. Thus, the controllers proposed in this thesis constitutes an new approach to assist knee movements based on motion intention, which and can be applied to assist movements and also for rehabilitation tasks. The fact that the controller is based on force feedback leaves opened the possibility of being applied in rehabilitation protocols in which the therapist can select the level of effort along sessions.

Finally, an evaluation of usability of ALLOR with the proposed controllers was performed. Results suggest that the device is safe, however, aspects of ease of use and comfort must be improved. For this, new materials to adjust the exoskeleton and to decrease the structure and the hardware weight will be considered. Also a user interface will be made available to facilitate the controller programing and to monitor variables, such as knee angle and torque, plantar pressure, number of steps, and other parameters of interest for the therapist.

5.2   Future Work

The knowledge and experience acquired during this research allows us to propose the following tasks: design of new control approaches for ALLOR, implementation of the entire system to be executed and integration of ALLOR with the UFES's Smart Walker for rehabilitation tasks.

Regarding the new control approaches using ALLOR, the idea is to allow patients with residual muscle function perform desired movements during training. Thus, position controller for swing phase can be used to release the leg in cases of muscle weakness. In addition, FES at hip can be used to induce movements and allow the functionality in subjects who require an active system for this joint.

Correlations between FSR activation, plantar pressure and knee joint impedance walking on treadmill and stair climbing phased also be studied, in order to increase the functionality of ALLOR with other tasks.

On the other hand, for the implementation of the entire system on-line, a portable sEMG acquisition system is required. Preliminary tests conducted with the system employed in (MAYOR, 2017), which is based on an NI USB-6009 data acquisition device and bipolar active electrodes (PL091060A - 60Hz) manufactured by Touch Bionics, suggest the applicability of the system for experimental tests.

The protocol proposed in Appendix B may be used for this purpose. Also, in order to execute rehabilitation therapies with the system here proposed, a graphical user interface will be adapted for the therapist who accompanies the rehabilitation. Based on therapist requirements, this interface must be contain the following facilities: a) manual control of knee impedance and velocity, b) control of the time for execution of each task (walking and knee flexion-extension); c) visualization of force at knee acquired from torque sensor and knee angle; d) control of the minimum and maximum knee angle and torque to avoid injuries and increase protection measures.

Finally, the integration of ALLOR with the *UFES's Smart Walker* (USW) can be explored to develop a system to improve mobility and safety during gait assistance/rehabilitation. The purpose is to allow the user to move around through the generation of voluntary commands. In this case, the motion intention can be detected through force sensors installed on the walker. of the devices. This may allow the user to learn how to control both *ALLOR* and thus *USW*, and improve his/her voluntary movements during rehabilitation therapies with safety. Preliminary tests with this system were already developed with promising.

5.3 Publications

This work has contributed to the scientific knowledge through the development of a control system for a robotic knee orthosis based on motion intention from sEMG of trunk. Different aspects of the research were published in the following papers:

Journal articles

1. Ana Cecilia Villa Parra, Denis Delisle Rodriguez, Jessica Souza Lima, Anselmo Frizera Neto and Teodiano Bastos. Knee Impedance Modulation to Control an Active Orthosis Using Insole Sensors. Sensors 17.12 (2017): 2751.

2. Ana Cecilia Villa Parra, Denis Delisle Rodriguez, Alberto López-Delis, Teodiano Bastos and Anselmo Frizera Neto. Exploración de Patrones de EMGs/EEG orientada al control de Exoesqueletos de Extremidad Inferior. Cognitive Area Nerworks, v. 3, p. 19-25, 2016.

3. Ana Cecilia Villa Parra, Leonardo Broche, Denis Delisle Rodriguez, Roberto Sagaró, Teodiano Bastos and Anselmo Frizera Neto. Design of active orthoses for a robotic gait rehabilitation system. Frontiers of Mechanical Engineering, v. 3, p. 242-254, 2015.

Conference Proceedings

1. Ana Cecilia Villa Parra, Thomaz Botelho, Denis Delisle Rodriguez, Anselmo Frizera Neto, Teodiano Bastos. Stance-Control of an Robotic Knee Orthosis based on admittance controller for Gait Assistance. XIII Simpósio Brasileiro de Automacao Inteligente Porto Alegre, 2017, ISSN 2175 8905, p. 1369-1374.

2. Ana Cecilia Villa Parra, Mario Jimenez, Jessica Souza Lima, Thomaz Botelho, Anselmo Frizera Neto, Teodiano Bastos. Robotic System to Improve Volitional Control of Movement During Gait. II Congreso Tecnología y Turismo para todas las Personas. Málaga, 2017, v. 1. p. 1-7.

3. Ana Cecilia Villa Parra, Thomaz Botelho, Denis Delisle Rodriguez, Alice Gomez, Teodiano Bastos and Anselmo Frizera Neto. Controle de um Exoesqueleto para Reabilitação de

Joelho baseado em Intenção de Movimento. Congresso Brasileiro de Automática, 2016, Vitória. Congresso Brasileiro de Automática. Vitória: UFES, 2016. v. 1. p. 50-55.

4. Ana Cecilia Villa Parra, Denis Delisle Rodriguez, Thomaz Botelho, Anselmo Frizera Neto and Teodiano Bastos. Knee-exoskeleton control for gait rehabilitation based on sEMG of trunk muscles. In: Cybathlon Symposium, 2016, Zurich. Cybathlon Symposium. Zurich: ETH Zurich, 2016. v. 1. p. 59-60.

5. Ana Cecilia Villa Parra, Denis Delisle Rodriguez, Alberto López Delis, Teodiano Bastos, Roberto Sagaró and Anselmo Frizera Neto. Towards a Robotic Knee Exoskeleton Control Based on Human Motion Intention through EEG and sEMG signals. Procedia Manufacturing, 2015, v. 3, p. 1379-1386.

6. Denis Delisle Rodriguez, Ana Cecilia Villa Parra, Teodiano Bastos, Anselmo Frizera Neto, Alberto López Delis. An Exploration of the Erector Spinae Muscle for Knee Exoskeleton Control. World Congress on Medical Physics ans Biomedical Engineering, IFMBE Proceedings, 2015.

7. Denis Delisle Rodriguez, Ana Cecilia Villa Parra, Teodiano Bastos, Anselmo Frizera Neto, Alberto López Delis. Protocol to Acquire sEMG and EEG Signals for Control of an Active Knee Orthosis Based on Detection of Movement Intention. International Workshop on Assistive Technologies IWAT, 2015.

8. Alberto López Delis, Denis Delisle Rodriguez, Ana Cecilia Villa Parra, Teodiano Bastos. Knee motion pattern classification from trunk muscle based on sEMG signals. 37th Annual International Conference of the IEEE Engineering in Medicine and Biology Society (EMBC), 2015.

9. Ana Cecilia Villa Parra, Diego Patiño, Martha Zequera, Teodiano Bastos. Control System for an Active AFO to Assist Ankle Dorsiflexion Movements in Swing Phase of Gait. Congresso Brasileiro de Engenharia Biomédica, 2014.

10. Ana Cecilia Villa Parra, Denis Delisle Rodriguez, Leonardo Broche, Roberto Sagaró, Teodiano Bastos, and Anselmo Frizera Neto. Proposal of an Assisted-Motion System for

Gait Rehabilitation. International Workshop on Wearable Robotics WeRob, 2014.

Book Chapter

1. Ana Cecilia Villa Parra, Teodiano Bastos, Resquin F, Moreno J.C., Leal E.R., Casco S., Rocon E., Del-Ama A., Prieto G. Estructura mecánica y actuación de exoesqueletos. In: CYTED & Red Reasiste. (Org.). Exoesqueletos Robóticos para Rehabilitación y Asistencia de Pacientes con Daño Neurológico. 1ed.Madrid-España, Vitória-Brasil: Programa Iberoamericano de Ciencia y Tecnología para el Desarrollo, 2016, v. 1, p. 63-87

2. Ana Cecilia Villa Parra, Denis Delisle Rodriguez, Flavia Loteiro, Carlos Valadao, Teodiano Bastos and Anselmo Frizera Neto. Robotic Systems for Gait Rehabilitation. Congresso Brasileiro de Engenharia Biomédica. (Org). 1ed. São Paulo: Canal 6 Editora, 2014, v. 1, p. 264-279.

Appendices

Appendix A

Features to sEMG signal processing

Mean Absolute Value (MAV): The mean absolute value of the signal in segment i which is N samples in length is given by

$$\bar{X}_i = \frac{1}{N} \sum_{k=1}^{N} |x_k| \qquad \text{for } i = 1, \ldots, I \tag{A.1}$$

where xi is the kth sample in segment i and I is the total number of segments over the entire sampled signal.

Root mean square (RMS): The amount of the RMS shows the activity level of the muscle. The RMS envelope of the EMG signal is calculated using a moving window, with each window of data calculated according to the following equation:

$$RMS = \sqrt{\frac{1}{N} \sum_{i=1}^{N} v_i^2} \tag{A.2}$$

where N is the number of the segments ($N = 400$) and v_i is the voltage at ith sampling.

Waveform length (WL): This feature could provide information on the waveform

$$l_i = \frac{1}{N} \sum_{k=1}^{N-1} |x_{k+1} - x_k| \qquad \text{for } i = 1, \ldots, I \tag{A.3}$$

Zero crossing (ZC): A simple frequency measure can obtained by counting the number of times the waveform crosses zero, which can be calculated as

$$z_i = \frac{1}{N} \sum_{k=1}^{N-1} f_k, \qquad f_k = \begin{cases} 1, & x_{k+1}x_k < 0 \text{ , and } |x_{k+1} - x_k| > th \\ 0, & \text{else} \end{cases} \qquad (A.4)$$

$$\text{for } i = 1, \dots, I$$

where th is a threshold to reduce the noise induced zero crossings.

Slope sign changes (SSC): Is a frequency measure by counting the number of times the slope of the waveform changes sign, and can be obtained as

$$c_i = \frac{1}{N} \sum_{k=2}^{N-1} f_k, \qquad f_k = \begin{cases} 1, & (x_k - x_{k-1})(x_{k+1} - x_k) < 0 \text{ , and} \\ & |x_k - x_{k-1}| > th \text{ or } |x_{k+1} - x_k| > th \\ 0, & \text{else} \end{cases} \qquad (A.5)$$

$$\text{for } i = 1, \dots, I$$

Variance (VAR):

$$VAR = \frac{1}{N-1} \sum_{k=1}^{N} x_k^2 \qquad \text{for } i = 1, \dots, I \qquad (A.6)$$

Wilson Amplitude (WAMP): This feature reflects the muscle contraction level

$$WAMP = \sum_{k=1}^{N} u(|x_k - x_{k+1}| - T) \qquad (A.7)$$

where T denotes a given threshold.

Mean frequency (MN):

$$MF = \sum_{i=1}^{N} h_i f_i / \sum_{i=1}^{N} h_i \qquad (A.8)$$

where f_i denotes frequency, and h_i denotes intensity of frequency spectrum.

Auto-regressive model (AR): An auto-regressive model of order P can be written as

$$X(k) = \sum_{i=1}^{P} A_i X_{k-i} + \epsilon_k \tag{A.9}$$

Appendix B

Protocol

Based on the results and with professional consulting of the therapist who accompanies the research, a protocol is proposed here for pilot tests using ALLOR with the system described in section 1.1.

For characterization of the sample, healthy adults and subjects with lower-limb movement and knee movements dysfunction during gait can be evaluated and compared. Hence, firstly healthy subjects participate and then, after modifications required by the therapist, the protocol is applied in post-stroke patients.

All volunteers must be informed about the background of this study, which was approved by the Ethics Committee of UFES CAAE: 64801316.5.0000.5542. All of them must also provide written informed consent prior to data collection.

A equipment based on a NI USB-6009 data acquisition device using reusable bipolar active electrodes (PL091060A - 60Hz) manufactured by Touch Bionics, with inbuilt 60Hz notch filter, pre-amplification, conditioning circuits, and adjustable gain, must be used to measure sEMG from trunk. The signals must be measured from *erector spinae* (ES) at levels T12 and L4. These sEMG signals must be measured on the right and left sides. The setup of the placement of the electrodes in each subject using ALLOR is shown in Figure B.1

The subjects must be cued through visual and sound stimuli with a period of 10 s to execute
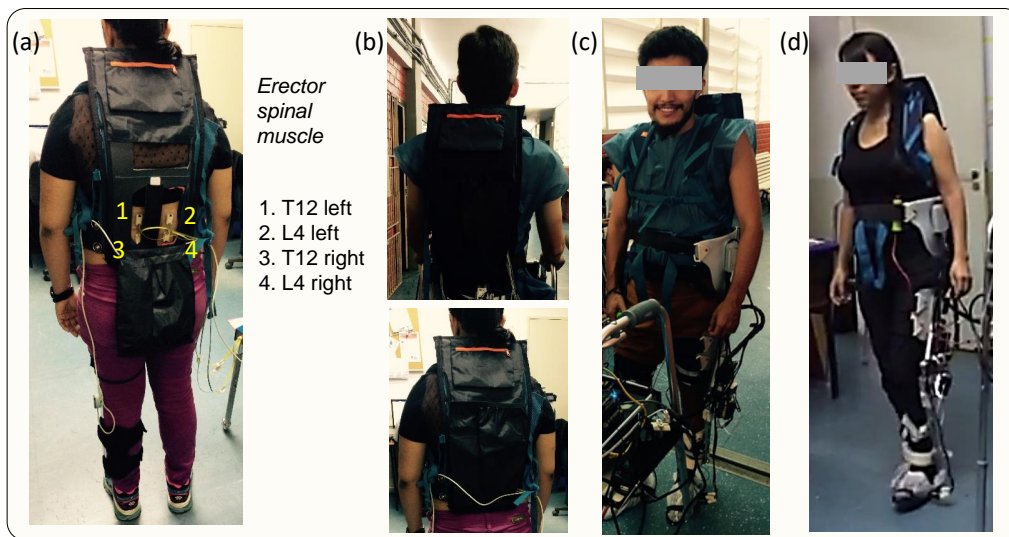
Figure B.1: Electrodes placement and setup for the execution of the motion classes during tests. (a) electrode position at trunk. The electrodes on the trunk are marked at the picture with numbers. (b) closed backpack to cover electrodes. (c) user during tests using the walker. (d) user during tests without walker while walking.

the following motor tasks: Stand-Up/Sit-Down (SU/SD), knee Flexion/Extension (F/E), gait walking (W), and Rest Stand-Up/Sit-Down positions (RSU/RSD). The two sequence of motor tasks, such as "sitting movements" and "standing movements" must be repeated in a random order. Three repetitions must be performed: the first one for adaptation and, after each test, there must be a rest from 5 to 10 minutes. The acquisition hardware must be attached to a mobile platform in order to follow the subjects, who must use a walker during the test.

During the movement execution, there must be constant monitoring of physical effort using the Borg Scale (VIVACQUA, 1992), (CHODZKO-ZAJKO et al., 2009).

To evaluate the applicability, functionality, usability and satisfaction with the use of ALLOR, QUEST 2.0 (CARVALHO et al., 2014) must be used.

For tests with post-stroke patients, initially, socio-demographic data, such as age, sex, scholarity, and body mass index must be collected, and the participants must be submitted to the Mini Mental State Exam (LOURENÇO; VERAS, 2006) and Berg Balance Scale (MIYAMOTO et al., 2004). These tests must be conducted in the own user's environment, with safety and privacy for him/her.

Bibliography

AGOSTINI, V.; BALESTRA, G.; KNAFLITZ, M. Segmentation and classification of gait cycles. *IEEE Transactions on Neural Systems and Rehabilitation Engineering*, IEEE, v. 22, n. 5, p. 946–952, 2014.

AI, Q. et al. Research on lower limb motion recognition based on fusion of semg and accelerometer signals. *Symmetry*, Multidisciplinary Digital Publishing Institute, v. 9, n. 8, p. 147, 2017.

AMA, A. J. del et al. Review of hybrid exoskeletons to restore gait following spinal cord injury. *Journal of Rehabilitation Research and Development*, v. 49, n. 4, p. 497–514, 2012. ISSN 1938-1352.

ANAM, K.; AL-JUMAILY, A. A. Active Exoskeleton Control Systems: State of the Art. *Procedia Engineering*, v. 41, p. 988–994, jan. 2012. ISSN 18777058.

ANDERS, C. et al. Trunk muscle activation patterns during walking at different speeds. *Journal of Electromyography and Kinesiology*, v. 17, n. 2, p. 245–252, abr. 2007. ISSN 1050-6411.

ARAZPOUR, M. et al. The influence of a powered knee–ankle–foot orthosis on walking in poliomyelitis subjects: A pilot study. *Prosthetics and orthotics international*, SAGE Publications Sage UK: London, England, v. 40, n. 3, p. 377–383, 2016.

ARNOS, P. *Age-related Changes in Gait: Influence of Upper-body Posture*. Tese (Doutorado) — University of Toledo, Madrid, 2007.

BACHSCHMIDT, R. A.; HARRIS, G. F.; SIMONEAU, G. G. Walker-assisted gait in rehabilitation: a study of biomechanics and instrumentation. *Ieee Transactions on neural systems and Rehabilitation Engineering*, IEEE, v. 9, n. 1, p. 96–105, 2001.

BALABAN, B.; TOK, F. Gait disturbances in patients with stroke. *PM&R*, v. 6, n. 7, p. 635–642, 2014. ISSN 1934-1482.

BENEDETTI, M. G.; AGOSTINI, V.; BONATO, M. K. a. P. Muscle Activation Patterns During Level Walking and Stair Ambulation. In: *Applications of EMG in Clinical and Sports Medicine*. 1. ed. CC BY: [s.n.], 2012. ISBN 978-953-307-798-7.

BENJAMIN, E. et al. Heart disease and stroke statistics—2017 update: A report from the american heart association. v. 135, p. CIR.0000000000000485, 01 2017.

BOTELHO, T. R. *Interface Multimodal Para o Uso em Reabilitação de Membros Inferiores Usando Predição de Movimento*. Tese (Doutorado) — Federal University of Espirito Santo, Brazil, 2017.

BRADLEY, S. M.; HERNANDEZ, C. R. Geriatric assistive devices. *American family physician*, v. 84, n. 4, 2011.

BUERGER, S. P.; HOGAN, N. Impedance and Interaction Control. In: *Robotics and Automation Handbook*. [S.l.: s.n.], 2004, (CRC Press 2004). ISBN 978-1-4200-3973-3.

BULEA, T. C. et al. A variable impedance knee mechanism for controlled stance flexion during pathological gait. *IEEE/ASME Transactions on Mechatronics*, IEEE, v. 17, n. 5, p. 822–832, 2012.

BULEA, T. C.; KOBETIC, R.; TRIOLO, R. J. Restoration of stance phase knee flexion during walking after spinal cord injury using a variable impedance orthosis. In: IEEE. *Engineering in Medicine and Biology Society, EMBC, 2011 Annual International Conference of the IEEE*. [S.l.], 2011. p. 608–611.

BURPEE, J. L.; LEWEK, M. D. Biomechanical gait characteristics of naturally occurring unsuccessful foot clearance during swing in individuals with chronic stroke. *Clinical Biomechanics*, v. 30, n. 10, p. 1102–1107, dez. 2015. ISSN 02680033.

BUURKE, J. et al. The effect of walking aids on muscle activation patterns during walking in stroke patients. *Gait & posture*, Elsevier, v. 22, n. 2, p. 164–170, 2005.

CALLAGHAN, M. et al. A comparison of the effects of first metatarsophalangeal joint arthrodesis and hemiarthroplasty on function of foot forces using gait analysis. *The Foot and Ankle Online Journal*, v. 4, n. 12, p. 1, 2011.

CAO, J. et al. Control strategies for effective robot assisted gait rehabilitation: the state of art and future prospects. *Medical engineering & physics*, Elsevier, v. 36, n. 12, p. 1555–1566, 2014.

CARVALHO, K. E. C. d. et al. Translation and validation of the quebec user evaluation of satisfaction with assistive technology (quest 2.0) into portuguese. *Revista brasileira de reumatologia*, SciELO Brasil, v. 54, n. 4, p. 260–267, 2014.

CECCATO, J.-C. et al. Comparison of trunk activity during gait initiation and walking in humans. *PLoS ONE*, v. 4, n. 12, p. e8193, 2009.

CHEN, B. et al. Recent developments and challenges of lower extremity exoskeletons. *Journal of Orthopaedic Translation*, Elsevier, v. 5, p. 26–37, 2016.

CHEN, B.; ZHENG, E.; WANG, Q. A locomotion intent prediction system based on multi-sensor fusion. *Sensors*, Multidisciplinary Digital Publishing Institute, v. 14, n. 7, p. 12349–12369, 2014.

CHEN, B. et al. A new strategy for parameter optimization to improve phase-dependent locomotion mode recognition. *Neurocomputing*, Elsevier, v. 149, p. 585–593, 2015.

CHEN, G. et al. A review of lower extremity assistive robotic exoskeletons in rehabilitation therapy. *Critical Reviews in Biomedical Engineering*, v. 41, n. 4-5, p. 343–363, 2013. ISSN 0278-940X.

CHODZKO-ZAJKO, W. J. et al. Exercise and physical activity for older adults. *Medicine & science in sports & exercise*, LWW, v. 41, n. 7, p. 1510–1530, 2009.

COWAN, R. et al. Recent trends in assistive technology for mobility. *Journal of NeuroEngineering & Rehabilitation (JNER)*, v. 9, n. 1, p. 20–27, 2012. ISSN 17430003.

DAWLEY, J. A.; FITE, K. B.; FULK, G. D. Emg control of a bionic knee prosthesis: exploiting muscle co-contractions for improved locomotor function. In: IEEE. *Rehabilitation Robotics (ICORR), 2013 IEEE International Conference On*. [S.l.], 2013. p. 1–6.

DONATI, M. et al. A Flexible Sensor Technology for the Distributed Measurement of Interaction Pressure. *Sensors*, v. 13, n. 1, p. 1021–1045, jan. 2013.

DZAHIR, M. A. M.; YAMAMOTO, S.-i. Recent trends in lower-limb robotic rehabilitation orthosis: Control scheme and strategy for pneumatic muscle actuated gait trainers. *Robotics*, Multidisciplinary Digital Publishing Institute, v. 3, n. 2, p. 120–148, 2014.

DíAZ, I.; GIL, J. J.; SáNCHEZ, E. Lower-Limb Robotic Rehabilitation: Literature Review and Challenges. *Journal of Robotics*, v. 2011, p. 1–11, 2011. ISSN 1687-9600, 1687-9619.

ESPINOSA, D. A. *Hybrid walking therapy with fatigue management for spinal cord injured individuals*. Tese (Doutorado) — Carlos III University, Madrid, 2013.

FARRIS, R. J.; QUINTERO, H. A.; GOLDFARB, M. Preliminary Evaluation of a Powered Lower Limb Orthosis to Aid Walking in Paraplegic Individuals. *IEEE Transactions on Neural Systems and Rehabilitation Engineering*, v. 19, n. 6, p. 652–659, dez. 2011. ISSN 1534-4320.

FETZ, E. E. Volitional control of neural activity: implications for brain–computer interfaces. *The Journal of Physiology*, Blackwell Publishing Ltd, v. 579, n. 3, p. 571–579, 2007. ISSN 1469-7793.

FIGUEIREDO, J. et al. Towards human-knee orthosis interaction based on adaptive impedance control through stiffness adjustment. In: IEEE. *Rehabilitation Robotics (ICORR), 2017 International Conference on*. [S.l.], 2017. p. 406–411.

FLEISCHER, C. et al. Application of EMG signals for controlling exoskeleton robots. *Biomedizinische Technik. Biomedical Engineering*, v. 51, n. 5-6, p. 314–319, dez. 2006. ISSN 0013-5585.

FUKUDA, T. Y. et al. Root mean square value of the electromyographic signal in the isometric torque of the quadriceps, hamstrings and brachial biceps muscles in female subjects. *J Appl Res*, v. 10, n. 1, p. 32–39, 2010.

HAYASHI, T.; KAWAMOTO, H.; SANKAI, Y. Control method of robot suit hal working as operator's muscle using biological and dynamical information. In: IEEE. *Intelligent Robots and Systems, 2005.(IROS 2005). 2005 IEEE/RSJ International Conference on*. [S.l.], 2005. p. 3063–3068.

HENDRICKSON, J. et al. Relationship between asymmetry of quiet standing balance control and walking post-stroke. *Gait & Posture*, v. 39, n. 1, p. 177–181, jan. 2014. ISSN 1879-2219.

HERR, H. Exoskeletons and orthoses: classification, design challenges and future directions. *Journal of NeuroEngineering and Rehabilitation*, v. 6, n. 1, p. 21, jun. 2009. ISSN 1743-0003.

HIROKAWA, S. et al. Energy consumption in paraplegic ambulation using the reciprocating gait orthosis and electric stimulation of the thigh muscles. *Archives of Physical Medicine and Rehabilitation*, v. 71, n. 9, p. 687–694, ago. 1990. ISSN 0003-9993.

HOF, A. L. et al. Speed dependence of averaged EMG profiles in walking. *Gait & Posture*, v. 16, n. 1, p. 78–86, ago. 2002. ISSN 0966-6362.

HOOVER, C. D.; FULK, G. D.; FITE, K. B. The design and initial experimental validation of an active myoelectric transfemoral prosthesis. *Journal of Medical Devices*, American Society of Mechanical Engineers, v. 6, n. 1, p. 011005, 2012.

HUO, W. et al. Lower limb wearable robots for assistance and rehabilitation: A state of the art. *IEEE systems Journal*, IEEE, v. 10, n. 3, p. 1068–1081, 2016.

HUSSAIN, S.; XIE, S. Q.; JAMWAL, P. K. Adaptive impedance control of a robotic orthosis for gait rehabilitation. *IEEE Transactions on Cybernetics*, IEEE, v. 43, n. 3, p. 1025–1034, 2013.

HUSSAIN, S.; XIE, S. Q.; LIU, G. Robot assisted treadmill training: Mechanisms and training strategies. *Medical Engineering & Physics*, v. 33, n. 5, p. 527–533, jun. 2011. ISSN 13504533.

IR, M.; AZUAN, N. Stance-control-orthoses with electromechanical actuation mechanism: Usefulness, design analysis and directions to overcome challenges. *Journal of Neurology and Neuroscience*, 2015.

JAHN, K.; ZWERGAL, A.; SCHNIEPP, R. Gait disturbances in old age. *Deutsches Ärzteblatt International*, v. 107, n. 17, p. 306–316, 2010. ISSN 1866-0452.

JAPKOWICZ, N.; SHAH, M. Evaluation learning algorithms a classification perspective. *Cambridge University Press*, v. 1, 2011.

JIMéNEZ-FABIáN, R.; VERLINDEN, O. Review of control algorithms for robotic ankle systems in lower-limb orthoses, prostheses, and exoskeletons. *Medical Engineering & Physics*, v. 34, n. 4, p. 397–408, maio 2012. ISSN 13504533.

JONSDOTTIR, J. et al. Functional resources to increase gait speed in people with stroke: strategies adopted compared to healthy controls. *Gait & Posture*, v. 29, n. 3, p. 355–359, abr. 2009. ISSN 1879-2219.

JOSHI, C. D.; LAHIRI, U.; THAKOR, N. V. Classification of gait phases from lower limb EMG: Application to exoskeleton orthosis. In: *2013 IEEE Point-of-Care Healthcare Technologies (PHT)*. [S.l.: s.n.], 2013. p. 228–231.

KANG, S. J. et al. Walker gait analysis of powered gait orthosis for paraplegic. In: SPRINGER. *World Congress on Medical Physics and Biomedical Engineering 2006*. [S.l.], 2007. p. 2889–2891.

KARTHIKBABU, S. et al. A review on assessment and treatment of the trunk in stroke. *Neural Regeneration Research*, v. 7, n. 25, p. 1974–1977, 2012. ISSN 1673-5374.

KIGUCHI, K.; HAYASHI, Y. *EMG-Based Control of a Lower-Limb Power-Assist Robot.* 2015.

KIGUCHI, K.; IMADA, Y. Emg-based control for lower-limb power-assist exoskeletons. In: IEEE. *Robotic Intelligence in Informationally Structured Space, 2009. RIISS'09. IEEE Workshop on.* [S.l.], 2009. p. 19–24.

KIGUCHI, K.; TANAKA, T.; FUKUDA, T. Neuro-Fuzzy Control of a Robotic Exoskeleton With EMG Signals. *IEEE Transactions on Fuzzy Systems*, v. 12, n. 4, p. 481–490, ago. 2004. ISSN 1063-6706.

KIM, J.; KIM, S. J.; CHOI, J. Real-time gait phase detection and estimation of gait speed and ground slope for a robotic knee orthosis. In: *2015 IEEE International Conference on Rehabilitation Robotics (ICORR)*. [S.l.: s.n.], 2015. p. 392–397.

KIM, S. Y. et al. Effects of Innovative WALKBOT Robotic-Assisted Locomotor Training on Balance and Gait Recovery in Hemiparetic Stroke: A Prospective, Randomized, Experimenter Blinded Case Control Study With a Four-Week Follow-Up. *IEEE Transactions on Neural Systems and Rehabilitation Engineering*, v. 23, n. 4, p. 636–642, jul. 2015. ISSN 1534-4320.

KONRAD, P. The abc of emg. *A practical introduction to kinesiological electromyography*, v. 1, 2005.

KOZLOWSKI, A. J.; BRYCE, T. N.; DIJKERS, M. P. Time and Effort Required by Persons with Spinal Cord Injury to Learn to Use a Powered Exoskeleton for Assisted Walking. *Topics in Spinal Cord Injury Rehabilitation*, v. 21, n. 2, p. 110–121, 2015. ISSN 1082-0744.

LAMOTH, C. J. C. et al. Effects of experimentally induced pain and fear of pain on trunk coordination and back muscle activity during walking. *Clinical Biomechanics (Bristol, Avon)*, v. 19, n. 6, p. 551–563, jul. 2004. ISSN 0268-0033.

LAMOTH, C. J. C. et al. Pelvis-thorax coordination in the transverse plane during walking in persons with nonspecific low back pain. *Spine*, v. 27, n. 4, p. E92–99, fev. 2002. ISSN 1528-1159.

LAUER, R. T. et al. Feasibility of Gait Event Detection Using Intramuscular Electromyography in the Child with Cerebral Palsy. *Neuromodulation: Technology at the Neural Interface*, v. 7, n. 3, p. 205–213, jul. 2004. ISSN 1525-1403.

LEE, H.-J. et al. Age-related differences in muscle co-activation during locomotion and their relationship with gait speed: a pilot study. *BMC geriatrics*, BioMed Central, v. 17, n. 1, p. 44, 2017.

LEE, M.-R. et al. Gait phase recognition based on EMG signal for stairs ascending and stairs descending. *Journal of the Institute of Electronics and Information Engineers*, v. 52, n. 3, p. 181–189, 2015. ISSN 2287-5026.

LEE, S. W. et al. Design of a gait phase recognition system that can cope with EMG electrode location variation. *IEEE Transactions on Automation Science and Engineering*, PP, n. 99, p. 1–11, 2015. ISSN 1545-5955.

LENZI, T. et al. Intention-based emg control for powered exoskeletons. *IEEE transactions on biomedical engineering*, IEEE, v. 59, n. 8, p. 2180–2190, 2012.

LEWEK, M. D. et al. The relationship between spatiotemporal gait asymmetry and balance in individuals with chronic stroke. *Journal of Applied Biomechanics*, v. 30, n. 1, p. 31–36, 2014. ISSN 1065-8483.

LI, J. et al. Structure design of lower limb exoskeletons for gait training. *Chinese Journal of Mechanical Engineering*, Springer, v. 28, n. 5, p. 878–887, 2015.

LOBO-PRAT, J. et al. Non-invasive control interfaces for intention detection in active movement-assistive devices. *Journal of NeuroEngineering and Rehabilitation*, v. 11, n. 1, p. 168, dez. 2014. ISSN 1743-0003.

LOTERIO, F. A. et al. Adaptation of a smart walker for stroke individuals: a study on semg and accelerometer signals. *Research on Biomedical Engineering*, SciELO Brasil, n. AHEAD, p. 0–0, 2017.

LOUIE, D. R.; ENG, J. J. Powered robotic exoskeletons in post-stroke rehabilitation of gait: a scoping review. *Journal of neuroengineering and rehabilitation*, BioMed Central, v. 13, n. 1, p. 53, 2016.

LOUIE, D. R.; ENG, J. J.; LAM, T. Gait speed using powered robotic exoskeletons after spinal cord injury: a systematic review and correlational study. *Journal of neuroengineering and rehabilitation*, BioMed Central, v. 12, n. 1, p. 82, 2015.

LOURENÇO, R. A.; VERAS, R. P. Mini-exame do estado mental: características psicométricas em idosos ambulatoriais. *Rev Saúde Pública*, SciELO Brasil, v. 40, n. 4, p. 712–9, 2006.

LOW, K. H.; YIN, Y. An integrated lower exoskeleton system towards design of a portable active orthotic device. *International Journal of Robotics and Automation*, v. 22, n. 1, p. 32–43, 2007.

LYNALL, R. C. et al. Reliability and validity of the protokinetics movement analysis software in measuring center of pressure during walking. *Gait & posture*, Elsevier, v. 52, p. 308–311, 2017.

MA, H. et al. Design and control of a powered knee orthosis for gait assistance. In: IEEE. *Advanced Intelligent Mechatronics (AIM), 2013 IEEE/ASME International Conference on*. [S.l.], 2013. p. 816–821.

MACKAY, J.; MENSAH, G. *The Atlas of Heart Disease and Stroke*. 1. ed. USA: World Health Organization, 2004. ISBN 978-92-4-156276-8.

MAEDA, N.; KATO, J.; SHIMADA, T. Predicting the probability for fall incidence in stroke patients using the berg balance scale. *Journal of International Medical Research*, Sage Publications Sage UK: London, England, v. 37, n. 3, p. 697–704, 2009.

MAHLKNECHT, P. et al. Prevalence and burden of gait disorders in elderly men and women aged 60–97 years: A population-based study. *PLoS ONE*, v. 8, n. 7, 2013. ISSN 1932-6203.

MAYOR, J. J. V. *Muscle-Computer Interface Based on Pattern Recognition of Myoelectric Signals for Control of Dexterous Hand and Finger Movements of Prostheses for Forearm Amputees*. Tese (Doutorado) — Universidade Federal do Espírito Santo, 2017.

MAYOR, J. J. V. et al. Dexterous hand gestures recognition based on low-density semg signals for upper-limb forearm amputees. *Research on Biomedical Engineering*, SciELO Brasil, n. AHEAD, p. 0–0, 2017.

MAZAHERI, R. et al. The Activation Pattern of Trunk and Lower Limb Muscles in an Electromyographic Assessment; Comparison Between Ground and Treadmill Walking. *Asian Journal of Sports Medicine*, In Press, n. In Press, jun. 2016. ISSN 2008-000X, 2008-7209.

MCGIBBON, C. A.; KREBS, D. E. Discriminating age and disability effects in locomotion: neuromuscular adaptations in musculoskeletal pathology. *Journal of Applied Physiology*, v. 96, n. 1, p. 149–160, jan. 2004. ISSN 8750-7587, 1522-1601.

McMillan, A. G. et al. Preliminary evidence for effectiveness of a stance control orthosis - , 2004 | american academy of orthotists & prosthetists. *Journal of Prosthetics and Orthotics*, v. 16, n. 1, 2004.

MELO, P. L. et al. Technical developments of functional electrical stimulation to correct drop foot: Sensing, actuation and control strategies. *Clinical Biomechanics*, v. 30, n. 2, p. 101–113, fev. 2015. ISSN 0268-0033.

MENG, M. et al. EMG signals based gait phases recognition using hidden markov models. In: *2010 IEEE International Conference on Information and Automation (ICIA)*. [S.l.: s.n.], 2010. p. 852–856.

MENG, W. et al. Recent development of mechanisms and control strategies for robot-assisted lower limb rehabilitation. *Mechatronics*, Elsevier, v. 31, p. 132–145, 2015.

MIYAMOTO, S. T. et al. Brazilian version of the berg balance scale. *Brazilian journal of medical and biological research*, SciELO Brasil, v. 37, n. 9, p. 1411–1421, 2004.

MIZRAHI, J. Mechanical impedance and its relations to motor control, limb dynamics, and motion biomechanics. *Journal of medical and biological engineering*, Springer, v. 35, n. 1, p. 1–20, 2015.

MUNOZ-ORGANERO, M. et al. Assessing walking strategies using insole pressure sensors for stroke survivors. *Sensors*, Multidisciplinary Digital Publishing Institute, v. 16, n. 10, p. 1631, 2016.

NAJI, M.; FIROOZABADI, M.; KAHRIZI, S. Evaluation of EMG features of trunk muscles during flexed postures. In: *2012 19th Iranian Conference of Biomedical Engineering (ICBME)*. [S.l.: s.n.], 2012. p. 71–74.

NEWMAN, W. S. Stability and Performance Limits of Interaction Controllers. *Journal of Dynamic Systems, Measurement, and Control*, v. 114, n. 4, p. 563–570, dez. 1992. ISSN 0022-0434.

NYMARK, J. R. et al. Electromyographic and kinematic nondisabled gait differences at extremely slow overground and treadmill walking speeds. *Journal of Rehabilitation Research and Development*, v. 42, n. 4, p. 523–534, ago. 2005. ISSN 1938-1352.

ONEN, U. et al. Design and Actuator Selection of a Lower Extremity Exoskeleton. *IEEE/ASME Transactions on Mechatronics*, p. 1–10, 2013. ISSN 1083-4435, 1941-014X.

OSKOEI, M.; HU, H. Support Vector Machine-Based Classification Scheme for Myoelectric Control Applied to Upper Limb. *IEEE Transactions on Biomedical Engineering*, v. 55, n. 8, p. 1956–1965, ago. 2008. ISSN 0018-9294.

OSKOEI, M. A.; HU, H. Myoelectric control systems—A survey. *Biomedical Signal Processing and Control*, v. 2, n. 4, p. 275–294, out. 2007. ISSN 1746-8094.

PEREIRA, L. M. et al. Electromyographic activity of selected trunk muscles in subjects with and without hemiparesis during therapeutic exercise. *Journal of Electromyography and Kinesiology: Official Journal of the International Society of Electrophysiological Kinesiology*, v. 21, n. 2, p. 327–332, abr. 2011. ISSN 1873-5711.

PERRY, J. *Gait Analysis: Normal and Pathological Function*. [S.l.]: Slack Incorporated, 2010. ISBN 978-1-55642-766-4.

PFEIFER, S. et al. Model-based estimation of knee stiffness. *IEEE Transactions on Biomedical Engineering*, IEEE, v. 59, n. 9, p. 2604–2612, 2012.

PHINYOMARK, A.; LIMSAKUL, C.; PHUKPATTARANONT, P. A novel feature extraction for robust emg pattern recognition. *arXiv preprint arXiv:0912.3973*, 2009.

PONS, J. L. *Wearable robots: biomechatronic exoskeletons*. Hoboken, N.J.: Wiley, 2008. ISBN 978-0-470-51294-4 0-470-51294-6.

PONS, J. L. et al. Lower-Limb Wearable Exoskeleton. In: *Rehabilitation Robotics*. Austria: [s.n.], 2007. ISBN 978-3-902613-04-2.

QUINTERO, H. A.; FARRIS, R. J.; GOLDFARB, M. A Method for the Autonomous Control of Lower Limb Exoskeletons for Persons With Paraplegia. *Journal of Medical Devices*, v. 6, n. 4, p. 0410031–0410036, dez. 2012. ISSN 1932-6181.

RAFIAEI, M. et al. The gait and energy efficiency of stance control knee–ankle–foot orthoses: A literature review. *Prosthetics and orthotics international*, SAGE Publications Sage UK: London, England, v. 40, n. 2, p. 202–214, 2016.

RAFIAEI, M. et al. The gait and energy efficiency of stance control knee-ankle-foot orthoses: A literature review. *Prosthetics and Orthotics International*, v. 40, n. 2, p. 202–14, 2016.

RIENER, R. et al. Patient-cooperative strategies for robot-aided treadmill training: first experimental results. *IEEE Transactions on Neural Systems and Rehabilitation Engineering*, v. 13, n. 3, p. 380–394, Sept 2005. ISSN 1534-4320.

RIENER, R.; LüNENBURGER, L.; COLOMBO, G. Human-centered robotics applied to gait training and assessment. *The Journal of Rehabilitation Research and Development*, v. 43, n. 5, p. 679, 2006. ISSN 0748-7711.

SALZMAN, B. Gait and balance disorders in older adults. *Am Fam Physician*, v. 82, n. 1, p. 61–68, 2010.

SANTOS, W. M. d.; SIQUEIRA, A. A. G. Robust torque control based on H inf criterion of an active knee orthosis. In: *5th IEEE RAS/EMBS International Conference on Biomedical Robotics and Biomechatronics*. [S.l.: s.n.], 2014. p. 644–649.

SARTORI, M. et al. Modeling and simulating the neuromuscular mechanisms regulating ankle and knee joint stiffness during human locomotion. *Journal of neurophysiology*, Am Physiological Soc, v. 114, n. 4, p. 2509–2527, 2015.

SAWICKI, G. S.; FERRIS, D. P. A pneumatically powered knee-ankle-foot orthosis (KAFO) with myoelectric activation and inhibition. *Journal of NeuroEngineering and Rehabilitation*, v. 6, n. 1, p. 23, 2009. ISSN 1743-0003.

SERIES, T. T. *The intrinsic back muscles*. 2017. Disponível em: <http://teachmeanatomy.info/back/muscles/intrinsic/>.

SHAMAEI, K. et al. Design and Evaluation of a Quasi-Passive Knee Exoskeleton for Investigation of Motor Adaptation in Lower Extremity Joints. *IEEE Transactions on Biomedical Engineering*, v. 61, p. 1809–1821, 2014. ISSN 0018-9294.

SHAMAEI, K.; DOLLAR, A. M. On the mechanics of the knee during the stance phase of the gait. In: IEEE. *Rehabilitation Robotics (ICORR), 2011 IEEE International Conference on*. [S.l.], 2011. p. 1–7.

SHAMAEI, K.; NAPOLITANO, P. C.; DOLLAR, A. M. Design and Functional Evaluation of a Quasi-Passive Compliant Stance Control Knee Ankle Foot Orthosis. *IEEE Transactions on Neural Systems and Rehabilitation Engineering*, v. 22, n. 2, p. 258–268, mar. 2014. ISSN 1534-4320.

SHORTER, K. A. et al. Technologies for Powered Ankle-Foot Orthotic Systems: Possibilities and Challenges. *IEEE/ASME Transactions on Mechatronics*, v. 18, n. 1, p. 337–347, fev. 2013. ISSN 1083-4435, 1941-014X.

SMITH, L. H. et al. Determining the Optimal Window Length for Pattern Recognition-Based Myoelectric Control: Balancing the Competing Effects of Classification Error and Controller Delay. *IEEE Transactions on Neural Systems and Rehabilitation Engineering*, v. 19, n. 2, p. 186–192, abr. 2011. ISSN 1534-4320.

STAM, D.; FERNANDEZ, J. Robotic gait assistive technology as means to aggressive mobilization strategy in acute rehabilitation following severe diffuse axonal injury: a case study. *Disability and Rehabilitation: Assistive Technology*, v. 0, n. 0, p. 1–7, abr. 2016. ISSN 1748-3107.

SUZUKI, K. et al. Intention-based walking support for paraplegia patients with robot suit hal. *Advanced Robotics*, Taylor & Francis, v. 21, n. 12, p. 1441–1469, 2007.

SWINNEN, E. et al. Methodology of electromyographic analysis of the trunk muscles during walking in healthy subjects: A literature review. *Journal of Electromyography and Kinesiology*, v. 22, p. 1 – 12, 2012.

SWINNEN, E. et al. Methodology of electromyographic analysis of the trunk muscles during walking in healthy subjects: a literature review. *Journal of Electromyography and Kinesiology: Official Journal of the International Society of Electrophysiological Kinesiology*, v. 22, n. 1, p. 1–12, fev. 2012. ISSN 1873-5711.

SèZE, M. de et al. Sequential activation of axial muscles during different forms of rhythmic behavior in man. *Experimental Brain Research*, v. 185, n. 2, p. 237–247, 2008. ISSN 1432-1106.

SèZE, M. P. de; CAZALETS, J.-R. Anatomical optimization of skin electrode placement to record electromyographic activity of erector spinae muscles. *Surgical and radiologic anatomy: SRA*, v. 30, n. 2, p. 137–143, mar. 2008. ISSN 0930-1038.

TABORRI, J. et al. Gait partitioning methods: A systematic review. *Sensors*, v. 16, n. 1, p. 66, 2016. ISSN 1424-8220.

TANG, G.; WANG, H.; TIAN, Y. semg-based estimation of knee joint angles and motion intention recognition. In: IEEE. *Intelligent Human-Machine Systems and Cybernetics (IHMSC), 2017 9th International Conference on.* [S.l.], 2017. v. 2, p. 390–393.

TO, C. S. et al. Stance control knee mechanism for lower-limb support in hybrid neuroprosthesis. *Journal of rehabilitation research and development*, NIH Public Access, v. 48, n. 7, p. 839, 2011.

TO, C. S. et al. Sensor-based stance control with orthosis and functional neuromuscular stimulation for walking after spinal cord injury. *JPO: Journal of Prosthetics and Orthotics*, LWW, v. 24, n. 3, p. 124–132, 2012.

TSUJI, T.; TANAKA, Y. Tracking control properties of human-robotic systems based on impedance control. *IEEE Transactions on Systems, Man, and Cybernetics - Part A: Systems and Humans*, v. 35, n. 4, p. 523–535, 2005.

TUCKER, M. R. et al. Design of a wearable perturbator for human knee impedance estimation during gait. In: IEEE. *Rehabilitation robotics (ICORR), 2013 IEEE international conference on.* [S.l.], 2013. p. 1–6.

TUCKER, M. R. et al. Control strategies for active lower extremity prosthetics and orthotics: a review. *Journal of NeuroEngineering and Rehabilitation*, v. 12, p. 1, 2015.

VILLAREJO, J. J. et al. Pattern recognition of hand movements with low density sEMG for prosthesis control purposes. In: *2013 IEEE International Conference on Rehabilitation Robotics (ICORR).* [S.l.: s.n.], 2013. p. 1–6.

VITECKOVA, S.; KUTILEK, P.; JIRINA, M. Wearable lower limb robotics: A review. *Biocybernetics and Biomedical Engineering*, v. 33, n. 2, p. 96–105, jan. 2013. ISSN 02085216.

VIVACQUA, E. *Ergometria e Reabilitação em Cardiologia*. Brazil: [s.n.], 1992.

WAFAI ALADIN ZAYEGH, J. W. S. M. A. L.; BEGG, R. Identification of foot pathologies based on plantar pressure asymmetry. *Sensors (Basel, Switzerland)*, v. 15, n. 8, p. 20392–20408, 2015.

WALDNER, A.; TOMELLERI, C.; HESSE, S. Transfer of scientific concepts to clinical practice: recent robot-assisted training studies. *Functional Neurology*, v. 24, n. 4, p. 173–177, dez. 2009. ISSN 0393-5264.

WATANABE, S. et al. Electromyographic activity of selected trunk muscles during bicycle ergometer exercise and walking. *Electromyography and Clinical Neurophysiology*, v. 46, n. 5, p. 311–315, set. 2006. ISSN 0301-150X.

WEERDESTEYN, V. et al. Falls in individuals with stroke. v. 45, n. 8, p. 1195–1213, 2008. ISSN 1938-1352.

WENTINK, E. C. et al. Intention detection of gait initiation using EMG and kinematic data. *Gait & Posture*, v. 37, n. 2, p. 223–228, fev. 2013. ISSN 1879-2219.

WHITE, S. G.; MCNAIR, P. J. Abdominal and erector spinae muscle activity during gait: the use of cluster analysis to identify patterns of activity. *Clinical Biomechanics*, Elsevier, v. 17, n. 3, p. 177–184, 2002.

WINTER, D. A. *Biomechanics and motor control of human movement*. 4th ed. ed. Hoboken, N.J: Wiley, 2009. ISBN 978-0-470-39818-0.

World Health Organization (Ed.). *World report on ageing and health*. Geneva, Switzerland: World Health Organization, 2015. ISBN 978-92-4-156504-2.

YAKIMOVICH, T.; LEMAIRE, E. D.; KOFMAN, J. Preliminary kinematic evaluation of a new stance-control knee–ankle–foot orthosis. *Clinical biomechanics*, Elsevier, v. 21, n. 10, p. 1081–1089, 2006.

YAKIMOVICH, T.; LEMAIRE, E. D.; KOFMAN, J. Engineering design review of stance-control knee-ankle-foot orthoses. *The Journal of Rehabilitation Research and Development*, v. 46, n. 2, p. 257, 2009. ISSN 0748-7711.

YAN, T. et al. Review of assistive strategies in powered lower-limb orthoses and exoskeletons. *Robotics and Autonomous Systems*, v. 64, p. 120–136, fev. 2015. ISSN 09218890.

ZACHARIAS, B.; KANNENBERG, A. Clinical benefits of stance control orthosis systems: An analysis of the scientific literature. *Journal of Prosthetics and Orthotics*, v. 24, n. 1, p. 2–7, 2012.

ZECCA, M. et al. Control of multifunctional prosthetic hands by processing the electromyographic signal. *Critical Reviews in Biomedical Engineering*, v. 30, n. 4-6, p. 459–485, 2002. ISSN 0278-940X.

ZEILIG, G. et al. Safety and tolerance of the ReWalk^{TM} exoskeleton suit for ambulation by people with complete spinal cord injury: a pilot study. *The Journal of Spinal Cord Medicine*, v. 35, n. 2, p. 96–101, mar. 2012. ISSN 1079-0268.

ZISSIMOPOULOS, A.; FATONE, S.; GARD, S. A. Biomechanical and energetic effects of a stance-control orthotic knee joint. *Journal of Rehabilitation Research and Development*, v. 44, n. 4, p. 503–513, 2007. ISSN 1938-1352.